Margit Midtgaard Bach

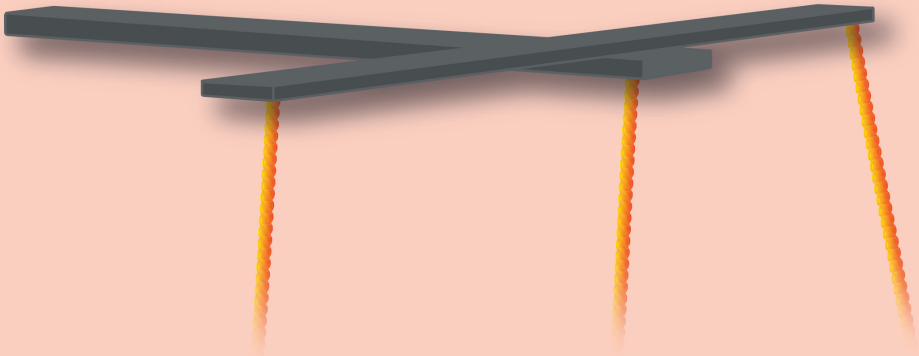

THE DEVELOPMENT OF RUNNING IN CHILDREN

There is more to the story than flight phase

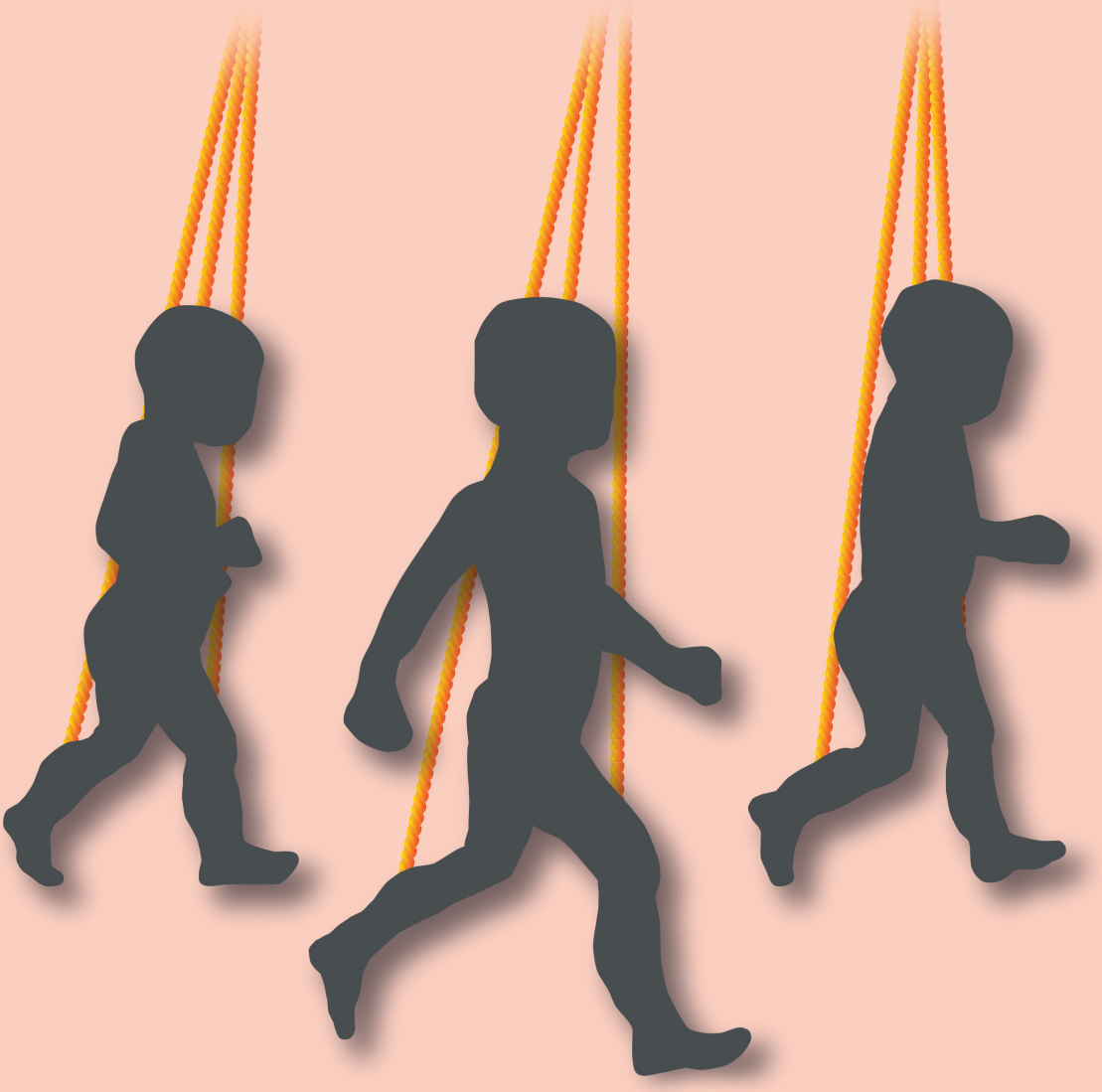

The development of running in children

There is more to the story than flight phase

Margit Midtgaard Bach

This PhD thesis was embedded within and supported by Amsterdam Movement Sciences Research Institute and Institute Brain and Behavior Amsterdam, at the Department of Human Movement Sciences, Vrije Universiteit Amsterdam, The Netherlands. The research was funded by the Netherlands Organisation for Scientific Research (NWO Vidi Grant FirSTeps #016.156.346) and the European Research Council (ERC Starting Grant Learn2Walk #715945).

ISBN: 978-94-6483-047-7

Cover design and Layout: Margit Midtgaard Bach

Printing: Ridderprint, www.ridderprint.nl

VRIJE UNIVERSITEIT

THE DEVELOPMENT OF RUNNING IN CHILDREN

There is more to the story than flight phase

ACADEMISCH PROEFSCHRIFT

ter verkrijging van de graad Doctor of Philosophy aan
de Vrije Universiteit Amsterdam,
op gezag van de rector magnificus
prof.dr. J.J.G. Geurts,
in het openbaar te verdedigen
ten overstaan van de promotiecommissie
van de Faculteit der Gedrags- en Bewegingswetenschappen
op dinsdag 9 mei 2023 om 11.45 uur
in een bijeenkomst van de universiteit,
De Boelelaan 1105

door

Margit Midtgaard Bach

geboren te Aarhus, Denemarken

promotor:	prof.dr. A. Daffertshofer
copromotor:	dr. N. Dominici
promotiecommissie:	prof.dr. H. Wagner prof.dr. V. Segers prof.dr. C.J.C. Lamoth dr. M. van der Krogt prof.dr. J.H. van Dieen

Sometimes the fastest way to get there is to go slow

Tina Dickow, Count to ten (2007)

Til min far

TABLE OF CONTENTS

Chapter 1

INTRODUCTION

As children gain confidence in their ability to walk, they increase their speed, eventually shifting from walking to running. Determining when and how running develops is a challenge, as there is no standard for measuring the development of running in children and the accompanying *motor control*. Biomechanics and neuromuscular control are two aspects that should be properly addressed when it comes to understanding the development of running skills. In the following sections, I delve into both aspects in greater detail and show what we may learn from them when studying the development of running in children.

Biomechanics of Locomotion

Biomechanics encompasses the analysis of movement patterns, muscle and joint forces, and energy expenditure during movement such as locomotion. Most biomechanical models of human locomotion are based on the gait patterns of adults. However, children cannot be considered merely scaled-down versions of adults (Rose & Arellano, 2021). Consequently, models used in adults are most likely to not be readily transferable to children. Before digging into this more, it is important to understand the models defining the most frequent gait patterns in adults: walking and running.

Walking can be modelled as a simple inverted pendulum swing where the center-of-mass (CoM) oscillates over the stance leg with the highest point at midstance (Alexander, 1976) cf. Figure 1.1, left panel. By contrast, *Running* can be modelled as a spring mass with the stance leg being compressed during stance (Blickhan, 1989; McMahon & Cheng, 1990) and the CoM is at its lowest point during midstance, cf. Figure 1.1, right panel. According to these models, the CoM's kinetic and potential energies are oscillating in-phase during walking and out-of-phase during running.

Both models found experimental support in adult studies which revealed that in walking, the transfer between kinetic and potential energy is out-of-phase during stance and around 65% of energy is recovered at the most optimal walking speed. By contrast, the transfer of energy between kinetic and potential energy of the CoM in running hardly exceeds 5% (Cavagna, Saibene, & Margaria, 1964; Cavagna, Thys, & Zamboni, 1976). Biomechanics-based energy estimates may hence serve as a classifier discriminating between walking and running.

Another common classifier to distinguish running from walking in adults is the presence or absence of a flight phase, i.e., a period where neither foot touches the ground. Put differently, walking can be distinguished from running by the double support phase during walking and flight phase during running. However, recent research suggests that running at slow speeds do not inherently result in a flight phase but the gait pattern still adheres to the spring mass model and result in in-phase oscillations of kinetic and potential energy (Bonnaerens et al., 2019; Bonnaerens et al., 2021; Shorten & Pisciotta, 2017).

When considering kinematics and kinetics, in adults, running is typically associated with a more flexed pattern compared to walking (Farley & Ferris, 1998). This can be observed in knee joint angles during stance, see Figure 1.1 for illustration. This, however, does not hold true in infants, not yet walking independently but supported while locomoting on a treadmill at high speeds (Vasudevan, Patrick, & Yang, 2016).

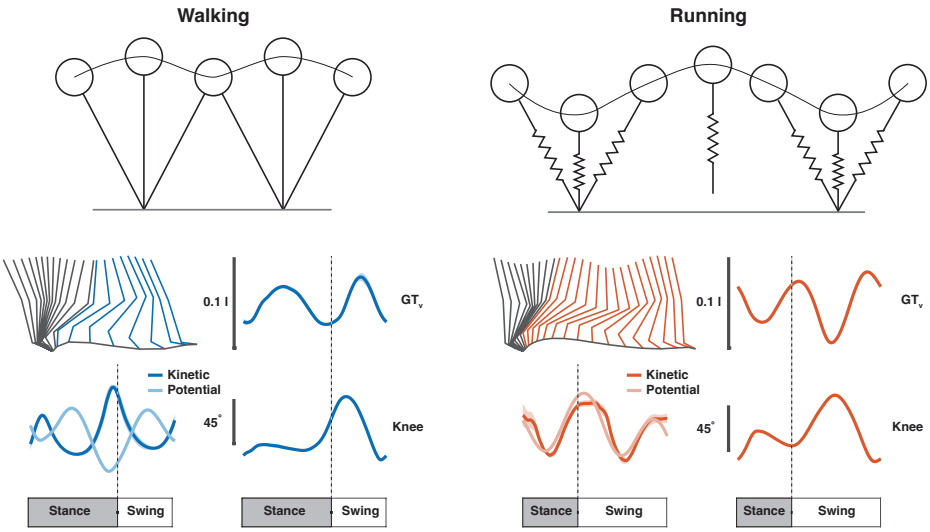

Figure 1.1: Schematic of walking and running models. Top, left: inverted pendulum swing mechanism for walking, top, right: spring mass model for running. Bottom: stick figures of an adult stride with the black indicating the stance and blue/red the swing phase for walking and running, respectively. Next to that are the kinetic and potential energies of the CoM, knee joint angle, and vertical hip displacement. Gait cycle bars represent mean stance and swing duration. Adapted from data acquired in Bach, Daffertshofer, and Dominici (2021a).

When children take their first independent steps, their gait pattern does not comply with the adult model of the pendulum swing mechanism, as there are no distinct oscillations of the CoM corresponding to the double oscillations in adults (Ivanenko, Dominici, et al., 2004). The exchange between kinetic and potential energies of the CoM is lower in children taking their first steps than in children older than two years (Ivanenko, Dominici, et al., 2004) and clearly lower than in adults (Hallemans, Aerts, Otten, De Deyn, & De Clercq, 2004). If children learning to walk are not exploiting the pendulum swing mechanism, it is conceivable that children learning to run also do not make full use of the spring mass model. This may affect the joint kinematics, ground reaction forces, and energy expenditure during running. Finally, running in children might not require a flight phase like fast running adults. This will affect the ability to run with a flight phase but possibly also the in-phase oscillations of kinetic and potential energies of the CoM that one observes in adults.

The question arises as to whether the two common classifiers, energy exchange and presence of a flight phase are also suitable for defining running in children. And, given that challenge, one may wonder how the *maturity of running* can be determined. If running cannot readily be classified, then it might not be possible to determine how mature a running pattern is. To solve this dilemma, I propose to use a combination of data such as whole-body kinematics, kinetics, and muscle activity patterns to infer the maturity of locomotor patterns. It is not clear which parameters are needed to explain running (development) in children, so state-of-the-art data mining and machine learning techniques can be utilized for blindly finding patterns in the data as these do not suffer from a priori parameter selections.

In recent years, machine learning algorithms have gained popularity in classifying the mode of locomotion and distinguishing people with gait impairments from healthy individuals (Figueiredo, Santos, & Moreno, 2018; Labarrière et al., 2020; Narayanan, Desai, Stewart, Duncan, & Mackay, 2020). Traditionally, the biomechanics of locomotion is investigated using one or a handful of kinematic variables such as joint angles, joint angular velocities, or joint moments. It is possible to detect some differences between walking and running via isolated kinematic parameters, however, many subtleties of the developing gait pattern remain opaque. It thus seems necessary to combine multiple kinematic and kinetic parameters to make inferences on the gait pattern. There are many ways to do so. A common approach relies on supervised learning, often closely related to mere linear regression. Supervised learning has several limitations and comes with the risk of overfitting. The alternative to avoid this risk, is unsupervised learning, and it comes as no surprise that it has been gaining popularity in recent years. In unsupervised learning, data are not necessarily pre-selected but analyzed for their predictive capacity. When it comes to data mining, a frequently used approach is hierarchical clustering that allows for circumventing selection bias when searching for patterns in data. Nonetheless, clustering can still suffer from the risk of classification bias and potentially yield invalid output. The primary reason for this is covariation in the data, which can be eliminated via principal component analysis (PCA), i.e., pre-whitening. Here I would like to note that, in more traditional gait analysis, PCA is typically used to identify and exploit covariance rather than eliminating it. PCA has indeed been used successfully to identify factors contributing to gait recovery in animals and humans after spinal cord injury by combining more than hundred kinematic and kinetic parameters (Courtine et al., 2009; Dominici et al., 2012; Friedli et al., 2015; Wenger et al., 2016).

Combining PCA with clustering is not new. Several studies looked at motor activity in chronic obstructive pulmonary disease (Sherrill, Moy, Reilly, & Bonato, 2005), classified gait patterns based on video data (DeCann, Ross, & Culp, 2014), and revealed distinct running patterns in healthy adults based on 3D kinematics (Phinyomark, Hettinga, Osis, & Ferber, 2015). This suggest that unsupervised learning could be an appropriate method to distinguish walking from running and determine the degree of maturity in locomotor patterns. I investigated this in

children aged three-nine years old and used this approach to specify the development of running longitudinally assessed over a one to four years age range combining both kinematic and neuromuscular parameters.

Neuromuscular control of locomotion

Steering the kinematics and kinetics during walking and running involves approximately 600 skeletal muscles. Controlling each muscle individually would require enormous computational load from the central nervous system (CNS). The CNS is believed to circumvent this by utilizing muscle synergies, groups of muscles that receive a common neural output. There is a plethora of studies starting with Bernstein (1967) that support the notion that the CNS reduces the degrees of freedom of control task by building on muscle synergies (Bernstein, 1967; Bizzi & Cheung, 2013; d'Avella, Saltiel, & Bizzi, 2003; Ting & Macpherson, 2005).

By non-invasively recording the activity of a group of muscles involved in a movement, muscle synergies can be extracted and analyzed. Here, muscle synergies were employed to determine the neuromuscular control of walking and running in children under the age of nine and gained new insights into the development of neuromuscular control in early childhood. I defined muscle synergies by decomposing multivariate electromyographic (EMG) signals – a proxy for muscle activity – via non-negative matrix factorization (NMF) (Dominici et al., 2011; Lee & Seung, 1999; Rabbi et al., 2020; Steele, Rozumalski, & Schwartz, 2015; Tresch, Cheung, & d'Avella, 2006).

The conventional NMF approach (Lee & Seung, 2001) is to estimate weighting coefficients W and activation waveforms C by minimizing the Frobenius norm between the enveloped signals and the sum of the synergies ($W \cdot C$, i.e., weightings $\times$ waveforms),

$$\| E - (W \cdot C) \|_F = min$$

E represents the EMG envelopes, as an $m \times t$ matrix (m = number of muscles, t = time samples), the weighting coefficients W an $m \times n$ matrix (n = number of synergies), and C the activation waveforms ($m \times t$ matrix), see Figure 1.2.

The muscle weights provide information about which muscles are contributing to a muscle synergy and the activation patterns provide the temporal information about when in the gait cycle the muscles are active and for how long.

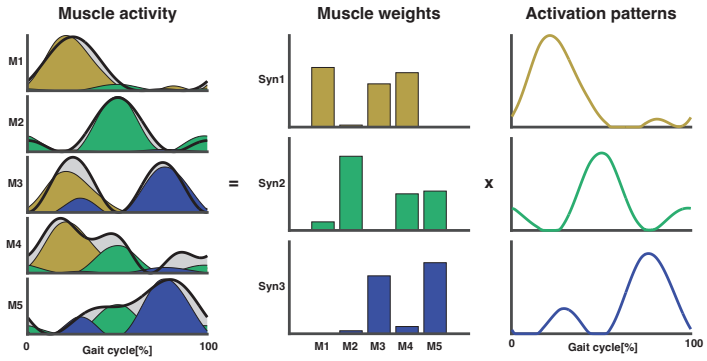

Figure 1.2: Schematic of muscle synergy extraction. Rectified muscle activity of five muscles (M1-M5; left) is decomposed into three synergies (syn1-syn3) comprising of muscle weights, (W; middle) and activation patterns (C; right). Each muscle contributes with a certain weight to each of the activation patterns illustrated with the shaded areas corresponding to each color of the synergies. As an example, M1, M3, and M4 are the contributors to the activation pattern of Synergy 1 (Syn1).

The decision about the number of synergies explaining the analyzed movement is often an arbitrary one. Meaning, the number of muscle synergies during movement analysis may differ based on the chosen methodology. Studies in adults have nonetheless found that five or less muscle synergies are involved with great consistency. This even holds during various types of locomotion such as level walking (Ivanenko, Poppele, & Lacquaniti, 2004; Kibushi, Moritani, & Kouzaki, 2022; Mileti et al., 2020), uneven walking (Santuz, Ekizos, Eckardt, Kibele, & Arampatzis, 2018), up or downhill walking (Dewolf, Mesquita, & Willems, 2020), direction changes (Chia Bejarano et al., 2017; Oliveira et al., 2013), perturbed walking (Chvatal & Ting, 2012; Hagedoorn, Zadravec, Olenšek, van Asseldonk, & Matjačić, 2022), walking at different speeds (Buurke, Lamoth, van der Woude, & den Otter, 2016; Kibushi, Hagio, Moritani, & Kouzaki, 2018), split-belt treadmill walking (Maclellan et al., 2014), running (Cappellini, Ivanenko, Poppele, & Lacquaniti, 2006; Oliveira, Gizzi, Ketabi, Farina, & Kersting, 2016; Santuz, Ekizos, Janshen, et al., 2018), and in older adults walking (Baggen et al., 2020; Monaco, Ghionzoli, & Micera, 2010). While healthy adults present with a stable number of muscle synergies independent of the type of locomotion the same cannot be observed in children learning to walk. When neonates are held over a stable surface to elicit their stepping reflex only two basic activation patterns are present (Dominici et al., 2011). Later, when taking their first independent steps, the two basic activation patterns are supplemented by two additional patterns that, combined with the two basic patterns, persist until adulthood (Dominici et al., 2011). This suggests that the number of synergies can be an indication of a mature walking pattern. A recent study found that four-year-old children who run display fewer muscle synergies than an untrained adult runner (Cheung et al., 2020). While the lower number of synergies in children running compared to untrained adults could be due to

immaturity of the running pattern, it may also be a result of co-contraction as well as an attempt to reduce the degrees of freedom available (Cheung et al., 2020).

Muscle synergy analysis can provide important insight into the neuromuscular control of running and informs about the differences between running and walking. In adults, it is established, that there is a shift in the timing of one muscle synergy related to the activation of the calf muscles which corresponds to a shorter stance phase (Cappellini et al., 2006; Yokoyama, Ogawa, Kawashima, Shinya, & Nakazawa, 2016). It is worth considering whether a similar pattern is present in children during the development and maturation of running. In fact, it has been observed that even during walking, the peak medial gastrocnemius activity shifts with increasing walking speeds in children aged 7-9 years from 45% at comfortable walking speeds to 25% at fast walking speeds in children aged 7-9 years but not older children (Tirosh, Sangeux, Wong, Thomason, & Graham, 2013).

In sum, studying muscle synergies, will provide insight into the neural capacity of children, with the synergy weights and activation waveforms revealing the motor control strategy used during a task, be that walking or running. Biomechanics, by contrast, which encompasses parameters, that represent the outcome of that strategy. By combining both, I expect to add to our understanding of the development of running in children aged 1-9 years.

Extending methods

Research on gait and running patterns in adults and children has been predominantly carried out in a laboratory setting designed for high-quality data acquisition including many strides (often required for synergy analysis). The latter usually involves a treadmill, and while locomoting on a treadmill is biomechanically like locomoting overground (van Ingen Schenau, 1980), treadmill requires habituation (Van Hooren et al., 2020). This certainly applies to very young children.

However, especially in children walking or running in a laboratory environment might not be representative of how they behave at home or on the playground. The main challenge with collecting data in their natural environment is that data quality recorded in natural environments might not match laboratory recordings. A central step in proper gait analysis is to detect stepping events, e.g., the moments at which the foot touches or lifts off the ground. In the lab this is realized via assessing ground-reaction forces that – if one can afford it – are integrated into a treadmill.

The shape of the vertical ground reaction forces can be estimated quite accurately from accelerometry (Horsley et al., 2021) or other wearable sensors, and neural networks is a promising tool to do so (Ancillao, Tedesco, Barton, & O'Flynn, 2018). I investigated the combination of accelerometers and machine learning in the form of artificial neural networks to first

predict ground reaction forces and, from this, the step events during walking and running in adults. Once a tool like that is developed, children's locomotion – especially their running development – can be investigated in children's natural environment in the future.

Research questions

In this thesis I will investigate the motor control of the development of running in children by combining neuromuscular and biomechanical measures using novel techniques and state-of-the-art-statistics. I structured my work along the following questions:

- **Q1.** How suitable are the common classifiers in running for children learning to run?
- **Q2.** How to determine the degree of maturity in locomotory patterns in children?
- **Q3.** What is the neuromuscular control of running in children?
- **Q4.** What is the longitudinal development of running in very young children?
- **Q5.** How can ground-reaction forces be estimated from shank accelerometer data?

Q1 & **Q2** are meant to reveal limitations of current analysis techniques and measures but first and foremost to provide solutions to overcome these limitations. With the suggested solutions at hand, answering **Q3** & **Q4** will contribute to our current understanding of the development of running in children. The answers to **Q5** will bring my scientific advances at step closer to the natural environment and real-life application.

Outline thesis

This thesis contains a set of experimental studies with the second and third chapters being cross-sectional, the fourth being longitudinal, and the fifth being exploratory in nature.

In the study summarized in **Chapter 2** I addressed the research questions **Q1** & **Q2**. I investigated whether the two most common classifiers of running are sensitive enough to classify mature running in children and subsequently combined these measures with more advanced statistical methods. In brief, I ranked locomotion patterns in children using clustering and, by comparing the locomotion patterns to those of adults, I determined their degree of maturity. To answer question **Q3**, in **Chapter 3** I focused on the neuromuscular control of the development of running in a cross-sectional design. I investigated the muscular activity and the number and structure of muscle synergies and related these findings to the ability to run with a flight phase. In the study underlying **Chapter 4** the aim was to elucidate the longitudinal development of running in very young children (**Q4**). I followed two children from their first independent steps until ~32 months since onset of independent walking and compare their locomotor patterns with those of adults. In this study I combined the knowledge gained on maturity of gait patterns with the knowledge gained on neuromuscular control. **Chapter 5**

answers question **Q5** by introducing a method to estimate vertical ground reaction force waveforms from accelerometer data to be able to accurately predict gait events. This method is the first step towards extending methods to the field.

The main findings are summarized in **Chapter 6** and further discussed against the literature.

Chapter 2

THE DEVELOPMENT OF MATURE GAIT PATTERNS IN CHILDREN DURING WALKING AND RUNNING

Bach, M.M., Daffertshofer, A., and Dominici, N.

Eur J Appl Physiol, 2021. 121(4): p. 1073-1085

Abstract

We sought to identify the developing maturity of walking and running in young children. We assessed gait patterns for the presence of flight and double support phases complemented by mechanical energetics. The corresponding classification outcomes were contrasted via a shotgun approach involving several potentially informative gait characteristics. A subsequent clustering turned out very effective to classify the degree of gait maturity.

Participants (22 typically developing children aged 2-9 years and 7 young, healthy adults) walked/ran on a treadmill at comfortable speeds. We determined double support and flight phases and the relationship between potential and kinetic energy oscillations of the center-of-mass. Based on the literature, we further incorporated a total of 93 gait characteristics (including the above-mentioned ones) and employed multivariate statistics comprising principal component analysis for data compression and hierarchical clustering for classification.

While the ability to run including a flight phase increased with age, the flight phase did not reach 20% of the gait cycle. It seems that children use a walk-run-strategy when learning to run. Yet, the correlation strength between potential and kinetic energies saturated and so did the amount of recovered mechanical energy. Clustering the set of gait characteristics allowed for classifying gait in more detail. This defines a metric for maturity in terms of deviations from adult gait, which disagrees with chronological age.

The degree of gait maturity estimated statistically using various gait characteristics does not always relate directly to the chronological age of the child.

Introduction

Running and walking – two everyday types of locomotion in humans – are distinguishable to the naked eye by obvious differences in kinematics and kinetics. When adults run, there is a well-defined flight phase during which none of the legs are in contact with the ground, unlike walking that comprises a double support phase during which both legs are on the ground together. It, therefore, comes as no surprise that the presence or absence of a flight phase is the most commonly used classifier to distinguish walking from running.

Turning to a more biomechanical perspective, walking may be modelled as an inverted pendulum swing: the center-of-mass (CoM) vaults over the stance leg (Alexander, 1976) resulting in peaks in the CoM trajectory during mid-stance and an out-of-phase exchange between potential and kinetic energies (Saibene & Minetti, 2003). Running, on the other hand, may be modelled as a spring, at least in adults: the stance leg compresses (Blickhan, 1989; McMahon & Cheng, 1990) resulting in a CoM trajectory with the lowest point at mid-stance and in-phase oscillations of potential and kinetic energies. In adults walking, the amount of saved energy, typically quantified as percentage of the recovered energy, is about 65% at the most optimal speed. In adults running, by contrast, the energy recovery does not depend on speed and fluctuates around 5% (Cavagna et al., 1964; Cavagna et al., 1976). This observation motivates an alternative and, by now, likewise accepted measure to distinguish walking from running, namely out-of-phase versus in-phase oscillations of potential and kinetic energies as well as the exchange between them.

In children, the ability to walk develops slowly from first independent steps to about 7 years of age, both in terms of mechanical energy and kinematics (Cheron, Bengoetxea, Bouillot, Lacquaniti, & Dan, 2001; Cheron, Bouillot, et al., 2001; Dominici, Ivanenko, Cappellini, Zampagni, & Lacquaniti, 2010; Hallemans et al., 2004; Ivanenko, Dominici, et al., 2004; Ivanenko, Dominici, Cappellini, & Lacquaniti, 2005; Ivanenko, Dominici, & Lacquaniti, 2007). It seems that efficient use of the pendulum mechanism during walking develops gradually, the recovery of mechanical energy is lower in toddlers during their first independent steps than in toddlers aged two and up who have more walking experience (Ivanenko, Dominici, et al., 2004), and it is much lower than in adults walking at comparable speeds (Hallemans et al., 2004).

Running in children is not as well researched. Vasudevan et al. (2016) showed that infants are able to take some steps with a flight phase when supported on a treadmill but that their kinematic patterns disagree with adult running. An earlier study in children running revealed instances in which the energy recovery exceeded 11% during slow running (Schepens, Willems, & Cavagna, 1998) and, hence, about twice as high as one may expect for running in adults. Since the corresponding experimental trials were excluded from further analysis, it

remains opaque whether or not exaggerated energy recovery values at slow speeds are part of the development of running. In any case, though, a mature and efficient walking pattern seems to develop gradually. This lets us believe that an equivalent gradual change should be visible in the development of running.

Current studies on energetics in children typically assessed over-ground locomotion with one or two strides recorded per trial (Ivanenko, Dominici, et al., 2004; Schepens, Bastien, Heglund, & Willems, 2004; Schepens & Detrembleur, 2009; Schepens, Willems, Cavagna, & Heglund, 2001). However, over-ground locomotion often introduces more variability in the gait speed than treadmill locomotion. Arguably, speed is easier to correct on the treadmill (Cavagna, Heglund, & Taylor, 1977), but certainly, one can record more strides per participant potentially providing more statistical power in the subsequent analyses. It is for that reason that we adopted this experimental design to answer: (i) how does running on a treadmill develop in children when running is defined as having a flight phase; and (ii) how does this change when defining running as the in-phase oscillations of kinetic and potential energies?

If 'proper' running in children is meant to resemble running patterns of adults in some sense, then the development of running implies an increasing *degree of gait maturity*. Yet, adult gait already comes with substantial variability, raising doubts as to whether identifying the presence of a flight phase or pinpointing phase relationship between the CoM's kinetic and potential energy will indeed provide a robust means to determine this degree of gait maturity. That is, while (i) & (ii) are relevant questions to ask, one may wonder whether or not the two characteristics they address suffice to quantify the (development of) running in children. In fact, the literature offers a plenitude of kinematic and kinetic parameters and other gait characteristics that might be informative about the gait maturity. We, therefore, supplemented flight phase presence and energy relationship by a large set of parameters that we chose based on previous studies that proved their capacity for categorizing gait patterns (Carriero, Zavatsky, Stebbins, Theologis, & Shefelbine, 2009; Courtine et al., 2009; Dewolf, Sylos-Labini, Cappellini, Lacquaniti, & Ivanenko, 2020; Dominici et al., 2012; Fortney, 1983; Friedli et al., 2015; Ivanenko, Cappellini, Dominici, Poppele, & Lacquaniti, 2007; Phinyomark, Petri, Ibanez-Marcelo, Osis, & Ferber, 2018; Roberts, Mongeon, & Prince, 2017; Van Hooren et al., 2020; Vasudevan et al., 2016; Wenger et al., 2016). Without informed pre-selection of parameters, however, such a shotgun approach faces the challenge that parameters may covary and – when combined – do not only yield redundant information but may cause a classification bias. Principal component analysis (PCA) is a common means to remove such covariation and, as such, it comes as no surprise that it has been applied extensively to identify types of locomotion in experimental settings (Courtine et al., 2009; Dominici et al., 2012; Friedli et al., 2015; Wenger et al., 2016). Here, we first applied PCA to rank-reduce our parameter set before clustering the parameters (DeCann et al., 2014; Phinyomark, Osis, Hettinga, & Ferber, 2015; Sherrill et al., 2005) to classify gait patterns in children by the degree they deviate from gait

patterns in adults. With this two-step procedure, we sought to answer (iii) if our 'blind' approach allows for pinpointing details of the development of gait in children, and whether it can serve to discriminate between mature and immature locomotion.

Methods

Participants

This study included 22 typically developing children aged 2-9 years and 7 young healthy adults as controls for mature patterns, where mature patterns here refer to adult performance. Exclusion criteria were known neurological and developmental diseases. Table 2.1 provides an overview of the relevant participant characteristics.

Table 2.1: Participant characteristics

	AGE (RANGE)	GENDER (M/F)	HEIGHT [CM]	WEIGHT [KG]
CHILDREN	26-106 months	10/12	122 (110-130)	22.5 (18.5-25.7)
ADULTS	22-28 years	4/3	180 (176-182)	69 (66-78)
MEDIAN (25TH-75TH PERCENTILE). AGE IS THE FULL RANGE				

The adult participants and the guardians/parents of the children provided written informed consent in compliance with the Declaration of Helsinki. The children provided assent. The experimental design was approved by The Scientific and Ethical Review Board of the Faculty of Behavioural & Movement Sciences, Vrije Universiteit Amsterdam, Netherlands (File number: VCWE-2016-149R1).

Setup

The experiment consisted of comfortable walking and running on the treadmill. Every condition was recorded for a minimum of 20 strides where possible and for maximum 100 strides.

Participants could familiarize themselves for several minutes on the treadmill during which walking and running were practiced. No set time was imposed. Subsequently, the comfortable speed was determined for both walking and running conditions by starting at a slow speed and increasing in intervals of 0.1 km/h until the participant reported a comfortable speed. In the following, the walking and running conditions refer to the prescribed condition that the participant was asked to perform (i.e., walking and running) during the specific recording.

Children participants wore a full body climbing harness (CAMP Bambino Full Body Harness, CAMP USA, Colorado) modified to also have a secure attachment point on the back. All participants wore their own shoes for the duration of the experiment.

Data acquisition

Kinematic data were recorded using an active marker system (Optotrak Motion System, NDI Measurement Sciences, ON, Canada) at 100 Hz. A camera was placed diagonally behind the treadmill on either side and one camera was placed diagonally in front on the right-hand side of the participant. Single markers were attached to the skin overlying the following bony landmarks on the right head of 5th metatarsal, right lateral malleolus (LM), right lateral femoral epicondyle (LE), and right greater trochanter (GT), right and left calcaneus (HE), right and left glenohumeral joint, right and left lateral humeral epicondyle, and right and left ulnar styloid. Kinematics of the right and left upper limbs were of poor quality and did not allow for further analysis. Kinematics could not be recorded in all participants (see *Supplementary Material* 2.3).

Vertical, mediolateral, and forwards ground reaction forces (F_v, F_{ml}, F_f GRFs) were sampled at 1 kHz for each belt via the two force plates in the instrumented dual-belt treadmill (Motek Medical BV, Culemborg, the Netherlands).

Foot switches (piezo-resistive pressure sensitive sensors: Zerowire; Cometa, Bareggio, Italy) were placed on the skin on the heel and the head of the first metatarsal underneath the right and the left foot and were secured with tape where necessary. Shoes and socks were placed over the foot switches. The foot switch signals were sampled at 2 kHz. Full-body electromyography recordings were made but not analyzed here. Kinematics, ground reaction forces, and foot switch data were synchronized. At the end of the recording session, anthropometric measurements were taken for every participant. These included mass (m) and stature of the participant as well as the lengths of the main body segments.

Data analysis

Flight and double support phases

Step events (heel strike and toe-off bilaterally) were determined based on the kinetic and kinematic data. The vertical ground reaction forces (F_v) were pre-processed with a Savitzky-Golay polynomial filter (3rd order, 121 samples; Savitzky & Golay, 2002). We defined heel strike (HS) and toe-off (TO) events as the first samples crossing a fixed threshold ($\mathrm{mean}(F_v)/10$). First and last HS and TO were excluded for further analysis to avoid transients. The HE markers in the vertical direction served to detect step events from the kinematics (Roerdink, Coolen, Clairbois, Lamoth, & Beek, 2008). The foot switch detection was based on a simple 'on/off' algorithm. All events were manually inspected, and events were added or removed when needed (e.g., when dragging/jumping). Events were primarily detected based on the F_v, but we supplemented with events based on kinematic and foot-switch detections whenever single foot GRF data were missing or did not allow for event detection. All relevant data were re-sampled to 1 kHz for this application. From the step events, we

determined double support and flight phases as well as the corresponding means and standard deviations over all strides per participant and condition. We also computed the walking Froude (Alexander & Jayes, 1983) for all participants and conditions based on the treadmill speed and leg length using:

$$Fr = \frac{v^2}{g \cdot l}$$

Potential and kinetic energies

The combined forces from the right and left force plates of the treadmill served to estimate the kinetic (E_k) and potential energy (E_p) of the CoM in the sagittal plane, following Cavagna (1975); Ivanenko, Dominici, et al. (2004); Saibene and Minetti (2003); Schepens et al. (2004); Schepens and Detrembleur (2009). For full calculations see *Supplementary Material* 2.1. In brief, the kinetic energy E_k was estimated based on the CoM's velocity in the vertical and the forward directions. Here, we would like to note that changes of kinetic energy in the mediolateral direction are usually much smaller than those observed in the vertical and forward directions (Tesio, Lanzi, & Detrembleur, 1998; Tesio & Rota, 2019), and that the lateral work can be assumed less than 10% of total work. That is, lateral components can be considered negligible (Schepens & Detrembleur, 2009). The potential energy E_p was determined via the CoM's position in the vertical direction by integrating the corresponding velocity. Then, we estimated the Pearson correlation coefficients r between E_k and E_p for each stride to quantify the degree of in-phase and out-of-phase oscillations of the energies.

To quantify the amount of mechanical energy that can be saved via a pendulum mechanism (see Introduction) we determined the relative recovered mechanical energy as (Cavagna et al., 1976):

$$R = 1 - \frac{W_{\text{ext}}}{W_f + W_v}$$

where the external work (W_{ext}) was based on the sum of $(E_k + E_p)$-increments over a stride and the work in forward and vertical directions (W_f and W_v) on the sum of increments of the forward and vertical CoM energies, respectively (Cavagna et al., 1976).

PCA and clustering

Based on the kinetics and right-side kinematics, numerous spatiotemporal, kinetic, and kinematic parameters were calculated that provided a comprehensive quantification of gait features. In total 93 parameters were determined for every participant when kinematic measurements were available (*n* = 18 participants; 13 children and 5 adults). The parameters can be split into themes that represent modalities of gait. To build on the findings of the ability to

run with a flight phase and have in-phase oscillations of potential and kinetic energies during running, we supplemented these parameters with additional temporal features (in total 9 parameters), additional features of the pendulum/swing mechanisms (in total 11 parameters), limb endpoint trajectories (12 parameters), stability measures (3 parameters), segmental and joint angles (21 parameters) and velocities (9 parameters), kinetics (6 parameters), intra-limb coordination (2 parameters), intersegmental coordination (14 parameters), and interlimb coordination (6 parameters). By including parameters from several strides per participant, we implicitly incorporated the variance across strides as this is a common measure for gait variability. For a detailed list of parameters see *Supplementary Material* 2.2. We normalized the parameters that were directly related to the size of the participant to body-size/body weight (e.g., step length, step height, vertical force; see *Supplementary Material* 2.2 for details). All the parameters were combined in a [(number of participants × condition × number of strides) × number of parameters] matrix [1530 × 93] and z-scored along the first dimension prior to PCA. As outlined above, PCA primarily served to rank-reduce the parameter matrix, which eliminates parameter covariations and, by this, allows for an unbiased classification via conventional clustering (see below). We selected the leading three principal components (PCs) as they turned out to suffice for our classification purposes (Courtine et al., 2009; Dominici et al., 2012; Friedli et al., 2015; Phinyomark, Osis, et al., 2015). To which degree the different 93 parameters influenced the first three PCs can be given by the corresponding $\text{loadings} = u \cdot \sqrt{\lambda}$, where u denotes the eigenvector of a PC and λ its eigenvalue. We considered a parameter a strong contributor to a PC when its loading exceeded the 95% confidence threshold $CI_{95} = 1.96/\sqrt{n}$, with n = 93.

Finally, we applied hierarchical clustering. In doing so, we first built a dendrogram or cluster tree (Milligan, 1980; Murtagh & Contreras, 2011; Xu & Wunsch, 2005) using average links (unweighted pair group method with arithmetic mean) based on the correlation distances across the 3D reduced parameter set (we also tested other distance measures, like Euclidean and Mahalanobis distances, but none of them yielded comparably proper clusters). The dendrogram was thresholded based on the cophenetic correlation coefficients (CCC; Sokal & Rohlf, 1962) and, for comparison, also by visual inspection, with the latter focusing on both categorization of walking versus running and classification of mature and immature locomotion. To distinguish mature from immature locomotion, we computed the average pairwise correlation distance from every participant belonging to a distinct walking cluster to the adults walking and from every participant belonging to a distinct running cluster to the adults running. Put differently, the correlation distance measures gait maturity with the adult gait pattern as reference.

Statistics

We assessed the influence of age on the presence of a flight phase (FP) during running, as well as the influence of age and condition on the presence a double support (DS) phase. For this, we used two linear regression models across both children and adults, the first one with FP as response variable and age as predictor, the second one with DS as response variable and age, condition, and the interaction between the two as predictors. For both models we considered $p < 0.05$ statistically significant.

We quantified the age-dependence of the correlation coefficients r and of the relative recovered energy R by least squares fitting exponential functions $a \cdot e^{-1/\tau(age-\gamma)} + b$, where τ was the time constant, and a, b, γ three constants, and report their explanatory power, in terms of adjusted R^2-values, unless specified otherwise.

Results

Although 29 participants were included in the analysis on the mechanical energies of the CoM, only 18 participants were included in the analysis of the effects of kinematic and kinetic parameters on distinguishing mature from immature gait and walking from running. All participant characteristics, as well as the numbers of strides included in each part of the analysis can be found in *Supplementary Material* 2.3. It is worthwhile adding that the minor differences between stride numbers relate to the quality of the data varying between datasets. The youngest participants that we recorded (< 50 months of age) were all locomoting with handhold from the experimenter or parent/guardian. We confirmed that this did not affect the kinetics post-recording.

Flight and double support phases

We expressed FP and DS relative to the gait cycle (Figure 2.1a). For the running condition, a FP was present in some participants and the linear regression revealed a significant effect of age ($p < 2 \cdot 10^{-16}$), i.e., FP increased with age. DS revealed main effects of both age and condition ($p < 2 \cdot 10^{-16}$, $p = 0$, respectively), and it decreased for running. We also found an interaction effect ($p = 5.8 \cdot 10^{-6}$) as summarized in Table 2.2. The normalized speeds given as Froude values differed between conditions for all participants; see Figure 2.1b.

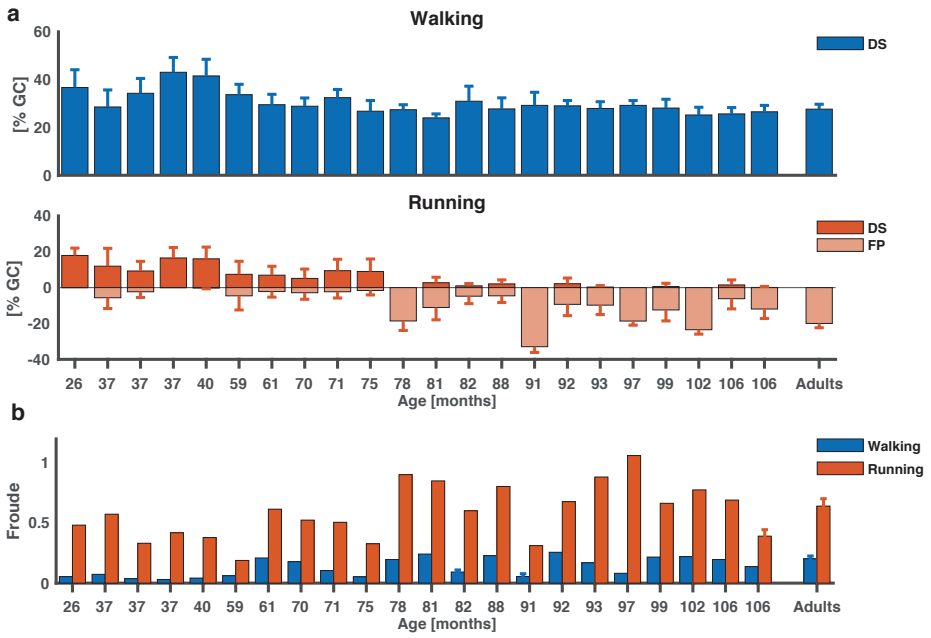

Figure 2.1: Temporal patterns during walking and running and normalized speed. a) Double support phase (positive numbers) and flight phase (negative numbers) expressed as a percentage of the gait cycle (mean± SD) for walking (upper panel) and running (lower panel), as a function of age (months-rounded to the nearest whole integer) for each child participant and adults as a grand average. b) Normalized speed expressed as the Froude value ($v^2 / g \cdot l$) for each participant and condition (walking in blue and running in red). Error bars signify standard deviations between participants for adults and differences between trials for the walking condition of the participants of 82 and 91 months and running condition for the second participant of 106 months.

Table 2.2: Linear regression of the effects of age and condition on double-support and flight phases

	FACTOR	ESTIMATE	SE	t	p-VALUE
DS	Intercept	31.03	0.26	117.50	0
	Age	-0.01	0.00	-9.57	<2·10-16
	Condition_Running	-24.40	0.38	-64.35	0
	Age:Condition_Running	-0.01	0.00	-4.54	5.8·10-6
FP	Intercept	4.63	0.38	12.24	<2·10-16
	Age	0.06	0.00	25.62	<2·10-16

Abbreviations: DS, double support; FP, flight phase; SE, standard error; t, t-statistics

The corresponding stick figures, vertical hip displacements, and knee joint angles of four representative participants are presented in Figure 2.2. For all participants, the vertical GT displacement (GT_v) was maximal during mid-stance of the load-bearing leg, adhering to the double-peaked profile of the pendular mechanism of the CoM during walking. During running, the GT_v was minimal during mid-stance of the load-bearing leg, suggesting a spring leg behavior of running. However, this was only present in the three oldest participants. In the youngest participants during running, GT_v was maximal at mid-stance. In Figure 2.2, GT_v and the knee joint angle for five strides for each of the displayed participants show a less pronounced pattern in the youngest participants compared to the adult, which suggests a more immature gait pattern in the younger participants and a mature one for the adult participant.

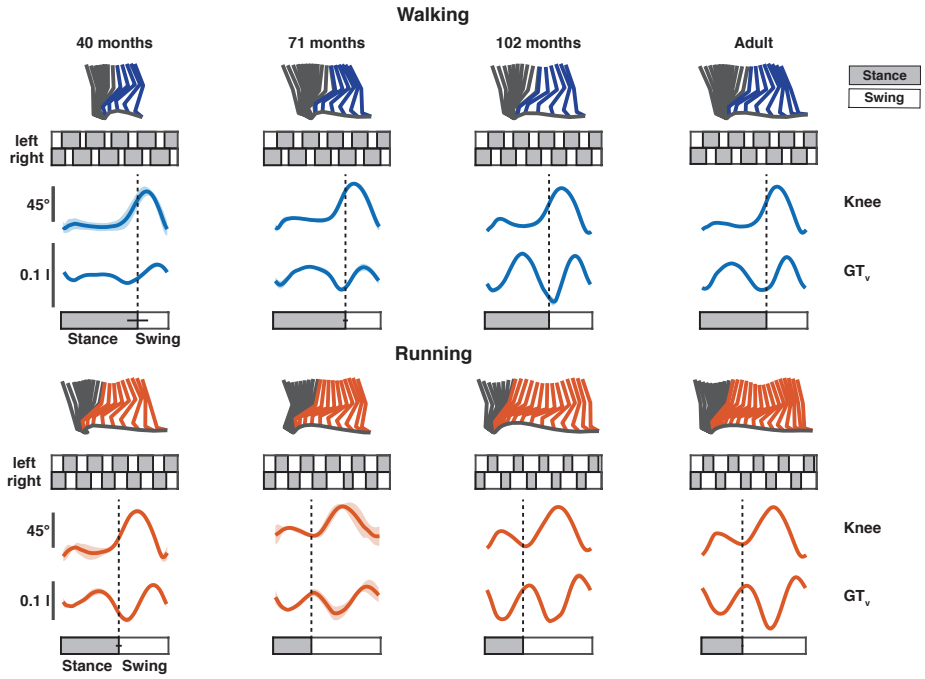

Figure 2.2: Kinematics during walking and running. Stick figures of representative strides of four representative participants during walking (upper panel) and running (lower panel). The black parts of the stick figures correspond to stance phase and the colored to the swing phase (blue for walking; red for running). Below, five representative strides are presented for each participant for left and right leg. Ensemble averages (±SD of five gait cycles) of knee joint angle and vertical hip displacement (GT_v) for each participant and condition. Gait cycle bars represent mean stance and swing duration for each participant with the horizontal black bar representing the standard deviation between strides. GT_v is expressed in relative units (normalized by the limb length l).

Potential and kinetic energies

We found a moderate exponential relationship between age and the correlation coefficients r for walking and running (R^2 = 0.53, R^2 = 0.51, respectively; Figure 2.3a), while the relative recovered energy R was strongly correlated with age for both walking and running (R^2 = 0.59, R^2 = 0.70, respectively; Figure 2.3b).

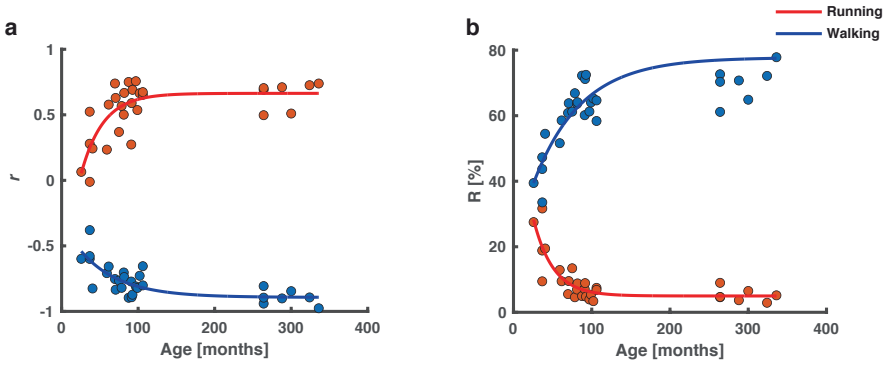

Figure 2.3: Effects of the mechanical energy of the CoM on age. a) The correlation coefficient r between E_k and E_p as a function of age for walking (blue) and running (red). There is an exponential relationship between age and r for both walking and running. b) The relative recovered energy R as a function of age for walking (blue) and running (red). There is an exponential relationship between R and age for both walking and running.

Shotgun and clustering

The first three PCs accounted for 57% of the total variance of the data while this might be considered a low proportion in conventional PCA, one has to realize that we z-scored the input variables which let us consider three PCs to cover a sufficient portion of data variance. The scatterplots in Figure 2.4 illustrate the separation between the prescribed walking and running patterns (filled and unfilled markers, respectively) with clear correlations illustrated in the PC1/PC2 plane. The loadings associated with these three PCs revealed that all parameters except for three were significantly larger than the 95% confidence interval, and thus uniformly influenced the variance in the data. The three exceptions were parameters 75, 76, and 82 (cf., *Supplementary Material* 2.2 and 2.4).

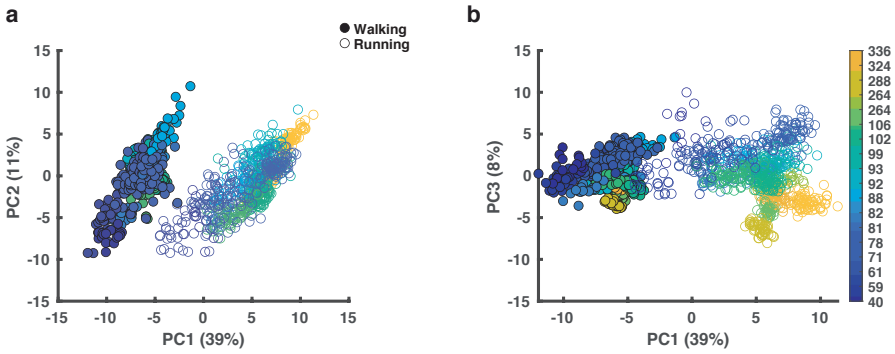

Figure 2.4: Principal component analysis (PCA) outcomes for walking and running. A) The outcome of the PCA in PC1-PC2 space. B) The outcome of the PC1-PC3 space. Each dot represents a stride and the color-coding refer to the age in months of the participants. The filled circles are the prescribed walking condition and the un-filled circles are the prescribed running condition.

The average linkage and correlation distance had a CCC of 0.92. There were no clear distinctions between the number of clusters when analyzing dissimilarity values. However, visual inspection of the dendrogram indicated that either four or eight clusters adequately represented the original data (see *Supplementary Material* 2.5). A Calinski Harabasz stopping rule (Milligan & Cooper, 1985) applied for 1-10 clusters confirmed this split, at least in parts, as it revealed two of the four clusters. Since we aimed for distinguishing mature from immature patterns as well as walking from running patterns, we continued with the four clusters identified visually.

In Figure 2.5, each of the clusters is represented with the relation every participant had to them. We expected adults to have a mature walking and running pattern and, accordingly, we grouped them together as a single node (indicated as 'A' in Figure 2.5). The thickness of the lines represents the percentage of strides, larger than 5%, belonging to a certain cluster. Every cluster is plotted in an individual color. Cluster 1 contained the adults running and 94.7% of the running strides from the participant aged 93 months. Cluster 2 contained between 74.6% and 100% of all prescribed running strides from the participants aged 71 to 106 months bar the participant of 93 months (5.3% of the strides from this participant belonged to cluster 2), together with around 50% of the prescribed running strides from the participants of 62 and 59 months. Cluster 3 covered between 42 and 100% of the prescribed walking strides from the participant aged 62 months to the adults and 16.1% of the walking strides from the participant of 59 months. Finally, cluster 4 contained around 50% of the prescribed running strides from participants of 59 and 62 months, 25% of the prescribed running strides from the participants of 71 months and all prescribed running and walking strides from the participant of 40 months, together with some walking strides from older participants, most

importantly, around 80% of walking strides from the participant of 59 months, around 50% of the walking strides from the participants aged 82, and 40% of the walking strides of the participant of 106 months (see *Supplementary Material* 2.6 for further details on the spread of strides into every cluster).

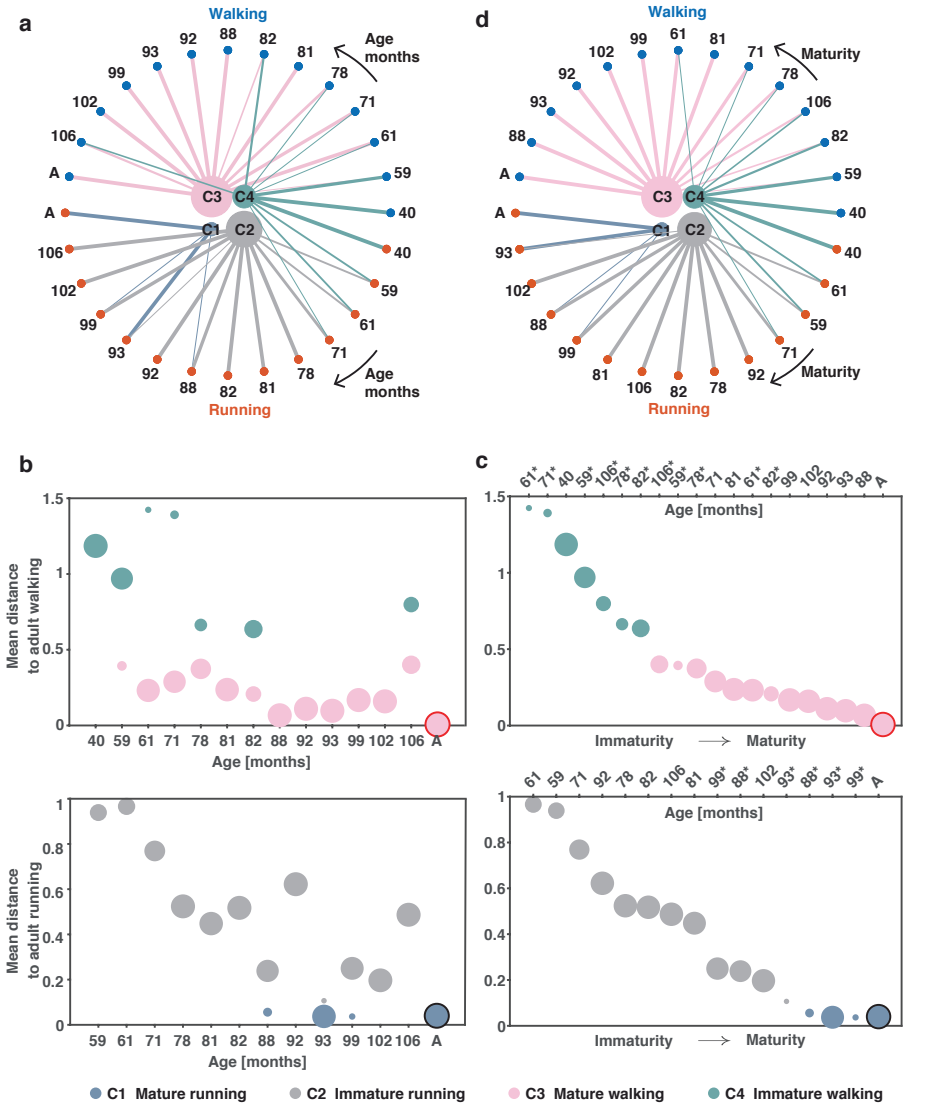

Figure 2.5: Clustering output. a) Output of clustering ordered based on age (months), with the youngest participant on the right side and the adults (A) on the left side for walking (blue circles) and running (red circles). The size of the clusters (C1-C4) depends on the amounts of strides belonging to each cluster, similarly the thickness of the lines connecting each cluster with a participant depends on the

percentage of data from each participant belonging to that cluster. b) Calculated average pairwise correlation distance to the mature walking patterns of the adults (A) (upper panel) and to the mature running patterns of the adults (A) (lower panel) as a function of age. c) Calculated average pairwise correlation distance to the mature walking patterns of the adults (A) (upper panel) and the mature running patterns of the adults (A) (lower panel) as a function of gait maturity. The upper axis in both plots represents the age of the participants in months (rounded to nearest whole integer). Note that the increase in age is not monotonic as it is a function of gait maturity (immature from left going to mature on right). Note also that the lower axis in both plots is not in units of the correlation distance (which is shown on the y-axis) but set to arbitrary values (indices of sorting); that is, the seeming exponential decay should not be interpreted as such. Color notation is the same as in a), C4 represents immature walking, C3 represents mature walking, C2 represents immature running and C1 represents mature running. The size of the circles depends on the amounts of strides belonging to each cluster. d) Output of clustering based on maturity with the least mature patterns on the right side and the most mature (adults - A) on the left side. For a full overview of the percentage of strides belonging to each cluster, see Supplementary Material 2.6.

As shown in Figure 2.5a, the younger children were grouped in separate clusters from the adult participants. The average pairwise distance to the adult patterns for walking and running separately, i.e., our measure for gait maturity is depicted in Figure 2.5b. Obviously, there was no directed relationship between our measure of gait maturity and the participants' age. To illustrate this further in Figure 2.5c, we ordered participants based on their respective distance to the mature pattern of the adults depending on whether their strides fall into the walking or running clusters, but here we also included the corresponding ages on the top x-axes. The participant of 40 months is only present in the walking clusters as the strides belonging to the prescribed running conditions are clustered with the walking strides of the other participants. Some participants are present twice as their strides fall into more clusters (see above). In Figure 2.5d, the order of the participants has been re-arranged following the maturity order in Figure 2.5c. When a participant had strides falling into two clusters, they were ordered based on the position in which most of their strides belong to.

Discussion

The aim of this paper was to investigate the development of running on a treadmill. Gait classification traditionally relies on the presence of a flight phase or the display of in-phase oscillations of kinetic and potential energies during running. Expectedly, both measures have their limitation in quantifying subtle changes in gait patterns. Hence, we supplemented them by a substantial set of alternative gait characteristics and followed a statistics-based classification of walking and running and the development thereof.

Not all children were able to run with a flight phase. Their running patterns clearly differed from that of adults, but also from (their own) walking. As such, their prescribed running should not be classified as walking. We found exponentially saturating changes in the correlation between kinetic and potential energies and the total amount of recovered mechanical

energy, implying there were in-phase oscillations of kinetic and potential energies during running and out-of-phase oscillations during walking. On top of that, our cluster analysis revealed the absence of a direct relationship between chronological age and maturity of the (prescribed) walking and running patterns in children aged 40-106 months.

Flight and double support phases

Running can be defined as having a flight phase. We showed that young children who are asked to run on a treadmill at comfortable speeds are not able to do so. This might be interpreted as they are in fact not running. At first glance, the gait patterns remind one of walking, but a closer look reveals that they are not walking either. It seems that children learning to run make use of what could be called a "walk-run strategy" that contains both double support and flight phases. The (relative) duration of the double support phase in running, is of course not comparable to that seen in walking. Interestingly, this also extends to the in-phase and out-of-phase oscillations of kinetic and potential energies.

Potential and kinetic energies

We already mentioned in the introduction that Schepens et al. (1998) studied running in children aged 2-16 years. In that study all trials were excluded in which the relative energy recovery R exceeded 11% as they were deemed not to be running trials. This is unfortunate as our finding support the idea that in the learning period the gait is a mix of a walking and a running pattern. That is, R may occasionally exceed 11% during running, in our case in six participants. When incorporating the correlation coefficients r, however it is still possible to distinguish between conditions for all participants as the potential energy oscillates out-of-phase for the walking conditions (r being negative) and in-phase for the running conditions (r being positive). In fact, the two types of locomotion (walking and running) are different in speed for all participants in our study (see Figure 2.1b and *Supplementary Material* 2.1), and despite the young participants sometimes running with double support phase, this is still different from the double support phases observed in the walking condition.

Yet, we have to admit that the overall findings in the energetics, with the exponential relationships between R and r and age are mostly influenced by the youngest participants. It seems that the energetics are not fine-grained enough to distinguish between older children and adults and thus will not reveal how running matures from children older than 3.5 to adults.

Shotgun and clustering

Chronological age and gait maturity of treadmill locomotion are not directly related in children aged 3.5-9 years old. Maturity of one type of locomotion is also not directly linked to that of the other type of locomotion and as such, a child can display mature walking, but not

mature running and vice versa. We defined gait maturity as the pairwise correlation distance from adult patterns and thus used the mean of the adult walking and running patterns, respectively, as a reference for mature patterns. This allowed us to rank participants based on their individual distance to the mature patterns of walking and running, separately.

These results appear more complete, indeed, when compared to those on flight phases and energetics only. We are, therefore, inclined to argue that a shotgun approach with proper pattern classification can provide additional insight in the development of running in children. In an earlier study, Phinyomark, Osis, et al. (2015) already showed that two distinct kinematic running patterns in adults running can be identified combining PCA and clustering analysis on separate kinematic waveforms. In our eight-cluster analysis, we found one adult with a separate running pattern from all other participants and this finding could be related to differences in the running pattern (see *Supplementary Material* 2.5). However, we here considered the adult group as a single group as, despite differences between adults they display a 'mature' pattern, and as such we chose the four-cluster result as the main result.

We 'blindly' selected 93 parameters, with which we succeeded to categorize gait patterns and classify their change in the course of development. The obvious next step is to identify which of these parameters have significant contributions to the classification. One can in fact isolate subsets of the parameter by their contribution to principal components (see e.g., Kaptein et al., 2014). In doing so, we found that the temporal parameters (such as flight phase/double support phase) and pendulum/swing mechanisms (e.g., the oscillations of kinetic and potential energies) do greatly influence PC1. However, others were also adding to it, like leg/joint velocities and limb endpoint velocities. That is, when it comes to the time course of development, many if not all these parameters seem to covary, a fact that of course also extends to PC2 and PC3. From the composition of PC1 one may conclude that – albeit important – the mere presence of flight phase and in-phase oscillations of potential and kinetic energies does not suffice to distinguishing walking from running. More information is needed to pinpoint the (type of) gait pattern and define its degree of maturity. Yet, one has to realize that in our gait classification PCA primarily served for rank reduction followed by hierarchical clustering. Isolating relevant parameters in the space spanned by three principal components for their contribution to the correlation distance based hierarchical clustering is clearly less trivial. Here we hope for future work to provide rigorous methods to determine which specific parameters play a role for each of the clusters; more advanced statistical models like genetic algorithms may help with this. Only if this or alternative methods will succeed, can our shotgun approach not only 'describe' the change of gait patterns, but may serve as unbiased means to determine which parameters are crucial for this change.

Limitations and choices

In the current dataset participants of around 4 years of age are absent due to recruitment or measurement issues. This leaves a relatively large gap of 19 months between the child of 40 months and the child of 59 months. We do not expect our outcomes to change qualitatively when that gap is filled, but without a doubt it can provide further information on the maturity of locomotion in the younger children.

The type of locomotion referred to throughout this paper is the prescribed locomotion and this means that despite asking the children to run and either them or their parent/guardian confirmed it as running, they might not have been able to run as they would have over ground. Despite this potential limitation, we are positive that –in our experiments– the prescribed running patterns were not like those one would expect for walking or even fast walking.

Our participants were walking and running on a treadmill at a constant comfortable speed during the whole trial, with the advantage that the amounts of strides analyzed for each condition varied between 15 and 76 strides (*Supplementary Material* 2.3). This is in contrast to most other studies on the mechanics of locomotion where participants walk or ran over ground and thus did not record more than two or three steps per trial with up to ten trials per participant (Ivanenko, Dominici, et al., 2004; Schepens et al., 2004; Schepens & Detrembleur, 2009; Schepens et al., 1998) amounting to a 10-15 strides per participant. Moreover, it is more difficult to control the speed of the participant when locomoting over ground compared to on a treadmill and as such more fluctuations in the speed of the participant are expected. Speed fluctuations are important to account for when analyzing the energetics during average locomotion (Cavagna et al., 1977).

A final note on data 'pre'-processing: Prior to performing PCA, data were z-scored along the first dimension. The normalization of parameters across strides results in the adult values not skewing the PCA and cluster analysis in terms of amplitude. When looking at Figure 2.4, it seems that the variability between and within participants was not larger in the older children than in the adults, arguably due to the normalization. Variability within participants hence appears an unlikely cause for larger correlation distances from the young children to the adults in our clustering approach. Moreover, not all parameters were normalized to body-size/body weight (see *Supplementary Material* 2.2) prior to the z-scoring, PCA, and subsequent clustering. The ones that were normalized directly relate to the size of the participant (e.g., step length, step height, vertical force), whereas for example joint and segmental angles are already considered dimensionless (see e.g., Hof, 1996). One may argue, however, that (almost) all the parameters might have been influenced by both the participants' size and the speeds performed. Yet, there were several instances of a single participant being split into

more than one cluster, while maintaining the same speed. We hence do not believe that speed or body size were influencing factors in our cluster results.

Kinematic and kinetic parameters are influenced by neural factors and vice versa. A recent comprehensive review on the neural circuitries and biomechanics of walking and running in development (Dewolf, Sylos-Labini, et al., 2020) showed that running patterns mature during childhood but that the underlying mechanisms are still not thoroughly investigated. Here, we give some insights into the underlying kinematics and kinetics of this development. However, we did not investigate the muscular components as part of this study. We know from adults that the muscle activity patterns differ between adults walking and running and that there is a reduction in the duration of contraction with age for both the medial gastrocnemius muscle in walking for typically developing children (Cappellini et al., 2016; Tirosh et al., 2013), as well as in the thumb adductor during pinching movements (Dayanidhi, Kutch, & Valero-Cuevas, 2013). These findings suggest that the immature locomotor patterns found in this study could be correlated to increased contraction time. A recent study in children with cerebral palsy showed that it was possible to change their kinematic gait patterns without influencing their selective motor control (Booth, van der Krogt, Harlaar, Dominici, & Buizer, 2019). However, whether this also applies to typically developing children should be confirmed with further analysis of the muscle activity signals. Another recent study investigating muscle activity patterns during running in preschoolers and adults with different training experience revealed substantial developmental and training-related plasticity suggesting a long-term reorganization to satisfy the biomechanical changes and functional requirements of locomotion (Cheung et al. 2020).

Conclusion

Clustering revealed that there is no direct agreement between chronological age and maturity in young children walking and running when comparing their gait patterns to those of adults. When learning to run, young children make use of a “walk-run-strategy”. This strategy provides the ability to run with a combination of strides with double support and flight phase and yields in-phase oscillations of potential and kinetic energies.

Supplementary Material 2.1

The following illustrates the steps taken to calculate the relevant energetic parameters.

First, the acceleration (a) of the center-of-mass (CoM) was calculated in the sagittal plane:

$$a_f = \frac{F_f}{m} \quad (1)$$

$$a_v = \frac{F_v}{m} - g \quad (2)$$

Where, F = Ground reaction forces, f = forward, v = vertical, m = body mass, g=9.81ms$^{-2,}$ gravitational acceleration.

Next, we calculated the velocity of the CoM in the sagittal plane:

$$v_i = \int a_i \, dt + c_i \quad (3)$$

Where *i* denotes either the forward, or vertical direction, c_i is the integration constant. The integration constants were found by calculating the mean speed of the GT marker on the assumption that GT is close to the CoM and so the corresponding velocity is equal to the mean speed of the CoM.

The instantaneous kinetic energy E_k of the CoM was then defined as:

$$E_k = \frac{1}{2} m \, v_f^2 + \frac{1}{2} m \, v_v^2 \quad (4)$$

Kinetic energy comprises of the vertical and forwards components computed in (3). The instantaneous potential energy E_p of the CoM was given as:

$$E_p = mg \int v_v \, dt + c \quad (5)$$

The integration constant *c* is arbitrary and was taken equal to 0.

The total mechanical energy of the CoM E_{tot} was the sum of E_k and E_p waveforms over a stride:

$$E_{tot} = E_k + E_p \quad (6)$$

The positive external work W_{ext} was calculated as the sum of increments of E_{tot} over a stride (Cavagna et al. 1976). As well as the forward work W_f and the vertical work W_v were computed as the sum of increments of E_f and E_v, respectively:

$$E_f = \frac{1}{2} m v_f^2 \tag{7}$$

$$E_v = E_p + \frac{1}{2} m\, v_v^2 \tag{8}$$

Finally, the percentage recovery R introduced by Cavagna et al. (1976) estimate the ability to save mechanical energy and was determined as:

$$R = 1 - \frac{W_{ext}}{W_f + W_v} \tag{9}$$

Since W_{ext} may depend on stride length and on the participants' anthropometry we normalized it via

$$W_{\text{ext}} \rightarrow \widehat{W}_{\text{ext}} = \frac{1}{m \cdot d} W_{\text{ext}}$$

where, m denotes the participant's body mass and d the stride length.

As a measure of the variability between strides we computed the standard deviation of r denoted by $\sigma(r)$. There was a moderate exponential relationship between age and $\sigma(r)$ of both walking and running (R^2 = 0.67, R^2 = 0.57, respectively; Figure S2.1a), whereas W_{ext} did not correlate with age (R2 = 0.16, R2 = 0.02, walking and running, respectively; Figure S2.1b).

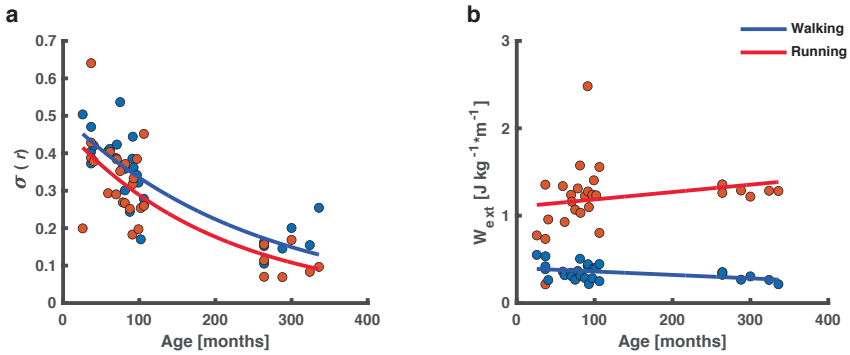

Figure S2.1: Effects of variability of the correlation between mechanical energies of the CoM and external work on age a) The variability of the correlation between E_k and E_p, $\sigma(r)$, as a function of age for walking (blue) and running (red). There is an exponential relationship between age and $\sigma(r)$ for both walking and running. d) The external work as a function of age for walking (blue) and running (red). There is no linear relationship between the external work and age for walking and running.

Effect of speed

Children of different sizes and adults ran and walked at different speeds and thus we correlated the measures to the Froude number, i.e., to the dimensionless speed. The Froude number is a measure for speed normalization across participants of different sizes. It is given by (Alexander & Jayes, 1983)

$$Fr = \frac{v^2}{g \cdot l}$$

here, v denotes the speed, g = 9.81ms^{-2} is the gravitational constant and l is the participant's leg length and measured as thigh (GT–LE) plus shank (LE–LM) length.

For the analysis of r, R, $\sigma(r)$, and W_{ext}, linear and exponential curves were fitted as appropriate to investigate the relationships with age and the normalized speed (walking Froude number), respectively. The adjusted R^2-value will be reported unless specified otherwise.

The spread in speeds was not (entirely) age dependent, as can be observed in the overlap of the lightest and darkest colors dots in Figure S2.2. The correlation coefficient r between E_k and E_p during walking and running was weakly correlated to the Froude number (R^2 = 0.31 and R^2 = 0.22, respectively; Figure S2.2a). There was no relationship between $\sigma(r)$ and the Froude number for running (R^2 = -0.02), although there was a weak to moderate relationship between $\sigma(r)$ and the Froude number during walking (R^2 = 0.36 Figure S2.2b). Furthermore, we found a moderate relationship between R and walking (R^2 = 0.58), while we could not identify any relationship between the R and the Froude number during running (R^2 = 0.133; Figure S2.2c). Likewise absent was a relationship between W_{ext} and the Froude number during walking and running (R2 = 0.14, R2 = -0.00, respectively; Figure S2.2d).

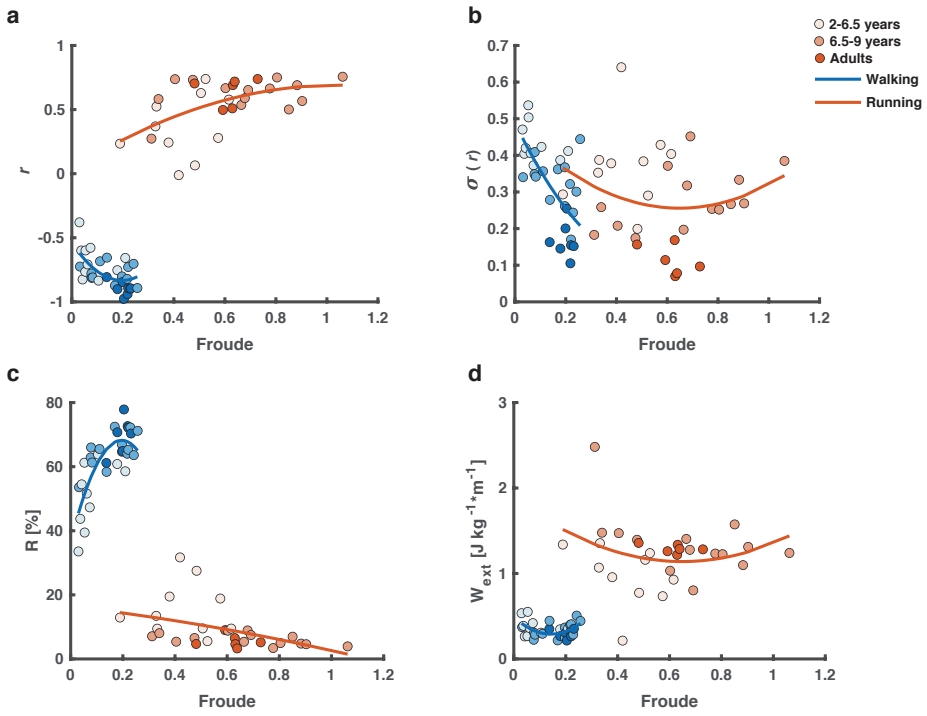

Figure S2.2: Effects of the mechanical energy of the CoM on dimensionless speed (Froude number). a) The correlation coefficient r between E_k and E_p as a function of the Froude number for walking (blue) and running (red). There is a second order polynomial relationship between the Froude value and r for both walking and running. b) The variability of the correlation r between E_k and E_p, $\sigma(r)$, as a function of the Froude number for walking (blue) and running (red). There is a relationship between $\sigma(r)$ Froude for walking, but not for running. c) The percentage recovery R as a function of Froude for walking (blue) and running (red). There is a relationship between R and Froude for walking, but not for running. d) The external work as a function of Froude for walking (blue) and running (red). There is no relationship between W_{ext} and Froude for walking and running. For all panels in the figure applies that the color-gradient refers to the age of the participant and the lightest colors are the youngest participants where the darkest colors are the adults

Hallemans et al. (2004) found that the maximal recovery during walking was around 40% in toddlers aged 12-18 months. The range we find in children aged 2-9 years is between 35%-70%, and we see an increase with age. In our study we find a relationship between the percentage recovery and the dimensionless speed. There is a direct link between the smaller stature (and thus slower speed) and the ability to recover energy when walking on a treadmill. Participants were walking at comparable dimensionless speeds.

We find no relationships between external work and age or dimensionless speed during running and a limited relationship during walking indicating that some participants are

locomoting at an optimal speed. The lack of relationship was also shown when comparing normal weight adolescents with their overweight counterparts running at the same speed (Taboga et al., 2012), however this is in contrast to the work presented in the introduction (Hallemans et al., 2004; Schepens et al., 2004; Van de Walle et al., 2010). We do not find any relationship for running due to the elastic energy which is not accounted for in external work in running (Cavagna et al., 1977; Saibene & Minetti, 2003). However, we would have expected some relationship between the external work and age and Froude value for walking. The finding can be related to the differences between over ground and treadmill running.

Supplementary Material 2.2

Computed gait parameters from kinematic and kinetic recordings. Parameter numbers refer to variables in PCA. Normalized parameters are denoted with square brackets [].

Table S2.1: Computed gait parameters from kinematic and kinetic recordings. Abbreviations: Param: Parameter; Norm: normalization; l, leg-length; FS, foot strike; TO, toe-off; SE, end-of-swing; AP, anterior-posterior; ML, medio-lateral; w, body weight; SS, single support; d, stride length (1D); Min, minimum; Max, maximum; Amp, amplitude; u, eigenvector; elev, elevation.

PARAM	DETAILED EXPLANATION	UNIT [NORM]
TEMPORAL FEATURES		
1	Stride duration	s
2	Froude velocity	
3	Stance duration	s
4	Percentage swing duration	% GC
5	Percentage stance duration	% GC
6	Percentage double support	% GC
7	Percentage flight phase	% GC
8	Stride length (1D)	[1/l]
9	Stride length (3D)	[1/l]
LIMB ENDPOINT (VM) TRAJECTORY		
10	Step length	[1/l]
11	Step height	[1/l]
12	Maximum backward position	[1/l]
13	Minimum forward position	[1/l]
14	Maximum velocity during swing	m/s
15	Relative timing of max velocity during swing	% GC
16	Acceleration at swing onset	m/s^2
17	Endpoint velocity	m/s
18	Orientation of velocity vector at swing onset	rad
19	Position of ankle with respect to hip at FS	[1/l]
20	Position of ankle with respect to hip at TO	[1/l]
21	Position of ankle with respect to hip at SE	[1/l]
STABILITY		
22	Lateral displacement of foot during swing	[1/l]
23	Step width (AP)	[1/l]
24	Step width (ML)	[1/l]
JOINT AND SEGMENTAL ANGLES		
25	Thigh elevation angle (Min)	deg
26	Shank elevation angle (Min)	deg
27	Foot elevation angle (Min)	deg
28	Main-leg elevation angle (Min)	deg
29	Thigh elevation angle (Max)	deg
30	Shank elevation angle (Max)	deg
31	Foot elevation angle (Max)	deg
32	Main-leg elevation angle (Max)	deg
33	Knee joint angle (Min)	deg

PARAM	DETAILED EXPLANATION	UNIT [NORM]
LEG/JOINT ANGULAR VELOCITY		
48	Ankle joint velocity (Min)	deg/s
49	Main-leg velocity (Max)	deg/s
50	Knee joint velocity (Max)	deg/s
51	Ankle joint velocity (Max)	deg/s
52	Main-leg velocity (Amp)	deg/s
53	Knee joint velocity (Amp)	deg/s
54	Ankle joint velocity (Amp)	deg/s
KINETICS		
55	Mean AP force during stance phase	N
56	Mean ML force during stance phase	N
57	Mean vertical force during stance phase	[1/w]
58	Mean AP force during SS phase	N
59	Mean ML force during SS phase	N
60	Mean vertical force during SS phase	[1/w]
INTRA-LIMB COORDINATION		
61	Correlation limb-arm AP direction	
62	Phase relationship between limb-arm	
INTERSEGMENTAL COORDINATION		
63	Percentage of variance (1st u)	
64	Percentage variance (2nd u)	
65	Percentage variance (3rd u)	
66	Projection of 1st u on thigh axis	
67	Projection of 1st u on shank axis	
68	Projection of 1st u on foot axis	
69	Projection of 2nd u on thigh axis	
70	Projection of 2nd u on shank axis	
71	Projection of 2nd u on foot axis	
72	Projection of 3rd u on thigh axis	
73	Projection of 3rd u on shank axis	
74	Projection of 3rd u on foot axis	
75	Area of the gait loop	deg^2
76	Ratio of left to right leg cycle duration	
INTERLIMB COORDINATION		
77	Phase difference hip and knee elev. angles	
78	Phase difference foot and shank elev. angles	
79	Max r (thigh and shank elevation angles)	

34	Ankle joint angle (Min)	deg	80	Max r (shank and foot elevation angles)	
35	Limb abduction (Min)	deg	81	Max r (knee and ankle joint angles)	
36	Knee joint angle (Max)	deg	82	Max r (ankle and foot joint angles)	
37	Ankle joint angle (Max)	deg	**PENDULUM/SPRING MECHANISM**		
38	Main-leg abduction (Max)	deg	83	Amplitude of vertical hip displacement	m
39	Thigh elevation angle (Amp)	deg	84	Amplitude of ML hip displacement	m
40	Shank elevation angle (Amp)	deg	85	Forwards work W_f	[1/w]
41	Foot elevation angle (Amp)	deg	86	Vertical work W_v	[1/w]
42	Main-leg elevation angle (Amp)	deg	87	External work W_{ext}	[1/d·w]
43	Knee joint angle (Amp)	deg	88	Recovery in percentage (R)	%
44	Ankle joint angle (Amp)	deg	89	Amplitude kinetic energy E_k	[1/w]
45	Main-leg medio-lateral angle (Amp)	deg	90	Amplitude potential energy E_p	[1/w]
LEG/JOINT ANGULAR VELOCITY			91	Amplitude total energy E_{tot}	[1/w]
46	Main-leg velocity (Min)	deg/s	92	Maximal correlation between E_k and E_p	
47	Knee joint velocity (Min)	deg/s	93	Lag between E_k and E_p	% GC

Supplementary Material 2.3

Number of strides analyzed for each child participant (CH) and the adults (AD) as a group for each condition in each analysis. A total of 29 participants were included in the analysis on the mechanical energies of the CoM (Energetics), and 18 participants were included in the analysis of the effects of kinematic and kinetic parameters (PCA-Clustering). Adult data are presented as the median (25th-75th percentile). For the adults, n= 7 for the energetic analysis and n = 5 for running PCA-clustering analysis and n = 4 for the walking analysis for the PCA-clustering.

Table S2.2: Number of strides analyzed for each child participant (CH) and the adults (AD) as a group for each condition in each analysis.

SUBJ	AGE (MONTHS)	ENERGETICS		PCA-CLUSTERING	
		Walking	Running	Walking	Running
CH1	26	24	57	-	-
CH2	37	21	24	-	-
CH3	37	35	61	-	-
CH4	37	22	17	-	-
CH5	40	15	17	13	16
CH6	59	26	32	26	31
CH7	61	32	29	31	29
CH8	70	40	40	-	-
CH9	71	71	38	71	38
CH10	75	14	30	-	-
CH11	78	64	86	64	83
CH12	81	22	23	22	23
CH13	82	26	26	26	26
CH14	88	29	31	29	31
CH15	91	15	40	-	-
CH16	92	30	34	30	34
CH17	93	76	56	76	56
CH18	97	17	28	-	-
CH19	99	56	62	56	62
CH20	102	68	45	68	45
CH21	106	40	45	-	-
CH22	106	71	12	71	12
A1-A7	Adults	39 (32.0-55.5) n=7	44 (28.5-50.0) n=7	53 (39.0-58.0) n=4	50 (41.9-59.5) n=5

Supplementary Material 2.4

The loadings related to the three PCs. The color-coding refers to the loading with a darker color meaning a higher loading for that factor and PC. For an overview of the parameters, see *Supplementary Material* 2.2.

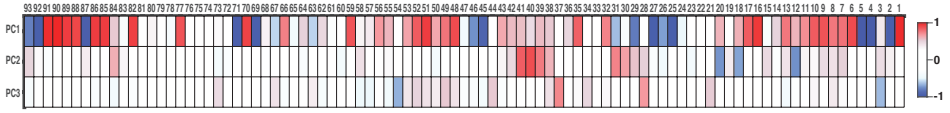

Figure S2.3: The loadings related to the three PCs.

Supplementary Material 2.5

Dendrogram showing the split into eight clusters. The clusters one to four (or cluster one and two in the four-cluster solution) are the clusters containing mostly the prescribed running condition (see *Supplementary Material* 2.6). Clusters five to eight (or clusters three and four in the four-cluster solution), are the clusters containing mostly the prescribed walking condition. The y-axis on the figure is a measure for the distance between clusters as measured with the correlation distance. The taller the links between two leaf nodes, the longer the leaf nodes (or clusters) are situated from each other in the 3D space.

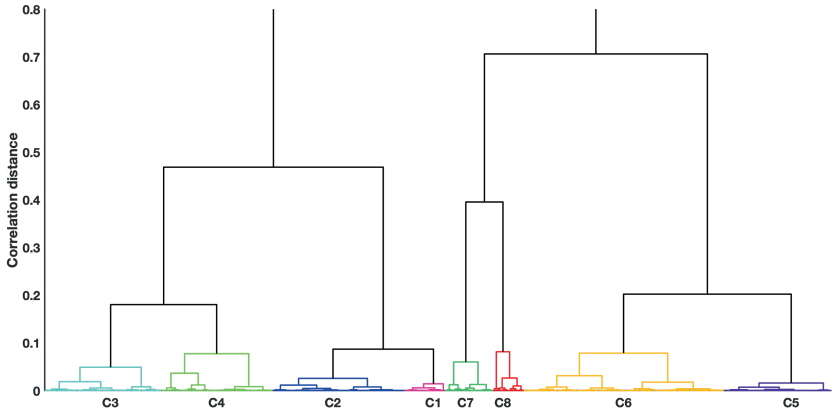

Figure S2.4:: Dendrogram showing the split into eight clusters.

Clustering output for eight clusters. Ordered based on age (months – rounded to the nearest whole integer), with the youngest participant on the right side and the adults (A) on the left for walking (blue circles) and running (red circles). The size of the clusters (C1-C8) depend on the amounts of strides belonging to each cluster, similarly the thickness of the lines connecting each cluster with a participant depend on the percentage of data from each participant belonging to that cluster. For a full overview of the percentage of strides belonging to each cluster, see *Supplementary Material* 2.6.

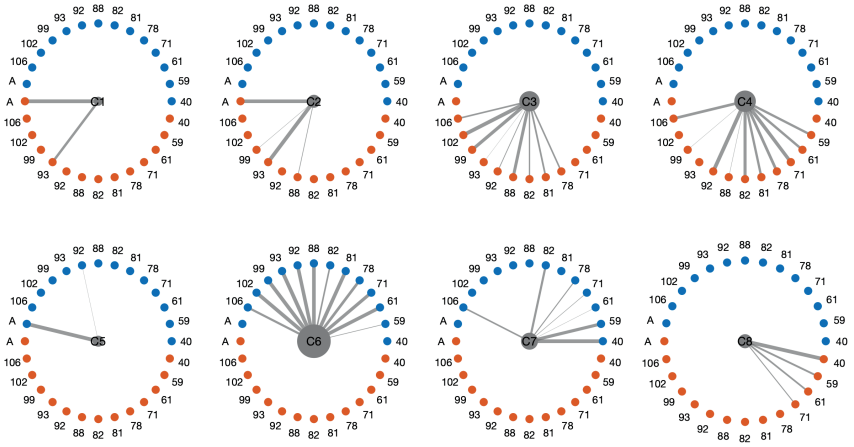

Figure S2.5: Clustering output for eight clusters.

Supplementary Material 2.6

The percentage of strides from each participant that belongs to each cluster for the four-cluster solution (left) and eight-cluster solution (right). Numbers in red are the percentage of strides smaller than five percent and are not considered in the figures presenting the cluster analysis.

Table S2.3: The percentage of strides from each participant that belongs to each cluster..

AGE	4 CLUSTERS				8 CLUSTERS							
	C1	C2	C3	C4	C1	C2	C3	C4	C5	C6	C7	C8
WALKING												
40				100.0							100.0	
59			16.1	83.9						16.1	83.9	
61			93.1	6.9						93.1	6.9	
71			86.8	13.2						86.8	13.2	
78			72.3	27.7						72.3	26.5	1.2
81			95.7	4.3						95.7	4.3	
82			42.3	57.7						42.3	57.7	
88			100.0						3.2	96.8		
92			100.0						5.9	94.1		
93			100.0							100.0		
99			100.0						1.6	98.4		
102			100.0						2.2	97.8		
106			58.3	41.7						58.3	41.7	
A1			100.0						100.0			
A2			100.0						100.0			
A3			100.0						100.0			
A4			100.0						98.2	1.8		
A5												
RUNNING												
40				100.0								100.0
59		50.0		50.0				50.0				50.0
61		51.6		48.4				51.6			3.2	45.2
71		74.6		25.4			1.4	73.2				25.4
78		100.0					40.6	59.4				
81	4.5	95.5				4.5	45.5	50.0				
82		100.0					34.6	65.4				
88	13.8	86.2				13.8	79.3	6.9				
92		100.0					20.0	80.0				
93	94.7	5.3			13.2	81.6	5.3					
99	7.1	91.1		1.8		7.1	85.7	5.4			1.8	
102	1.5	98.5				1.5	98.5					
106		100.0					42.3	57.7				
A1	100.0					100.0						
A2	97.3	2.7				97.3	2.7					
A3	100.0					100.0						
A4	96.6	3.4				96.6	3.4					
A5	100.0				100							

Chapter 3

MUSCLE SYNERGIES IN CHILDREN WALKING AND RUNNING ON A TREADMILL

Bach, M.M., Daffertshofer, A., and Dominici, N.

Front Hum Neurosci, 2021. 15: p. 637157

Abstract

Muscle synergies reflect the presence of a common neural input to multiple muscles. Steering small sets of synergies is commonly believed to simplify the control of complex motor tasks like walking and running. When these locomotor patterns emerge, it is likely that synergies emerge as well. We hence hypothesized that in children learning to run the number of accompanying synergies increases and that some of the synergies' activities display a temporal shift related to a reduced stance phase as observed in adults. We investigated the development of locomotion in 23 children aged 2–9 years of age and compared them with seven young adults. Muscle activity of 15 bilateral leg, trunk, and arm muscles, ground reaction forces, and kinematics were recorded during comfortable treadmill walking and running, followed by a muscle synergy analysis. We found that toddlers (2–3.5 years) and preschoolers (3.5–6.5 years) utilize a "walk-run strategy" when learning to run: they managed the fastest speeds on the treadmill by combining double support (DS) and flight phases (FPs). In particular the activity duration of the medial gastrocnemius muscle was weakly correlated with age. The number of synergies across groups and conditions needed to cover sufficient data variation ranged between four and eight. The number of synergies tended to be smaller in toddlers than it did in preschoolers and school-age children, but the adults had the lowest number for both conditions. Against our expectations, the age groups did not differ significantly in the timing or duration of synergies. We believe that the increase in the number of muscle synergies in older children relates to motor learning and exploration. The ability to run with a FP is clearly associated with an increase in the number of muscle synergies.

Introduction

Muscle synergies reflect a common neural input to multiple muscles easing the control of complex motor tasks like locomotion (Bernstein, 1967; Bizzi & Cheung, 2013). The central nervous system can activate large groups of muscles by small sets of descending neural signals at specific moments during the gait cycle (Bizzi & Cheung, 2013; d'Avella et al., 2003; Ting & Macpherson, 2005).

When children develop walking skills, the number of muscle synergies that accompany the cyclic movement of the lower extremities increases (Dominici et al., 2011). In neonates, two muscle synergies are present resembling the reflexive stepping pattern seen at birth, while in toddlers two additional are present, i.e., a total of four synergies can be observed that persist to and during adulthood (Dominici et al., 2011; Sylos-Labini et al., 2020). The shape of the synergies' waveforms evolves from wide, sinusoidal shapes to more focal ones with shorter activation duration from toddlers to preschoolers and adults (Dominici et al., 2011). Here, we ask whether there is similar change in the number of synergies and the shape of their waveforms during the development of running. Is it generally true that an immature locomotor pattern is represented by fewer muscle synergies and less focal activation peaks?

Running may be defined as having a flight phase (FP) in contrast to walking where there is a double support phase (DS). Infants without independent walking experience toddling on a treadmill but with body-weight support show a shift from DS to FP at speeds of around 0.75 m/s (Vasudevan et al., 2016). Children, at the age of 6–18 years can run with FP though seemingly only in about 90% of the strides (Rozumalski, Novacheck, Griffith, Walt, & Schwartz, 2015). Given the relatively rare presence of FP, one may expect that children learning to run employ a so-called *walk-run strategy*, i.e., a mixture of DS and FP.

Running in adults differs from walking in that the activation timing changes in several muscles, amplitudes increase, or activation profiles may alter all together (Cappellini et al., 2006; Hagio, Fukuda, & Kouzaki, 2015; Ivanenko, Cappellini, Poppele, & Lacquaniti, 2008; Yokoyama et al., 2016). Muscle synergy analysis revealed, in particular, a shift in timing that is related to the activation of the calf muscles in line with a shorter stance phase in running compared to walking (Cappellini et al., 2006). One may ask whether such a pattern is also present in children during the development and maturation of running. In fact, already without running, the peak medial gastrocnemius activity of children at the age of 7–9 years does shift to earlier in the gait cycle during walking from ~45% at comfortable speeds to ~25% at fast speeds (Tirosh et al., 2013). Yet, it seems that the medial gastrocnemius muscle is pivotal for the development of walking as its full-width half-maximum (FWHM) decreases with age in typically developing children aged 1–12 years (Cappellini et al., 2016). The FWHM is a measure of the duration of the peak activation and any reduction of this measure suggests an increased

ability to contract the muscle. But how do all these changes relate to (the emergence of) the aforementioned, common neural input?

We sought to answer these questions by investigating the development of both walking and running in children aged 2–9 years old. Using electromyographic (EMG) signals from 15 bilateral leg, trunk, and arm muscles, we extracted muscle synergies and related their number and waveforms with the ability to run with a FP. We expected the youngest children to make use of the afore-introduced walk-run strategy. We also hypothesized that the pivotal role of the medial gastrocnemius muscle extends to the development of running and expected its FWHM to reduce with increasing age for both walking and running. If this assumption holds, this will imply a (gradual) maturation of muscle synergies toward resemblance of adult patterns by means of an increased number of synergies accompanied by a temporal shift related to a reduced stance phase. To anticipate, we failed to find support for some of these hypotheses.

Materials and Methods

Participants

Thirty healthy participants were included in this study (23 children aged 2–9 years old and 7 young adults; see Table 3.1) with exclusion of those with known developmental disease or neurological disorders. Participant groups were selected based on the ability to manage the speeds on a treadmill with FP (~ running, see below): toddlers (range: 25.7–40.4 months), preschoolers (range: 59.0–75.0 months), school-age (range: 78.4–106.1 months), and adults (range: 22–28 years).

Table 3.1: Participant characteristics. Mean (SD)

	TODDLERS	PRESCHOOLERS	SCHOOL-AGE	ADULTS
AGE	35.3 (5.6) months	66.1 (6.5) months	92.9 (9.5) months	24.15 (2.5) years
GENDER (M/F)	2/3	3/3	6/6	4/3
HEIGHT [CM]	96.2 (2.8)	117.2 (7.7)	130.2 (6.8)	178.7 (5.7)
WEIGHT [KG]	15.0 (2.0)	20.8 (3.3)	25.4 (4.9)	71.3 (8.3)

Adult participants and guardians/parents of the children provided written informed consent in compliance with the Declaration of Helsinki. Ethical approval was given by The Scientific and Ethical Review Board of the Faculty of Behavioural & Movement Sciences, Vrije Universiteit Amsterdam, Netherlands (file number: VCWE-2016-149R1).

Setup

Participants were instructed to walk or run on the treadmill (Motek Medical BV, Culemborg, the Netherlands) at a comfortable speed. Each of these conditions was repeated until a minimum of 20 consecutive strides had been recorded, where possible (Oliveira, Gizzi, Farina, &

Kersting, 2014). When more than twenty gait cycles were recorded, the middle twenty cycles were chosen for analysis.

Walking and running were practiced and comfortable speeds were first determined by starting at a slow pace that was increased in steps of 0.1 km/h until the participant reported a comfortable speed. In two instances, participants were unable/unwilling to continue after practicing and we included the data recorded during these familiarization trials for analysis (one for walking and another for running).

Children participants wore a full body climbing harness (CAMP Bambino Full Body Harness, CAMP CO, United States) modified to also have a secure attachment point on the back at all times when on the treadmill. All participants wore own shoes for the duration of the experiment.

Data Acquisition

Behavior

Vertical, mediolateral, and anteroposterior ground reaction forces were sampled at 1 kHz for every trial via the two force plates in the instrumented treadmill.

Foot switches (piezo-resistive pressure sensitive sensors: Zerowire; Cometa, Bareggio, Italy) were placed on the skin on the heel and the head of the first metatarsal underneath the foot and were secured with tape; shoes and socks were placed over the foot switches. Foot switch data were sampled at 2 kHz.

Kinematic data were recorded bilaterally using an active marker system (Optotrak motion system, NDI Measurement Sciences, Ontario, Canada) and sampled at 100 Hz. Two cameras were placed diagonally behind the treadmill, and one was placed diagonally in front on the right-hand side of the participant. Single markers were attached to the right head of 5^{th} metatarsal, right lateral malleolus (LM), right lateral femoral epicondyle (LE), and right greater trochanter (GT), right and left calcaneus, right and left glenohumeral joint, right and left lateral humeral epicondyle, and right and left ulnar styloid. Here, kinematic and foot switch data merely served for step detection in the case the vertical ground reaction data were unreliable.

Electrophysiology

Bipolar electromyographic (EMG) signals were recorded with a wireless system (Mini wave plus, Zerowire; Cometa, Bareggio, Italy; sampled at 2 kHz after online band-pass filtering between 10 and 500 Hz) using pediatric Ag-AgCl pre-gelled EMG disk-electrodes for children (inter-electrode distance: 19 mm: DuoTrode, Myotronics, Kent, WA, United States) and pre-gelled Ag-AgCl electrodes for adults (BlueSensor H5; Ambu, Ballerup, Denmark). Skin was cleaned with alcohol and excess hair was removed prior to electrode placement on the bulk

of the muscle belly parallel to the muscle fiber direction, conform SENIAM recommendations (Hermens et al., 1999).

We targeted the following 16 bilateral muscles: tibialis anterior (TA), gastrocnemius medialis (MG), biceps femoris (BF), vastus medialis oblique (VMO), rectus femoris (RF), tensor fascia latae (TFL), adductor longus, gluteus maximus (GM), erector spinae–L2 level (ES), latissimus dorsi (LD), deltoid–anterior part (AD), deltoid–posterior part (PD), trapezius–descending part (TRAP), triceps brachii (TB), biceps brachii (BB), and brachioradialis (BR). Adductor longus was, on the basis of the quality of the recorded muscle activity, excluded for all participants for further analysis leaving 15 bilateral muscles.

A single participant was recorded in a different lab using a slightly different setup. The kinematics was measured at 100 Hz using a passive marker system (Vicon Motion Systems Ltd., Oxford, United Kingdom). The reflective markers (14 mm in diameter) were placed bilaterally in the same positions as the other participants. Twelve cameras were placed around the ceiling of the room. The treadmill (Motek Medical BV, Amsterdam, the Netherlands), measured only vertical ground reaction forces. The EMG protocol and equipment did not differ from the other participants.

Data Analysis

Behavior

While step events were mainly detected based on the vertical ground reaction forces (F_v), they were supplemented with the events detected from the heel markers and foot switches when F_v data were not sufficient for the event detection. The F_v were filtered with a Savitzky-Golay filter (3rd order, 121 framelength; Savitzky & Golay, 2002). Heel strike (HS) and toe-off (TO) were defined as the first sample crossing the threshold [mean(F_v) /10]. First and last HS and TO were excluded for further analysis. Heel markers were used to detect step events from the kinematics (Roerdink et al., 2008). The foot switch detection was based on an on/off algorithm. Foot switch data and kinematic data were re-sampled to 1 kHz for this application. All events were visually verified. The FP and DS were determined for up to twenty strides for every participant and condition.

All behavioral data were time-normalized to the right HS. Based on HS and TO, the percentage stance and swing of each gait cycle were determined. Velocity was normalized to leg length yielding the walking Froude number (Alexander & Jayes, 1983)

$$Fr = \frac{v^2}{g \cdot l}$$

where, v denotes stride speed as measured by the treadmill (m/s), g represents the gravitational constant (9.81ms^{-2}) and l is the leg length (m) as the combined measured distance of

thigh (GT-LE) and shank (LE-LM). Normalizing to the walking Froude number is considered suitable when comparing gait patterns at different speeds in participants of different size (Ivanenko, Dominici, et al., 2004).

Electrophysiology

Electromyographic data were visually inspected, and artifacts were removed using a custom-written burst-detection algorithm. EMG data were high-pass (2nd order bi-directional Butterworth filter at 20 Hz; De Luca, Gilmore, Kuznetsov, & Roy, 2010; Willigenburg, Daffertshofer, Kingma, & van Dieen, 2012) and notch filtered (bi-directional stop notch filter around k·50 Hz, k = 1,…,10, with half-bandwidth of 0.5 Hz). Subsequently, EMG data were rectified using the modulus of the analytic signal and finally low-pass filtered (bidirectional 2nd order filter at 10 Hz) to obtain the corresponding EMG envelopes (Oliveira et al., 2016). These envelopes were time-normalized to 200 samples per gait cycle. Right-side EMG signals were normalized to the right HS and left-side EMG normalized to the left HS.

To characterize differences in the duration of EMG activity, we computed the FWHM. The FWHM was calculated as the number of samples exceeding each cycle's half maximum, after subtracting the cycle's minimum. We determined FWHM for each condition as the grand average within groups and across right and left side and expressed it as a percentage of the gait cycle. While we determined FWHM for every muscle per group, in view of our hypothesis we also expressed FWHM of the MG muscle as a function of age. Moreover, we estimated the phase shift τ between the walking and running mean activity patterns of the MG muscle (Ivanenko, Poppele, et al., 2004) using the cross-correlation. The cross-correlation was computed as (Nelson-Wong, Howarth, Winter, & Callaghan, 2009):

$$R_{\alpha\beta}(\Delta) = \frac{\int \alpha(t) \cdot \beta(t+\Delta)dt}{\sqrt{\int \alpha^2(t)dt \cdot \int \beta^2(t)dt}}$$

where α and β denote the two mean-subtracted waveforms during walking and running and Δ refers to a time lag between the two. Then, the maximum correlation peak was determined as well as its corresponding time lag τ. Positive τ values indicate a lag of the MG signal during walking relative to running. To ease interpretation, we expressed the time lag τ in percent of the gait cycle.

For the subsequent synergy analysis, the concatenated EMG envelopes (concatenation leads to higher reconstruction accuracy (RA); Oliveira et al., 2014) were amplitude normalized to the mean value for every individual muscle (Goudriaan et al., 2018; Halaki & Gi, 2012; Torricelli et al., 2014). To increase the signal-to-noise ratio for the synergy analysis, the muscle synergy analysis was performed on each participant side (Clark, Ting, Zajac, Neptune, & Kautz, 2010), and thus, EMG envelopes were concatenated in a (15 muscles) × (20 strides × 200 samples) matrix for every condition and side for each participant. To ease comparison of our

experimental findings with the literature, we also performed the muscle synergy analysis on only the lower limb muscles (TA, MG, BF, VMO, RF, TFL, GM, and ES), which resulted in an (8 muscles) × (20 strides × 200 samples) matrix for each participant, condition, and side (see *Supplementary Material* 3.1 for details).

For dimensionality reduction we first employed a principal component analysis (PCA) on the mean-centered data (Boonstra et al., 2015). The appropriate number of muscle synergies was determined as the minimum number required to explain 80% of the variance. Then, a rank-reduced dataset was reconstructed, and the mean was added back. Subsequently, we employed non-negative matrix factorization (NMF) as a decomposition tool (Dominici et al., 2011; Lee & Seung, 1999; Rabbi et al., 2020; Steele, Tresch, & Perreault, 2015; Tresch et al., 2006) to identify the relevant muscle synergies. Similar to PCA, NMF is an optimization method but is supplemented by the constraint that both the extracted weighting coefficients and activation waveforms are non-negative. This accounts for the constructive (non-negative) superposition of neural and muscle activations. Following the conventional NMF approach, weightings W and activation waveforms C were estimated by minimizing the Frobenius norm between (rank-reduced) envelope data E and the sum of synergies ($W \cdot C$, i.e., weightings × waveforms):

$$\|E - W \cdot C\|_F = \min$$

E denotes the aforementioned data, i.e. it resembles an $m \times t$ matrix (m = 15 muscles and t = 20 strides × 200 samples), the weighting coefficients W comprise an $m \times n$ matrix (n = number of synergies), and C contains the activation waveforms ($m \times t$ matrix) (Lee & Seung, 1999). We employed a multiplicative algorithm (Berry, Browne, Langville, Pauca, & Plemmons, 2007, implemented in Matlab, The Mathworks, Natick, MA, United States, ver. 2019b; 200 replicates, 3000 iterations, convergence threshold 10-6 and termination tolerance 10-8) that requires an a-priori choice of the number of muscle synergies. Capitalizing on the optimized Frobenius norm, we also estimated the RA following (Kerkman, Bekius, Boonstra, Daffertshofer, & Dominici, 2020; Zandvoort, van Dieen, Dominici, & Daffertshofer, 2019) that is defined as

$$RA = 1 - \frac{\|E - (W \cdot C)\|_F}{\|E\|_F}$$

In addition, we verified that the selected number of synergies adequately reconstruct the activity of each muscle by computing the RA per muscle, condition, and participant side.

The output of the NMF is (pseudo-)random for every optimization run. Hence, we ordered the outcomes by their correlation across participants. To do so, a separate NMF analysis was carried out on the grand-average of the adult data and the waveforms were arranged based

on the timing of the main peaks of the activation pattern (Cappellini et al., 2006; Santuz et al., 2020). Subsequently, this serve as a "model-order" for the outputs of the NMF from all other participants which were then correlated to that model-order and ranked based on the largest Pearson correlation coefficient.

Finally, we determined the FWHM of every activation waveform for each participant side and the time lag τ between walking and running activation waveforms.

Statistics

Descriptive statistics included the calculation of the mean and standard deviation (SD).

Behavior

To test for effects of *age* on FP and for effects of *age* and *condition* (levels: instructed walking and running) on DS, we used two linear regression models. Next to main effects, the second one also served to identify interactions *age* × *condition*. The significance threshold was set to $\alpha = 0.05$.

Group differences in stance duration, stride duration, and Froude values were assessed using Kruskal-Wallis tests for every condition (with corresponding Bonferroni correction for multiple comparison); note that Kolmogorov-Smirnov tests revealed significant deviations from normality arguably due to small group sizes, which let us choose for non-parametric testing. Only *p*-values below 0.01 were considered significant in order to correct for the multiple corrections.

Electrophysiology

Along the same lines of the behavioral data, the time lag between walking and running and the FWHM of muscle activations and the waveforms of the muscle synergies were compared non-parametrically for every condition (Kruskal-Wallis tests with Bonferroni correction). Moreover, we detailed the age-dependency of the MG's FWHM by fitting exponentially saturating functions. To quantify the corresponding goodness-of-fit we report the adjusted R^2-value unless specified otherwise.

Results

We failed to record the aimed-for minimum of 20 strides for all participants (between 14 and 20 strides were analyzed). All the children in the toddler group were assisted with handhold by either a researcher or their parent/guardian ($N = 5$). Yet, we are confident that this did not affect the level of body-weight support during locomotion as we verified the level of vertical ground reaction forces via the toddler's body weight (range of body-weight support was 0-7%). The conditions referred to in the following are the instructed conditions.

Behavioral Results

As expected, the young children in this study used a combination of DS and FP when running on a treadmill (see Figure 3.1A). For FP there was a significant main effect of *age* ($p < 0.001$) and the FP increased with increasing age. A similar significance could be established for the main effect of *age* on DS ($p < 0.001$) but, opposite to FP, DS decreased with increasing age. And there was a significant main effect of *condition* on DS ($p < 0.001$), which turned out to be smaller during running than during walking. Moreover, we found a significant *age* × *condition* interaction effect on DS ($p = 0.0012$); see Table 3.2 for overview.

Table 3.2: Linear regression estimates

	FACTOR	ESTIMATE	SE	t	p-VALUE
DS	Intercept	29.59	0.39	74.95	0
	Age	-0.02	0.00	-6.31	$4 \cdot 10^{-10}$
	Condition Running	-22.79	0.55	-41.20	$<2 \cdot 10^{-16}$
	Age:Condition Running	-0.01	0.00	-3.25	0.0012
FP	Intercept	3.95	0.59	6.82	$2 \cdot 10^{-11}$
	Age	0.07	0.00	19.73	$<2 \cdot 10^{-16}$

Abbreviations: DS, double support phase; FP, flight phase; SE, standard error; t, t-statistic.

We could not establish significant differences in stride duration between *groups* for walking, while during running stride duration of preschoolers and the school-age group differed significantly from that of the adults ($p = 0.0008$, $p = 0.0061$, respectively, Figure 3.1B). We also found a significant difference in stance duration between the toddlers and both the school-age group and the adults, both during walking ($p = 0.0072$, $p = 0.0077$, respectively) and running ($p = 0.0045$, $p = 0.0003$, respectively). And the stance duration of preschoolers differed significantly from that in the adults for running ($p = 0.0095$); see Figure 3.1C.

The aforementioned differences are particularly interesting since for dimensionless speed we only found significant differences between toddlers and adults during walking ($p = 0.0027$) and between toddlers and adults during running ($p = 0.0061$); see Figure 3.1D.

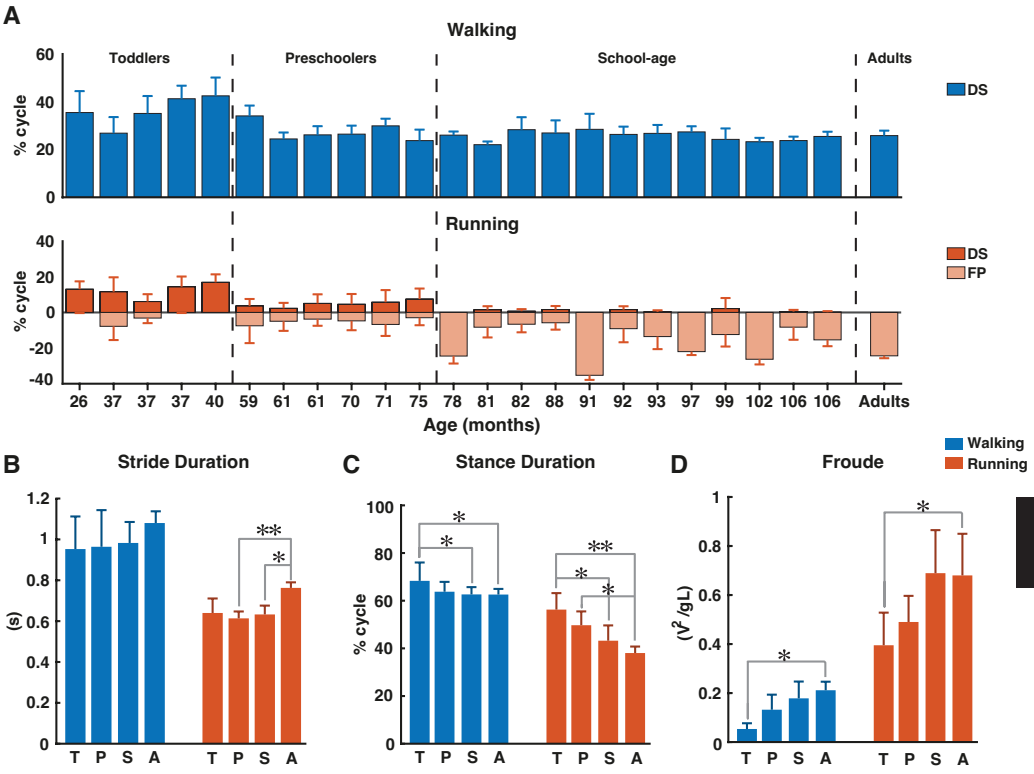

*Figure 3.1: Temporal gait parameters. (A) Percentage double support and flight phase during walking (blue) and running (red). Flight phase is depicted with negative numbers. Vertical dotted lines separate the different groups: Toddlers, Preschoolers, School-age, and Adults, (B) Stride duration for walking and running, (C) Stance duration for walking and running, (D) Froude number for walking and running. Abbreviations: DS, double support; FP, flight phase; s, seconds; T, toddlers; P, preschoolers; S, school-age; A, adults; V, velocity, g, gravitational constant; L, leg length; * = $p < 0.01$, ** = $p < 0.001$.*

Electrophysiology

The ensemble-averaged EMGs of all muscles depicted in Figure 3.2A appeared consistent with those reported in the literature for school-age and adult participants (e.g., Cappellini et al., 2006; Cappellini et al., 2018; Rozumalski, Steele, & Schwartz, 2017; Tirosh et al., 2013).

During walking, lower leg activity had about the same overall modulation across groups with wider peaks of activity in the toddler group that was reduced in the older groups. Activity patterns in arm muscles were relatively flat during the gait cycle across all groups, while trunk muscles showed a clear modulation with increasing intensity in all the groups, but the adults. The gluteus maximus activity showed only a single major peak in the beginning of the stance phase in the toddlers, while in adults two isolated peaks were present with the additional one being early swing, in agreement with earlier reports (Cappellini et al., 2016; Cappellini et al.,

2006; Dominici et al., 2011; Kerkman et al., 2020; Olree & Vaughan, 1995). Likewise, the erector spinae activity showed a single, prolonged activation peak for about 50% of the gait cycle in the toddlers, whereas in adults we could observe two distinct peaks.

During running, EMG activity increased in all muscles, but most pronounced in the adults' lower extremities. In the toddlers, the EMG patterns of upper trunk muscles largely agreed with those of the other groups, but peak activity was less pronounced. A clear pattern of activation in arm muscles was visible in all groups except toddlers with more consistent EMG activity in the adults. The upper trunk (TRAP and PD) muscles changed from a pattern with two negligible peaks to a pattern with two prominent ones. The lower trunk muscle (ES) changed from a unimodal pattern with a small burst of activity during heel strike to a prominent bimodal pattern with bursts of activity in early stance and mid-swing (Figure 3.2A).

As expected, the most notable differences between the two conditions (instructed walking vs. running) were found in the time lag of peak activity of the calf muscle (MG) toward earlier in the gait cycle during running. The toddlers displayed a significantly smaller shift than the adults (p= 0.0071) and, when looking at all groups, there was a clear trend of shift increase with increasing age. The time lag in the toddler group had a mean (±SD) of 8.8 ± 8.0% of the gait cycle, where the others' time lags were 16.3 ± 5.7%, 18.5 ± 7.8%, and 20.5 ± 7.1% (for preschoolers, school-age, and adults, respectively); cf. Figure 3.5B.

For the MG's FWHM we found a decreasing function of age for both instructed walking and running conditions with goodness-of-fit values of R^2 = 0.26 and R^2 = 0.30, respectively (Figure 3.2C and 2D).

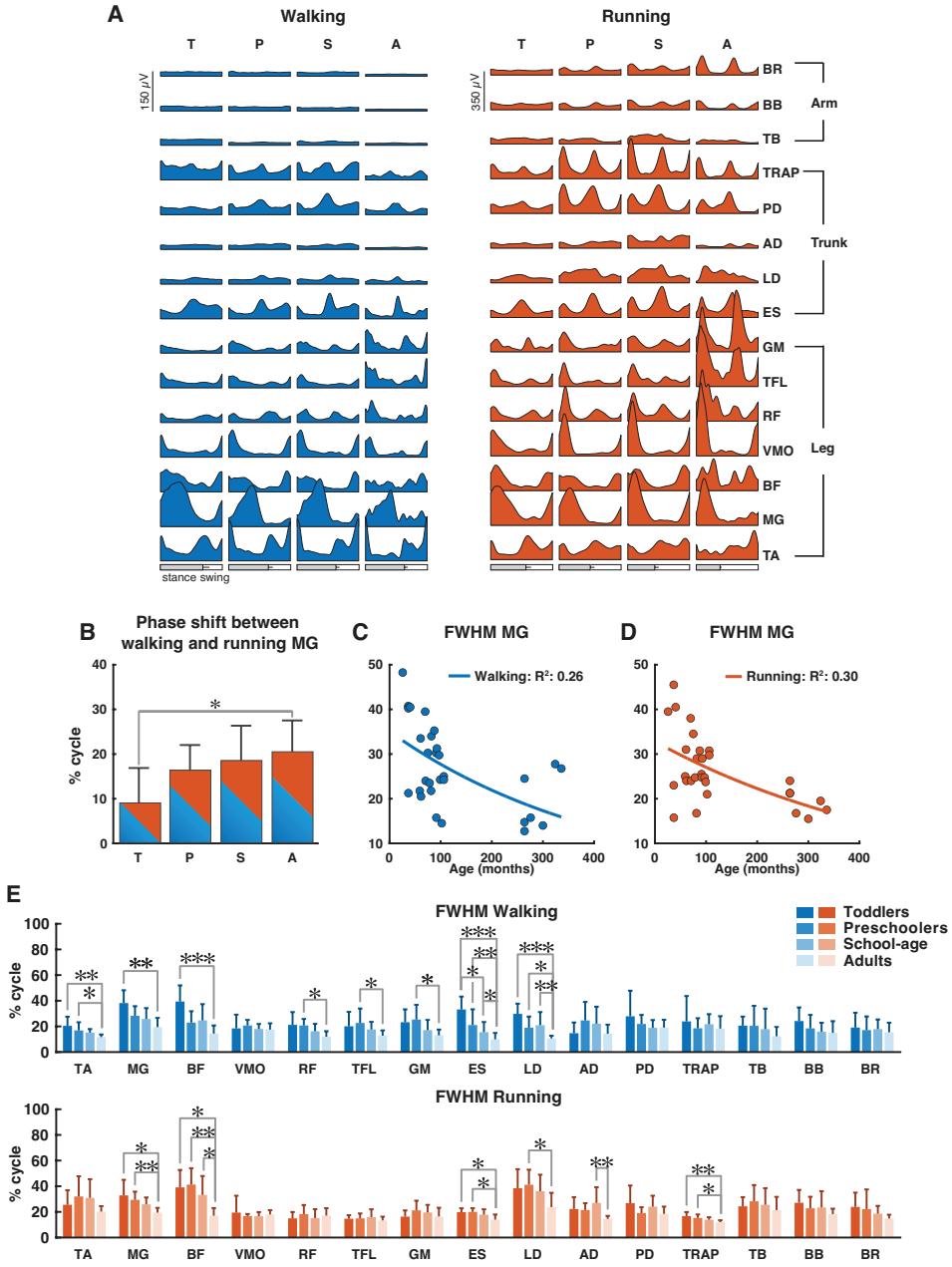

Figure 3.2: Characteristics of EMG signals. (A) Grand averages of 15 EMG activity patterns for walking (blue) and running (red) for all four groups, data are plotted vs. normalized gait cycle, relative duration of stance varied across groups, a bar indicates an amount of variability in the stance phase duration across groups. (B) Phase shift between the peak activation of medial gastrocnemius (MG) for walking and running for each group, positive value indicates a lag of walking signal relative to running signal. (C + D) Full-width half-maximum (FWHM) of the MG activity as a function of age for walking (C) and

*running (D). Continuous lines represent exponential fittings, note the decrease in values with age. (E) FWHM of all muscles (means + SD) for the four groups. Abbreviations: TA, tibialis anterior; MG, medial gastrocnemius; BF, biceps femoris; VMO, vastus medialis oblique; RF, rectus femoris; TFL, tensor fascia latae; GM, gluteus maximus; ES, erector spinae; LD, latissimus dorsi; AD, anterior deltoid; PD, posterior deltoid; TRAP, trapezius; TB, triceps brachii; BB, biceps brachii; BR, brachioradialis; T, toddlers; P, preschoolers; S, school-age; A, adults; FWHM, full-width half-maximum. * = $p < 0.01$, ** = $p < 0.001$, *** = $p < 0.0001$.*

Last but not least, we found significant differences in the FWHM between groups for eight muscles in the walking condition and six muscles in the running condition (Figure 3.2E). In the lower leg muscles, we found significant differences between the toddler group and the adults (TA: p = 0.00012, MG: p = 0.00011, BF: p < 0.00006) for walking (MG: p = 0.0017, BF: p = 0.0018) and for running; between the preschoolers and the adults in the TA muscle during walking (p = 0.0064) and the MG and BF muscles during running (p = 0.0009, p = 0.00017, respectively); and between school-age and adults in the BF muscle during running (p = 0.0048). In the upper leg muscles the only differences were found in the walking condition between the preschoolers and the adults in the RF, TFL, and GM muscles (p = 0.0021, p = 0.0097, p = 0.009, respectively). In the lower trunk muscles the ES muscle was significantly different between toddlers and the school-age group, toddlers and adults, the preschoolers and the adults, and finally the school-age children and the adults for walking (p = 0.002, p < 0.00001, p = 0.0001, p = 0.0085, respectively) but also the toddlers and preschoolers were significantly different from the adults (p = 0.0071, p = 0.0024, respectively) during running. The LD was significantly different between all children groups and the adults for walking (p < 0.00001, p = 0.0056, p = 0.0006, respectively) and between the preschoolers and adults for running (p = 0.0054). In the upper trunk muscles the only differences were visible in the running condition with significant differences between the school-age group and adults in AD (p = 0.00026), and the toddlers as well as the preschoolers were significant different from the adults in TRAP (p = 0.0004, p = 0.0053, respectively). No significant differences were found in the arm muscles for any condition.

Number of Synergies

The results for the analysis involving all muscles are illustrated in Figure 3.3. Across participant sides and conditions, PCA revealed that four to eight components were needed to explain 80% of the variance with the highest numbers needed for the walking condition compared to the running condition (Figure 3.3A). In the toddlers walking, 70% of the group required six synergies (range: five-seven), while in the preschoolers and the school-age groups, the majority required seven synergies (50% and 55%, respectively, range: four-seven and five-eight, respectively), and finally in the adult group five-six synergies were needed with 72% requiring five synergies. For running, 80% of the toddlers required six synergies (range: five-six), in the preschoolers 50% of them required six synergies (range: five-seven), and school-age group there was an almost even distribution between participants requiring six and seven synergies

(40%, respectively, range: four-seven synergies), whereas in the adults five synergies explained the variance of the data for 70% of the participants, with a range of four-five. After NMF, the percentage of RA remained approximately 70% across groups and conditions (Figure 3.3B) and RA across single muscles exceeded 70% as a group average across conditions.

The results of the lower limb analysis and the number of synergies extracted can be found in *Supplementary Material* 3.1. Between two and five synergies were needed to explain the variance across all participants and conditions with the majority of the participants requiring four synergies during walking and the majority requiring three during running. Similarly, to the full-body analysis, the percentage RA on the lower limb analysis varied around 70%.

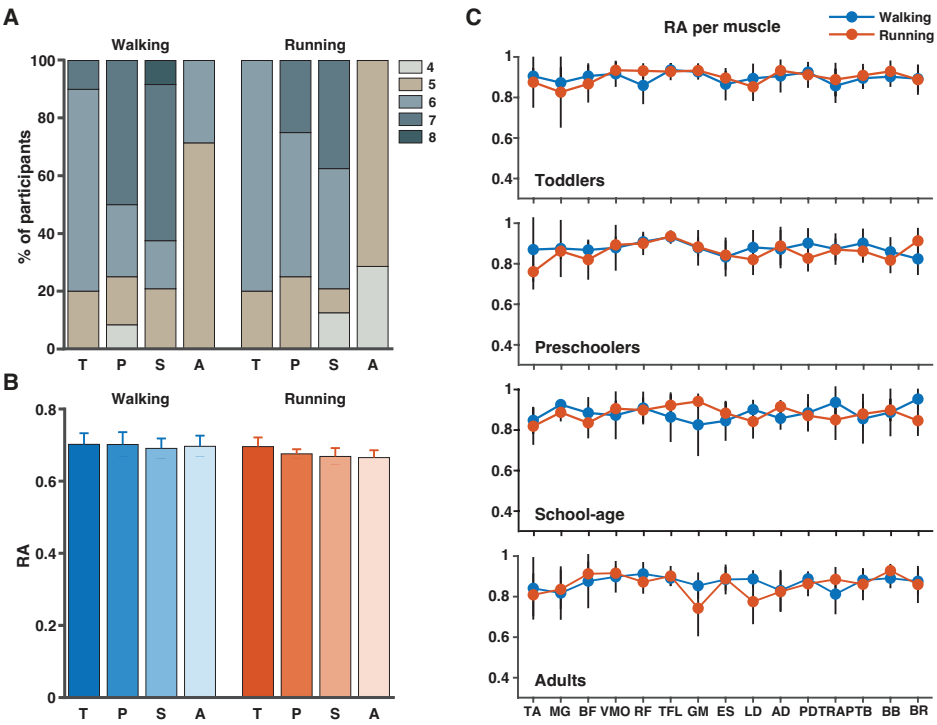

Figure 3.3: Number of synergies and accuracy. (A) Number of synergies needed to account for the cycle-to-cycle variability of EMG activity during walking and running for each group as determined by principal component analysis PCA (>80% of variance). (B) The corresponding reconstruction accuracy (RA) after rank-reduction with PCA followed by NMF. (C) The RA (mean ± SD) for each muscle and condition (blue = walking, red = running). Abbreviations: TA, tibialis anterior; MG, medial gastrocnemius; BF, biceps femoris; VMO, vastus medialis oblique; RF, rectus femoris; TFL, tensor fascia latae; GM, gluteus maximus; ES, erector spinae; LD, latissimus dorsi; AD, anterior deltoid; PD, posterior deltoid; TRAP, trapezius; TB, triceps brachii; BB, biceps brachii; BR, brachioradialis; T, toddlers; P, preschoolers; S, school-age; A, adults.

Structure of Muscle Synergies

Based on the number of muscle synergies identified per participant in the previous section, the activation waveforms and corresponding weighting coefficients were grouped; cf. Figure 3.4. Every waveform showed a peak at a specific moment during the gait cycle. In Figure 3.4, the first waveform for all groups represented the loading response around the foot contact moment. On average, the lower limb muscles among others, the BF, VMO, and GM largely contributed to the first synergy during walking and running in the toddlers, while for the older children and the adults VMO contributed more to it. The second waveform peaked at mid-stance and due to the relatively shorter stance phase for running compared to walking, this pattern was shifted to earlier in the gait cycle during running compared to walking. As expected, this waveform was mostly influenced by the MG (Cappellini et al., 2006). The third waveform peaked prior to foot off in the walking condition across groups, and after foot-off for the running condition except for the toddler group, where it peaked around the foot-off event. This synergy was primarily influenced by the ES and the other trunk and arm muscles during walking and running. The fourth waveform reached its maximum at the early swing and was dominated by the TA muscle, presumably because the foot needs to clear the floor at this moment in the gait cycle, whereas the fifth waveform peaked at the end of swing in preparation for the foot contact. Higher order waveforms, if present, were more variable between participants and less defined when it comes to the main peak: the fifth synergy was not dominated by any particular muscles but predominantly influenced by the trunk and arm muscles, and this applies also to the sixth, seventh, and eighth synergies when present across groups.

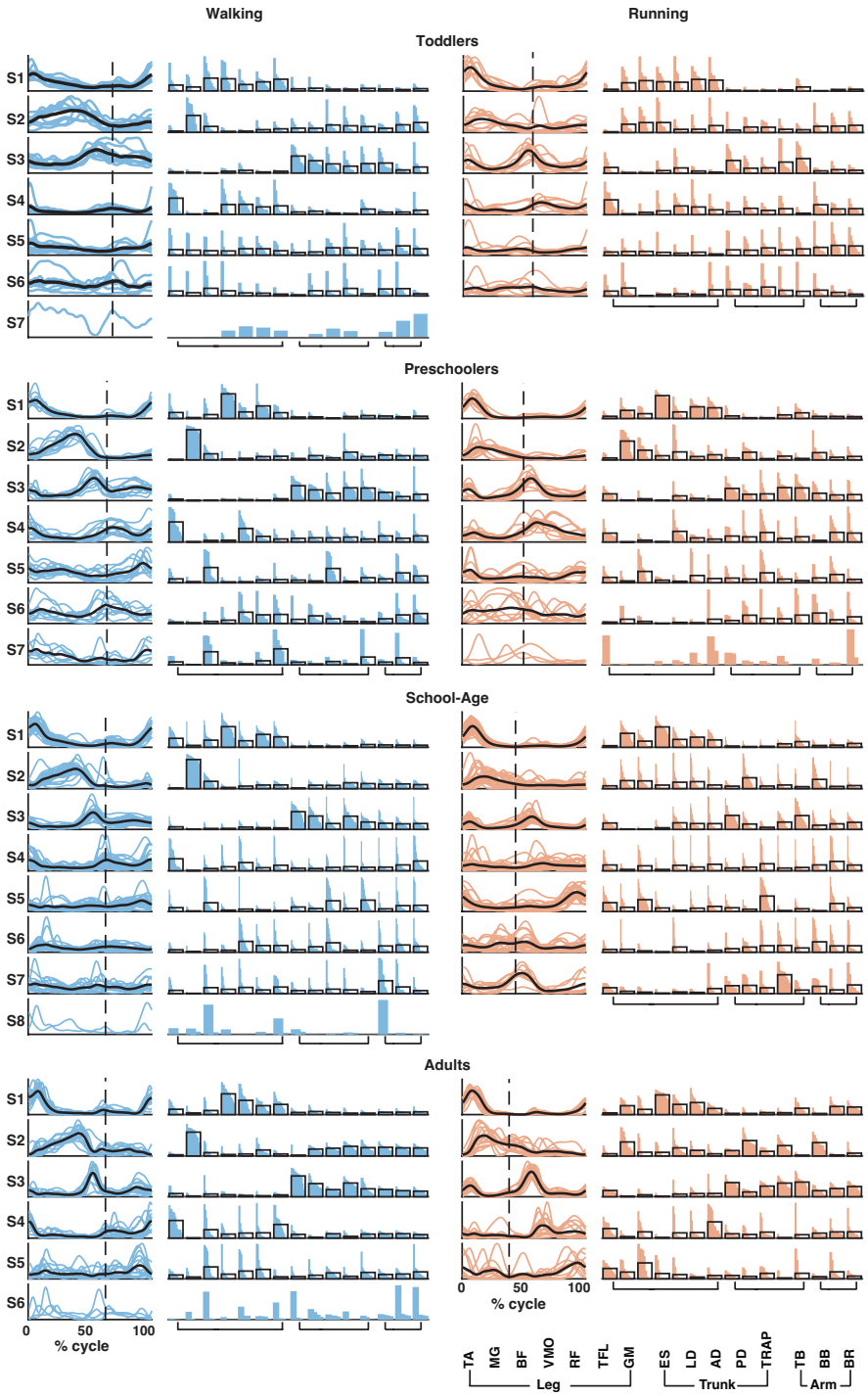
Walking
Running
Toddlers
S1
S2
S3
S4
S5
S6
S7
Preschoolers
S1
S2
S3
S4
S5
S6
S7
School-Age
S1
S2
S3
S4
S5
S6
S7
S8
Adults
S1
S2
S3
S4
S5
S6
0
50
100
% cycle
TA
MG
BF
VMO
RF
TFL
GM
Leg
ES
LD
AD
PD
TRAP
Trunk
TB
BB
BR
Arm

Figure 3.4: Muscle synergy structure for the four groups for walking (left; in blue) and running (right; in red). Vertical dotted line in activation timing plots represents the end of the stance phase. Each colored line represents a participant side, leading to one line for right side and one line for left side for each participant resulting in a total of (n=10) for the toddler group, (n=12) for the preschoolers, (n=24) for the school-age group, and (n=14) for the adult group. Black lines represent the mean. Y-axis is in arbitrary units. In the weighting plots, each colored bar represents the weighting coefficient for one participant side, the weightings are ordered based on their size. The black outlines represent the mean for the group. Abbreviations: TA, tibialis anterior; MG, gastrocnemius medialis; BF, biceps femoris; VMO, vastus medialis oblique; RF, rectus femoris; TFL, tensor fascia latae; GM, gluteus maximus; ES, erector spinae; LD, latissimus dorsi; AD, anterior deltoid; PD, posterior deltoid; TRAP, trapezius; TB, triceps brachii; BB, biceps brachii; and BR, brachioradialis.

Using FWHM for the temporal activation waveforms (Figure 3.5), we found a significant difference between the toddler group and adult group in the third waveform in walking (p = 0.0013). For running, the only significant differences were found in waveform four between the preschoolers and adults (p = 0.0084) and in waveform five between the school-age group and the adults (p = 0.0074). There was a trend toward a larger FWHM in the younger groups for waveform two in walking, and a trend toward a reduction in the FWHM in running with increasing age, but with a similar duration of the FWHM in the adult group compared to the toddlers in running. There were no significant differences between groups for the phase shift of the activation waveforms between walking and running due to the large variabilities between participant sides.

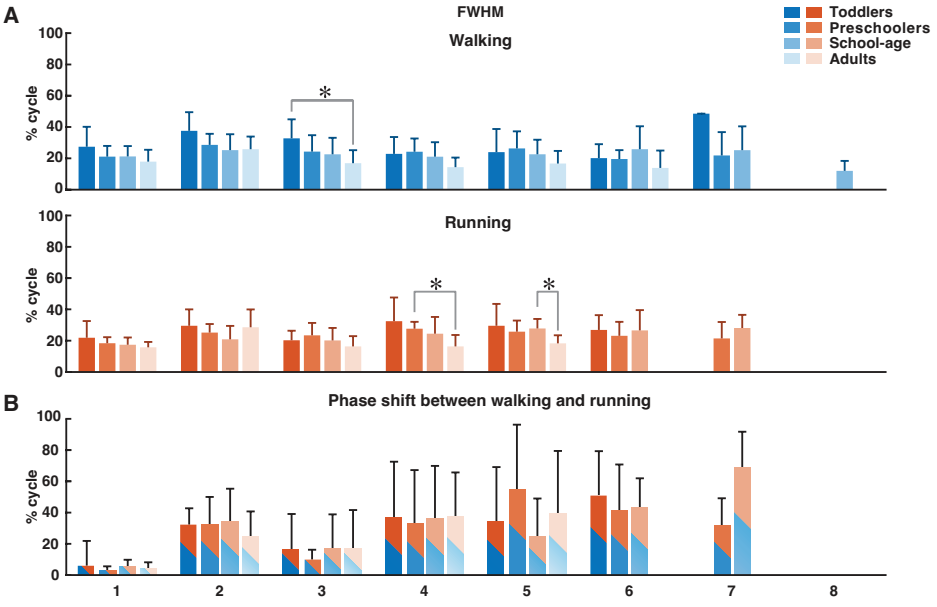

Figure 3.5: FWHM of consistent activation waveforms and phase shift between walking and running activation waveforms. (A) FWHM of all waveforms as a function of the percentage of the gait cycle for each group. Colour-coding refer to the groups. (B) Phase shift as a function of the gait cycle, determined

*using the cross-covariance between the waveforms for walking and running. Means and standard deviations are given per group. Abbreviations: FWHM, full-width half-maximum. * = $p < 0.01$.*

Previous findings in adults from Cappellini et al. (2006) showed a characteristic time lag in the temporal activation pattern corresponding to the second synergy (weighted primarily on the calf muscles) to an early moment in the gait cycle in running compared to walking. We found a similar phase shift in all groups but no significant differences between the four groups.

Discussion

Children make use of a walk-run strategy when learning to run. A weak exponential relationship between age and the FWHM of the MG muscle for both walking and running indicates this muscle to be important for development. We found a varying number of synergies between participant sides when investigating the muscle synergies during comfortable walking and running in 15 leg, trunk, and arm muscles in four age groups. It seems that a smaller number of synergies are active in the toddler group and adult groups compared to the preschoolers and school-age groups. Despite tendencies to wider activation patterns in the youngest groups, there were few significant differences between the groups. Yet, we did not find any significant differences in time lags between activation patterns between walking and running across the four groups.

Behavioral Results

We found very similar stride duration and normalized speed across groups, with only few significant differences. However, we found several significant differences in the stance duration across groups in the running condition (Figure 3.1C). This difference in stance duration appears correlated to the split of the groups, which was based on the ability to manage the running condition with a FP; cf. Figure 3.1A. Here it seems that a longer stance duration with decreasing age is directly related to the reduced ability to run with a FP.

There are two traditional ways of defining running: having a FP or the kinetic and potential energies of the center of mass being in-phase. Here, we argue that all children were running despite the lack of a FP. That is, they did not have a FP in the instructed running conditions, but their double support phases differ from the double support phases observed during walking (see, e.g., Table 3.2: Linear regression estimates). Hence, we refer to this as making use of a "walk-run strategy." Our previous research into the development of mature running patterns revealed that even in young children walking and running are distinguishable from each other and that a multitude of kinetic and kinematic parameters can serve to discriminate between immature and mature gait patterns (Bach et al., 2021a).

Muscle Activity

Tirosh et al. (2013) found that the difference of the peak MG activation for children aged 7-9 years old was around 20% of the gait cycle between walking at comfortable and fast speeds. In this study we found a shift of around 9% of the gait cycle for the toddlers (2-3.5 years), increasing to around 16% for preschoolers (3.5-6.5 years) and 19% for school-age (6.5-9 years). Put differently, the shift between walking and running in our oldest children group was comparable to what Tirosh et al. (2013) found in their study between walking and fast walking. The fast walking speed in the study of Tirosh et al. (2013) were of similar speed as the comfortable running speeds in this study for the oldest children (0.65-0.75 Froude vs 0.75 Froude in our study).

To test the hypothesis of the existence of a walk-run strategy, we examined the EMG patterns in the children for four types of locomotion: prescribed running with only FP, prescribed running with only DS, prescribed running with a mix of FP and DS within the gait cycle, and prescribed walking (see *Supplementary Material* 3.2). We found that the EMG patterns corresponding to the prescribed running condition are more similar to each other despite the lack of FP in terms of amplitude and pattern compared to the EMG patterns of the walking condition.

Number of Synergies

When employing the NMF algorithm, certain *post hoc* decisions have to be made, the most important being the number of synergies to run the NMF algorithm over. The most common methods to determine this number is to either apply a threshold or to calculate the "best-linear-fit" (e.g., Cheung, d'Avella, Tresch, & Bizzi, 2005; d'Avella, Portone, Fernandez, & Lacquaniti, 2006). The thresholds are applied to the centered R^2-value (e.g., Booth et al., 2019; Delis, Panzeri, Pozzo, & Berret, 2014; Oliveira et al., 2016; Santuz et al., 2020; Short, Damiano, Kim, & Bulea, 2020; Singh, Iqbal, White, & Hutchinson, 2018), the uncentered R^2-value (e.g., Kim, Bulea, & Damiano, 2018; Steele, Munger, Peters, Shuman, & Schwartz, 2019; Torres-Oviedo, Macpherson, & Ting, 2006), and the RA based on Frobenius norm (Kerkman et al., 2020; Zandvoort et al., 2019). Here, we opted for a different approach in that we first applied a PCA algorithm to the data as the outcome of the PCA is more likely to converge. After applying the PCA with a set threshold of 80% of the variance of the data explained, the data was reconstructed and after this, the NMF algorithm was applied. One may argue that continuing with the PCA rank-reduced dataset would be sufficient for a muscle synergy analysis. Following this route, however, may hamper the physiological interpretation of the outcome due to negative weightings and the interpretation of them. When applying NMF, the outcome is constrained to be positive which corresponds to the summation of muscle contractions which by hypothesis are always positive. We confirmed that applying PCA followed

by NMF did not greatly influence the amount of signal content lost and as such is a sound approach for the determination of muscle synergies during locomotion tasks.

We hypothesized the muscle synergies for running to "gradually" mature by means of an increased number of synergies. Our data, however, did not reveal this. Instead, we found an increase in the number of synergies with age but with a much larger number of synergies across children groups compared to the adults with a relatively larger number of synergies in the older children compared to the youngest children. Combined with what is known from motor learning and the variability we maintain in the data by concatenating across strides, the large range of synergies needed across groups and conditions to explain the variance of the data seems related to motor learning and optimizing the locomotion pattern. This is also visible in the relatively larger percentage of participant sides in the preschoolers and school-age groups needing more than six synergies in the walking condition and in the same two groups in the running condition. The relatively larger number of synergies required to explain the same variation could be due to exploration and motor learning where the lack of this increase in the toddler group could be due to the use of a "simpler" locomotor strategy to manage the tasks (Dominici et al., 2010). Adults have fine-tuned their locomotion patterns and thus we see a comparatively low number of synergies across all participant sides and conditions. The duration of the peaks of the activation patterns computed using the FWHM confirm this finding, that we consider a trend toward activation bursts for all synergies and conditions compared to the adults, who have indeed the same number of synergies as the toddlers. Another reason for the different number of synergies across groups could be due to splitting of synergies, also known as fractionization. It has been found that children aged 3-5 years, all with the ability to run over ground with a FP, show synergies that later split into more synergies for novice adult runners (Cheung et al., 2020). Likewise, the study also showed that from sedentary adults to elite adult runners, a merging of synergies occurred, which suggests that with experience, a smaller number of synergies are needed as a larger number of muscles is represented in each synergy. That is confirmed with the findings of this study. We found an increase in number of synergies from the toddlers to the school-age group, and a subsequent decrease of the number of synergies in the adult group.

Structure of Muscle Synergies

We focused the analysis on all 15 muscles recorded from the lower limb, trunk, and upper limb, but also carried out an analysis on a subset of these muscles in order to confirm the findings from the literature where the main focus is often on the lower limb muscles (*Supplementary Material* 3.1). We found that the number of synergies across groups were much lower and comparable to what has previously been found in walking in children and adults (e.g., Dominici et al., 2011; Hinnekens, Berret, Do, & Teulier, 2020; Mileti et al., 2020; Oliveira et al., 2016; Sylos-Labini et al., 2020) where four synergies is one of the most common

findings. The activation patterns and the weighting coefficients were also comparable to what has previously been found in literature. The FWHM had smaller variability within groups which suggests that the variability we observed in the full-body analysis was due to the larger set of muscles and the possible larger contribution of the trunk and arm muscles to the waveforms.

In the synergy results of the full-body analysis there was large variability in the activation patterns and the weightings within groups. These large variabilities were participant-specific, and we hypothesized that they may be related to motor-learning: children are exploring their own abilities to be able to run on a treadmill. In the adult patterns, there were a few outliers in every synergy in both activation patterns and weightings, but in general, the results were robust across participants.

There were significant differences in especially the stance duration between groups influencing the appearance of the muscle synergies. The FWHM of the synergies that appeared not significantly different between groups as a function of the full gait cycle might be considered different when identifying the relatively longer stance duration in the toddler group as running. Yet, there were fewer significant differences in the FWHM when expressed as a function of the stance duration (see *Supplementary Material* 3.3). Despite the relative differences in the stance duration for especially running, this suggests that the FWHM of the synergies did not depend on the duration of the stance phase and that differences between groups did not increase when taking the altered stance duration into account.

In the EMG signals the phase shift of the peak MG muscle activity was significantly smaller in the toddler group compared to the other groups. We expected that this would also be visible in the synergy analysis. However, we do not find any statistically significant differences in the phase shift between groups for the activation pattern (S2), commonly reported to relate to the shank muscles. In the walking conditions, the MG muscle activity clearly dominated the second synergy. In the running conditions, however, the MG muscle activity was frequently split between the first and the second synergy. This might explain why the influence of the shift in the single muscle analysis did not come to the fore in the synergy analysis.

Limitations

One limitation in this study is the large gap in age between the participant of 40 and 59 months where, for several reasons, it was not possible to recruit and measure any children. We do not expect having this data would have changed the outcomes significantly, but it would have given a larger insight into the development of running on a treadmill in this age as well.

All children in the toddler group were assisted not only with the harness during treadmill locomotion but also with handhold from either a researcher or their parent/guardian. This did not apply to any children in any of the other groups. We verified with the recorded ground reaction forces that there were no added effects of handhold compared to the harness, but the effect is present in the arm muscles on the side of the handhold as there will be less muscle activity compared to the other side. We indirectly corrected for this in the analysis by normalizing the muscle activity, not to the maximum activation for that particular muscle, but to the mean activity of that muscle. By normalizing to the mean activity of all muscles, we ensured that even muscles with low activity would not dominate the muscle synergy analysis.

Finally, all conditions referred to in this study are the prescribed conditions. This means, that the participant themselves confirmed the recorded speed was comfortable walking or running speed for them. We confirm in the Froude values that there are only significant differences between the walking speed for the toddler and adult group and the running speed between the toddler and school-age group. We also confirm that there are significant differences between the prescribed walking and running conditions for all groups (p = 0.0039, p = 0.009, $p = 3.2 \cdot 10^{-5}$, p = 0.0017, respectively).

Conclusion

Children follow a walk-run strategy when learning to run on a treadmill. Older children incorporate exploratory muscle synergies when “optimizing” their walking and running pattern on the treadmill whereas the youngest children below 3.5 years of age make use of a “simpler” motor control pattern trending toward larger bursts of activation. We believe that the increase in the number of muscle synergies for individual participant sides relates to motor learning and exploration.

Supplementary Material 3.1

Muscle synergy analysis of the 8 lower limb muscles, tibialis anterior (TA), medial gastrocnemius (MG), biceps femoris (BF), vastus medialis (VMO), rectus femoris (RF), tensor fascia latae (TFL), gluteus maximus (GM), and erector spinae (ES). The muscle synergy analysis was carried out in a similar fashion to the main text. Briefly, a principal component analysis (PCA) was applied to the mean-centered data with a cut-off of 80% of the variance explained. The mean was then added back to the now reconstructed rank-reduced dataset. Subsequently a non-negative matrix factorization (NMF) was applied on this rank-reduced dataset and run for the corresponding number of synergies for each participant side. Figure S3.1A shows that on the lower limb analysis the chosen threshold led to two-to-five synergies per group and condition. The number of synergies per participant side was larger for the walking condition compared to the running condition where more participants only required three synergies. Figure S3.1B shows that a corresponding reconstruction accuracy (RA) based on the Frobenius norm of the output of the NMF on the rank-reduced dataset resulted in a range of 65-75%. Figure S3.1C shows that for the number of synergies required for each participant side, result in an average of more than 75% reconstruction accuracy for each muscle.

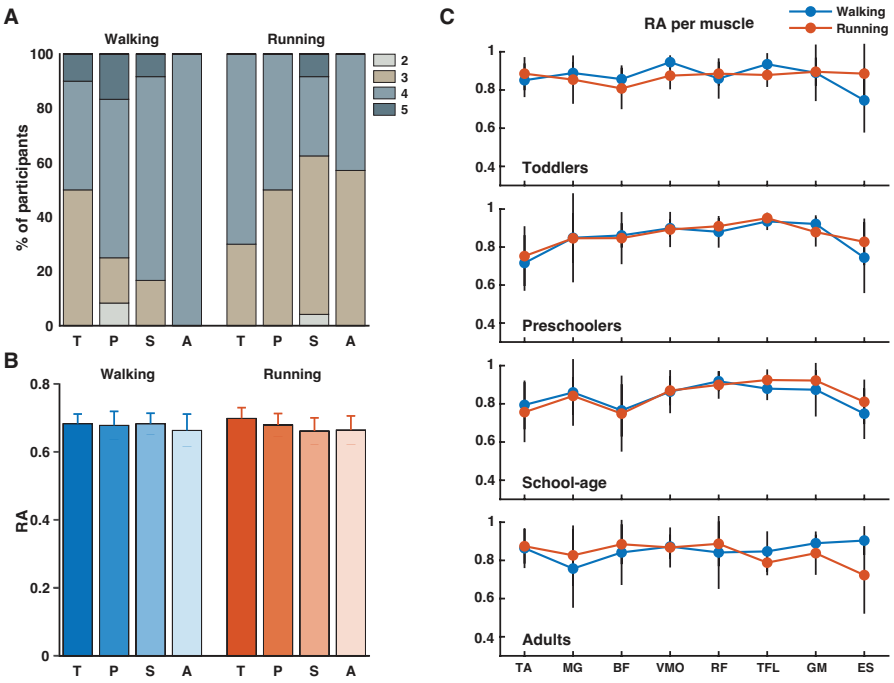

Figure S3.1: Number of synergies based on lower limb analysis and accuracy of the muscle synergy analysis. A) Number of synergies needed to account for the cycle-to-cycle variability of the lower limb EMG activities during walking and running for each group as determined by principal component analysis PCA (>80% of variance). B) The corresponding reconstruction accuracy (RA) after rank-reduction

with PCA followed by NMF. C) The RA (mean ± SD) for each muscle and condition (blue = walking, red = running). Abbreviations TA, tibialis anterior; MG, medial gastrocnemius; BF, biceps femoris; VMO, vastus medialis oblique; RF, rectus femoris; TFL, tensor fascia latae; GM, gluteus maximus; ES, erector spinae; T, Toddlers; P, Preschoolers; S, School-age; A, Adults.

The activation waveforms and the weighting coefficients of the muscle synergies of the lower limb analysis can be found in Figure S3.2. The waveforms of the first synergy peaked just after heel strike, ~5-10% of the gait cycle, and are mostly loaded on VMO, RF, TFL and GM, providing body support during weight acceptance. The waveform belonging to the second muscle synergy peaked around mid-stance for all groups and conditions and due to the relatively shorter stance duration for running, the peak is shifted to earlier in the gait cycle. The second synergy is mostly loaded by the MG muscle, especially in walking whereas in running, also the hamstring (BF) become involved. The peak of the waveform belonging to the third synergy peaked just before foot-off in the walking condition and just after in the running condition for the older children and adults, and around the foot-off for toddlers. The muscle with the largest contribution to this muscle synergy is TA for foot lift, and ES. The waveform belonging to the fourth synergy peaked during swing and was variable in which muscles contribute the most. In the case of a fifth synergy, the same applies, with large variability between participants.

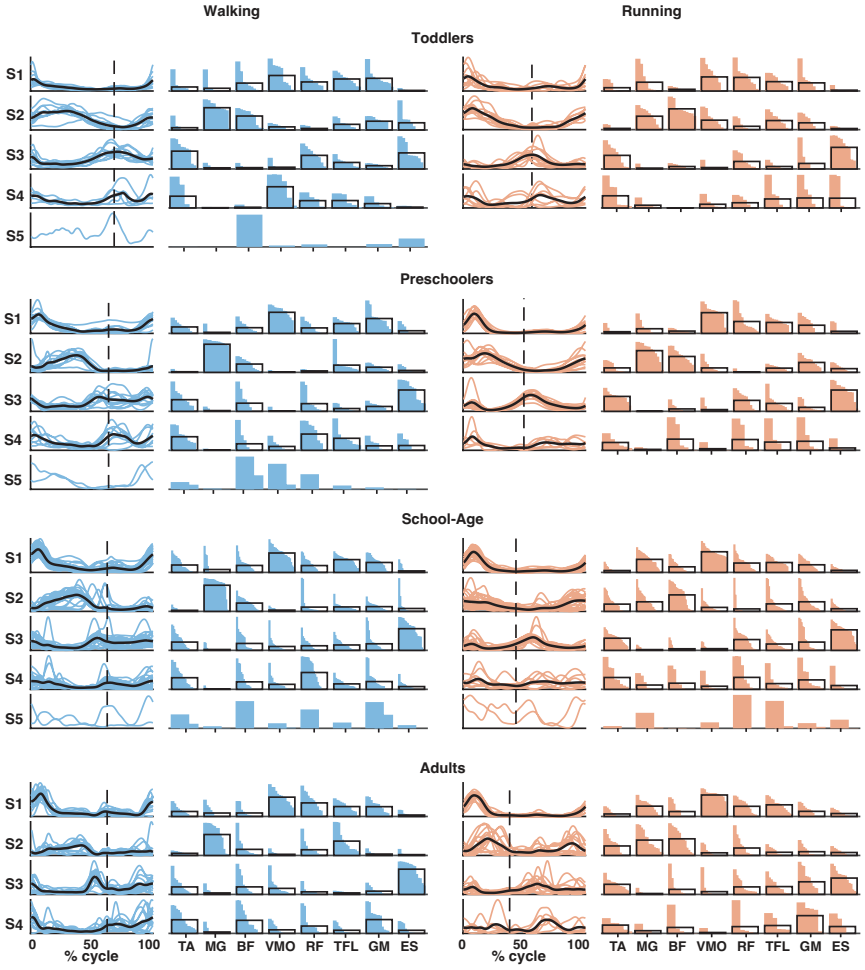

Figure S3.2: Muscle synergy structure for the four groups for walking (left in blue) and running (right in red). Vertical dotted line in activation timings plots represents the end of the stance phase. Each colored line represents a participant side, leading to one line for right side and one line for left side for each participant resulting in a total of (n=10) for the toddler group, (n=12) for the preschoolers, (n=24) for the school-age group, and (n=14) for the adult group. Black lines represent the mean. Y-axis is in arbitrary units. In the weighting plots, each colored bar represents the weighting coefficient for one participant side, the weightings are ordered based on their size. The black outlines represent the mean for the group. Abbreviations: TA, tibialis anterior; MG, gastrocnemius medialis; BF, biceps femoris; VMO, vastus medialis oblique; RF, rectus femoris; TFL, tensor fascia latae; GM, gluteus maximus; ES, erector spinae.

The results of the FWHM analysis of the lower limb analysis can be found in Figure S3.3. We found significant differences in the second synergy in the activation duration, where the toddler group had a significant longer activation duration than all other three groups (p = 0.0038, p = 0.00051, $p = 6 \cdot 10^{-5}$, respectively). We also found a significant difference in the third

synergy between the toddlers and the adults (p = 0.0058). Finally, there were no significant differences in the running condition, however, there was a trend towards the toddlers being significantly different from the adult group (p = 0.0162) in the second waveform. There were no significant differences in the phase shift between groups, similarly to the whole-body analysis.

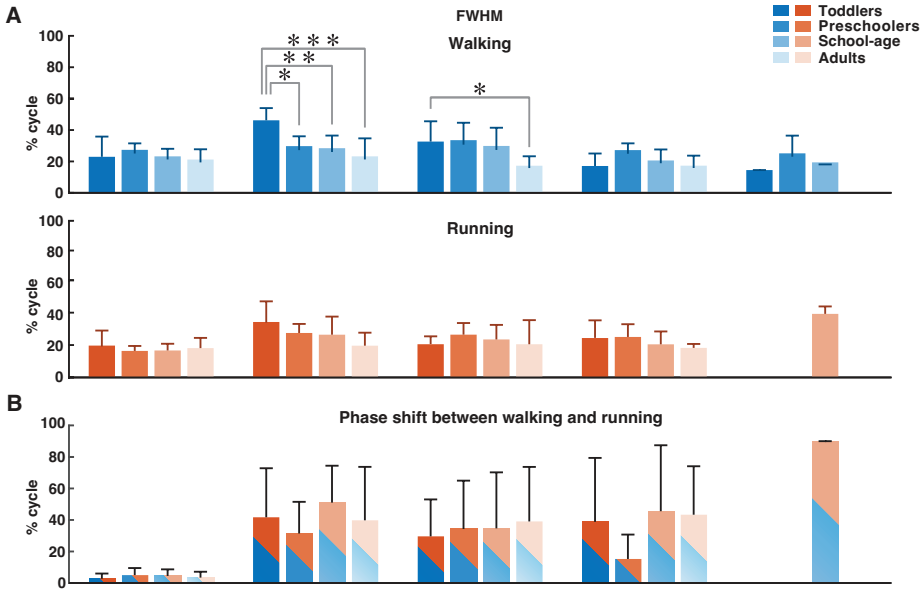

*Figure S3.3: FWHM of consistent activation waveforms and phase shift between walking and running activation waveforms. A) FWHM of all waveforms as a function of the percentage of the gait cycle for each group. Color-coding refers to the groups. B) Phase shift between walking and running activation waveforms as a function of the gait cycle, determined using the cross-covariance between the waveforms for walking and running. Means and standard deviations are given per group. Abbreviations: FWHM, Full-width half-maximum. * = $p < 0.01$, ** = $p < 0.001$, *** = $p < 0.0001$.*

Supplementary Material 3.2

EMG patterns for children participants split into four categories based on the presence of the DS or FP in the gait cycle: prescribed running with only FP, prescribed running with only DS, prescribed running with both FP and DS present (Mix) in the gait cycle, and prescribed walking.

We show that the walking condition is different from the prescribed running conditions independent of the behavioral patterns, i.e., flight phase or double support phase or a mix thereof.

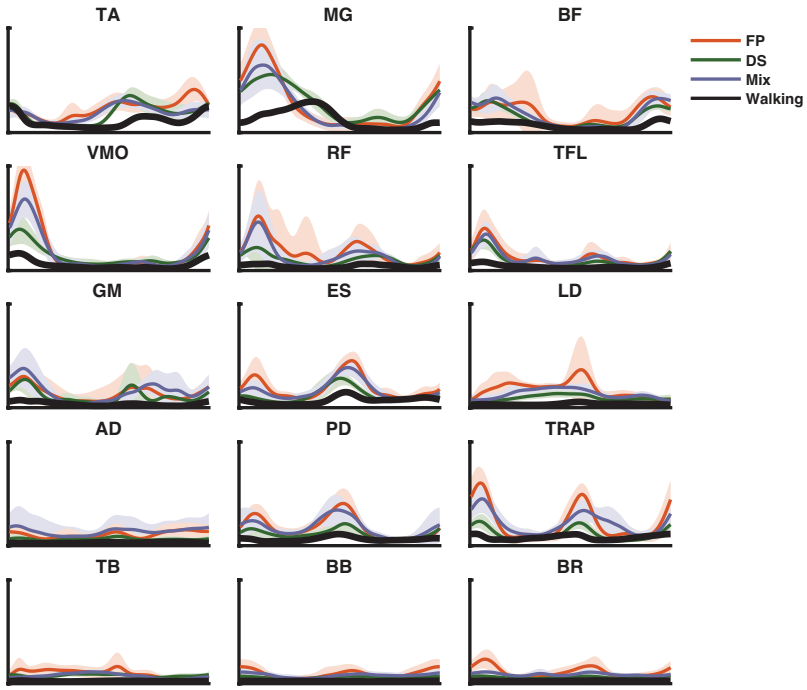

Figure S3.4: Ensemble averaged EMG patterns of the children participants split into behavioral patterns. Four patterns are shown: prescribed running with only flight phase (FP in red), prescribed running with only double support (DS in green), prescribed running with a mixture of FP and DS within the gait cycle (Mix in blue) and prescribed walking (black). The shaded areas refer to the standard deviations across participants for the three prescribed running conditions. Abbreviations: TA, tibialis anterior; MG, gastrocnemius medialis; BF, biceps femoris; VMO, vastus medialis oblique; RF, rectus femoris; TFL, tensor fascia latae; GM, gluteus maximus; ES, erector spinae; LD, latissimus dorsi; AD, anterior deltoid; PD, posterior deltoid; TRAP, trapezius; TB, triceps brachii; BB, biceps brachii; and BR, brachioradialis.

Supplementary Material 3.3

FWHM of synergy one-eight, of the full-body analysis, expressed as a percentage of the mean stance phase for each group can be found in Figure S3.5. Data are presented as the group means and error bars represent standard deviations. There is only one significant difference between the groups in terms of FWHM which are related to synergy three for walking (p = 0.0086). There is a trend for the FWHM for running to be larger with younger age, whereas there is a trend towards the opposite for walking. This could be a factor of the relatively longer stance phase in running for the youngest group compared to the other groups.

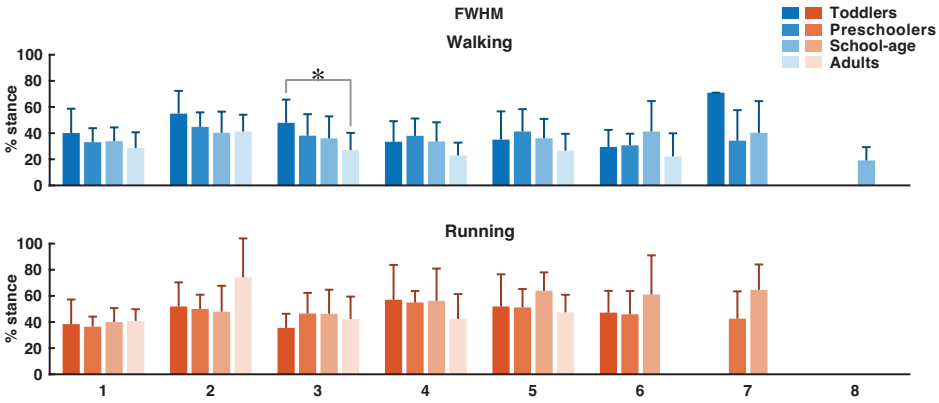

*Figure S3.5: FWHM of consistent activation waveforms of full-body analysis, expressed as percentage of the mean stance phase duration. Color-coding refers to the groups. Means and standard deviations are given per group. Abbreviations: FWHM, Full-width half-maximum. * = $p < 0.01$.*

Chapter 4

DEVELOPMENT OF RUNNING IS NOT RELATED TO TIME SINCE ONSET OF INDEPENDENT WALKING, A LONGITUDINAL CASE STUDY

Bach MM, Zandvoort CS, Cappellini G, Ivanenko Y, Lacquaniti F, Daffertshofer A, and Dominici N

Front Hum Neurosci, 2023, 17: p. 1101432

Abstract

Children start to run after they master walking. How running develops, however, is largely unknown. We assessed the maturity of running pattern in two very young, typically developing children in a longitudinal design spanning about three years. Leg and trunk 3D kinematics and electromyography collected in six recording sessions, with more than a hundred strides each, entered our analysis. We recorded walking during the first session (the session of the first independent steps of the two toddlers at the age of 11.9 and 10.6 months) and fast walking or running for the subsequent sessions. More than 100 kinematic and neuromuscular parameters were determined for each session and stride. The equivalent data of five young adults served to define mature running. After dimensionality reduction using principal component analysis, hierarchical cluster analysis based on the average pairwise correlation distance to the adult running cluster served as a measure for maturity of the running pattern. Both children developed running. Yet, in one of them the running pattern did not reach maturity whereas in the other it did. As expected, mature running appeared in later sessions (>13 months after the onset of independent walking). Interestingly, mature running alternated with episodes of immature running within sessions. Our clustering approach separated them. An additional analysis of the accompanying muscle synergies revealed that the participant who did not reach mature running had more differences in muscle contraction when compared to adults than the other. One may speculate that this difference in muscle activity may have caused the difference in running pattern.

Introduction

Independent walking is a major developmental milestone for children. In typically developing children it commonly occurs between 9 and 15 months of age (Piper & Darrah, 1994; Storvold, Aarethun, & Bratberg, 2013). While most parents can recall at what age their children started walking independently, almost none of them can put a finger on when the children started running. One reason for this might be the difficulty to tell walking and running apart. This is not so in adults' locomotion, where even a still picture may serve to distinguish walking from running. Obviously, the presence of a phase of flight can do the job, i.e., when no leg touches the ground. In very young children, discriminating walking from running is often not that straight-forward. Early running may appear as fast walking which raises the question on which parameters these two locomotory states really differ.

In a previous work we studied 5-9-year-old children (Bach et al., 2021a). There we realized that classical measures for classifying walking and running mostly fail. Neither the presence of a flight phase nor the phase relation of energetics was sufficient to distinguish mature from immature running patterns in these children. We suggested using a 'shotgun' approach involving a large set of kinetic and kinematic parameters with subsequent principal component analysis (PCA) and hierarchical clustering that allowed for separating the degree of maturity of walking and running with great success.

As it turns out, there is no immediate agreement between the chronological age and the maturity of treadmill walking and running patterns (Bach et al., 2021a). Yet, the amount of walking experience clearly influences the walking pattern and that improves with practice (Cheron, Bouillot, et al., 2001; Forssberg, 1985; Ivanenko et al., 2005; Sutherland, Olshen, Cooper, & Woo, 1980). Be it the recovery of mechanical energy, the external work, or the inter-segmental kinematic coordination, all these features gradually evolve toward those of adults when walking experience increases (Ivanenko, Cappellini, et al., 2007; Ivanenko, Dominici, et al., 2004). Not only do joint kinematics and kinetics improve progressively (Hallemans, De Clercq, & Aerts, 2006), but also the duration of electromyographic activity of the gastrocnemius medialis muscle is reduced (Cappellini et al., 2016). We believe that the (gain of) walking experience also influences the development of running which ultimately tends toward the mature pattern observed in adults. Very recently, it has been shown that the motor control of running is influenced by motor exploration and learning (Bach, Daffertshofer, & Dominici, 2021b). As such, it seems quite likely that developmental characteristics of walking are also mirrored in the development of running.

Tackling such commonalities is a challenge, which may fail when following more traditional routes in studying locomotion, namely from either a sole neuromuscular (e.g., Ivanenko, Poppele, & Lacquaniti, 2006) or a sole biomechanics perspective (e.g., Liu et al., 2022;

Rozumalski et al., 2015). We advocate combining both perspectives as several recent studies suggest their interdependence during infancy (Bekius et al., 2021; Cappellini et al., 2016; Dewolf, Sylos-Labini, et al., 2020; Dominici et al., 2011; Forssberg, 1985). At the onset of independent locomotion, walking and running may overlap so strongly for their neural and biomechanical control that some consider walking and running in infants not as distinct modes of locomotion as they are in adults (Dewolf, Sylos-Labini, et al., 2020; Vasudevan et al., 2016). If walking and running are intertwined when infants learn to walk, then at which moment will they 'separate' as much as in adults?

Answering the relation between the onset of independent walking and the development of running requires longitudinal assessments spanning several years. To quantify the influence of time since onset of independent walking, one must assess participants at the very onset of independent walking (in fact assesement have to start even before that). And recordings must be frequent enough to properly sample the development of running. We monitored two typically developing children for about three years after their first independent walking steps. We conducted seven experimental sessions during each of which we guaranteed more than 100 running strides when recording leg and trunk 3D kinematics and electromyography (EMG). Using the aforementioned shotgun method that encompasses kinematics and neuromuscular data, we investigated the earliest development of running. Possible mechanisms underlying the coordinated locomotion were explored through muscle synergy analysis and by integrating some of the corresponding outcome parameters in the shotgun approach. We expected this approach to allow for determining the degree of maturity also in very young children who just learned / are learning to run. We expected the development of running maturity to be similar, if not identical, to the onset of independent walking when stratifying its time course.

Methods

Participants

We recruited two children and five adults. The two children (1 male / 1 female) were recruited before taking their first independent steps as part of a larger study (Zandvoort, Daffertshofer, & Dominici, 2022). The adult participants (4 male / 1 female, 30-45 years old) were recruited by word-of-mouth as part of a previous study (Cappellini et al. 2006). Both the adults and the legal guardians of both children gave written informed consent in compliance with the Declaration of Helsinki. The inclusion of the children was approved by The Scientific and Ethical Review Board of the Faculty of Behavioural & Movement Sciences, Vrije Universiteit Amsterdam, Netherlands (File number: VCWE-2016-082). The inclusion of adults was in accordance with the procedures of the Ethics Committee of the Santa Lucia Institute, Rome, Italy (Prot. CE-AG4-PROG.99-155).

The first recording session of each child participant took place within 9 days of taking at least four consecutive steps without support. The time of first indpendent steps were relayed by the parents to the researchers.

Setup

Seven sessions were recorded from first steps (FS) to ~32 months after onset of independent walking for each of the two children (P1 and P2). The initial plan was to record each child every three months from their first independent steps until one year after onset of independent walking with a follow-up every six months from that timepoint. As this was not achieved with the first child, we matched the second child to the spacing of the recordings of the first child. As sketched in Figure 4.1, the following sessions were recorded: first steps session (FS), 2 months after the FS (denoted +2), as well as 6 months (+6), 9 months (+9), 13 months (+13), 19 months (+19), and finally 32 months after FS (+32).

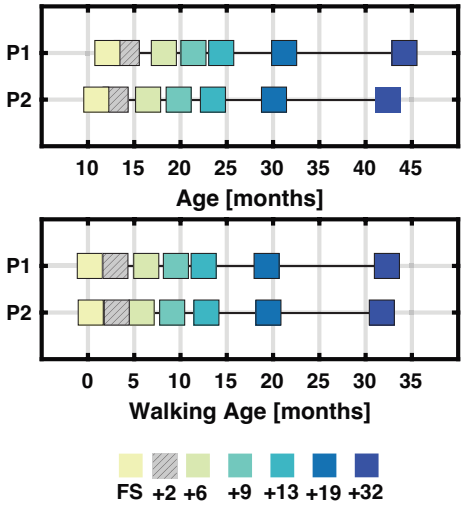

Figure 4.1: Overview of age and walking age (time since onset of walking) for each session/child. A total of seven sessions were recorded for each child. At the end, six sessions were analyzed for each child, and these were matched based on walking age (bottom plot) in months. A few weeks separate the different sessions between P1 and P2. +2 is hatched as not analysed due to poor data quality. FS: First steps, +2, +6, +9, +13, +19, +32 refers to the number of months since first steps, i.e., time since onset of independent walking.

The experiments consisted of locomoting overground and on a pediatric treadmill (N-Mill 60 × 150 cm, Motek Medical BV, Amsterdam, the Netherlands) with either no support or trunk/hand support. During the first session (FS), only walking was recorded. During the subsequent sessions, we recorded both walking and fast walking and/or running. Children were tasked to move from one end of the lab to the other end. They were instructed to either walk or run, sometimes enticed with toys or food. When the child was instructed to run, but the speed was between their normal running and walking speed, then the trial was noted as "fast walking". For sessions +6, +9, +13, +19, and +32, only the trials labelled as fast walking or running were retained for further analysis.

All children sessions, except one, were recorded in the BabyGaitLab of the Department of Human Movement Sciences at the Vrije Universiteit Amsterdam, The Netherlands; the remaining session was recorded at the clinical gait laboratory of the Department of Rehabilitation Medicine at the Amsterdam UMC (location VUmc). The adults were recorded in the laboratory of the Santa Lucia Foundation, Rome, and included in a previous publication (Cappellini et al., 2006).

The children were barefoot during all recordings and wore only diapers or underpants. When locomoting overground, they were encouraged by researchers/parents to walk/run in a straight line. Sometimes they were supported by handhold. When on the treadmill, the speed was adjusted to a comfortable speed and type of locomotion (walk or run). On the treadmill, the children were supported on trunk or by handhold by the researcher/parent. Adults were running at 7 and 9 km/h on a treadmill (EN-MILL, 3446.527, Bonte Zwolle BV, Netherlands) wearing shoes.

Data acquisition

Toddlers

During each session for P1 and P2, bilateral 3D kinematics was recorded using reflective markers and Vicon motion capture system (Oxford, UK) with 10 (12 for the session recorded at VUmc) infrared cameras affixed to the ceiling, sampled at 100 Hz and one (four for the session recorded at VUmc) video camera (Vicon camera Oxford, UK) sampled at 100 Hz (50 Hz for the session recorded at VUmc). Reflective markers (14 mm) were placed bilaterally on the acromion (SHO), iliac crest (IL), greater trochanter (GT), lateral femur epicondyle (LE), lateral malleolus (LM) and fifth metatarsal (VM). For each session, a static trial was recorded where the participant was standing still to be used for correction of the joint angles. We recorded electromyography (EMG) bilaterally from the following 16 muscles: tibialis anterior (TA), medial gastrocnemius (MG), lateral gastrocnemius (LG), soleus (SOL), rectus femoris (RF), vastus medialis oblique (VMO), vastus lateralis oblique (VLO), semitendinosus, biceps femoris (BF), tensor fascia latae (TFL), gluteus maximus (GLM), erector spinae level L2 (ES), latissimus dorsi, trapezius, deltoid, and biceps brachii. EMG was recorded using mini-golden reusable surface EMG disc-electrode pairs (15-mm-diameter electrodes, acquisition area of 4 mm^2), placed at the approximate location of the muscle belly on the cleaned skin, with interelectrode spacing of ~1.5 cm. The placement followed the SENIAM recommendations (Hermens et al., 1999), and were sampled at 2 kHz. Movement artifacts were minimized by fixating the electrodes and wireless EMG sensors to the leg using elastic gauzes. EMG was recorded with a wireless system (Mini wave plus, Zerowire; Cometa, Bareggio,Italy) and saved in Nexus software as backup. EMG recordings included an online bandpass filter 10 Hz-1 kHz. For each session, we also recorded electroencephalogram (EEG) using pre-gelled caps (ANT

neuro, Hengelo, The Netherlands) which could not be included in the analysis due to too many artefacts.

The pediatric treadmill recorded vertical ground reaction forces with a sampling frequency of 1 kHz. For each session, the anthropometrics of the child was measured and recorded, such as the total length, the weight measured by weighing scales m, the body weight measured by treadmill $bw_{\mathrm{treadmill}}$, and the length and circumference of the main body segments (Schneider & Zernicke, 1992). The segment lengths estimated from the static trials were used to determine leg length.

When running on the treadmill, children were supported on the trunk or by handhold by the researcher/parent. The amount of body weight support (BWS) provided to the children during treadmill trials were estimated as the percentage reduction of the mean vertical forces compared to $bw_{\mathrm{treadmill}}$. More than 30% of BWS may result in altered foot trajectories and temporal patterns of the muscle synergies in toddlers walking (Dominici, Ivanenko, & Lacquaniti, 2007; Kerkman, Zandvoort, Daffertshofer, & Dominici, 2022). Thus, only strides with less than 30% BWS were retained for further analysis (∼22 and ∼28% of strides were removed for P1 and P2, respectively).

Adults

Data acquisition has been described previously in Cappellini et al. (2006). In brief, we used reflective markers (14 mm) and Vicon motion capture system (Vicon camera Oxford, UK, sampling at 100 Hz) with 9 infrared cameras spaced around the treadmill to record bilateral 3D kinematic. Reflective markers were placed bilaterally on SHO, IL, GT, LE, LM, heel, and VM; these are the same anatomical locations as used for P1 and P2 (except for the heel marker). The following 32 muscles were recorded unilaterally: TA, flexor digitorum brevis, LG, MG, SOL, peroneus longus, VLO, VMO, RF, sartorius, BF, semitendinosus, adductor longus, TFL, GLM, gluteus medius, external oblique, internal oblique, latissimus dorsi, iliopsoas, rectus abdominis, erector spinae recorded at T1, T9, and L2 (ES), biceps brachii, triceps brachii, deltoideus (anterior and posterior portions), trapezius (inferior and superior portions), sternocleidomastoid, and splenius using Delsys electrodes (model DE2.1, Delsys, Boston, MA). The signals were amplified, filtered (20-450 Hz), and sampled at 1 kHz. Height and weight were recorded for all participants. Leg lengths were not recorded but could be inferred from the 3D kinematics.

Data analysis

Kinematics and gait parameters

Foot contact and foot-off were manually determined for both sides by visual inspection using digitial video recordings and the foot marker trajectories from the Nexus software (Vicon, Oxford, UK) in the children. For the adults, foot contact was defined as the local minima of

the heel marker and foot off as the lift-off of the VM marker by 2 cm from the minimum detected at stance (Cappellini et al., 2006). Strides with jumping, dragging etc. were excluded from further analysis as was gait initiation and termination. Flight phases and double support phases were determined based on right and left foot contact and foot off. The Froude number (Fr) is a dimension-less parameter suitable for the comparison of locomotion in subjects of different size (Alexander & Jayes, 1983). The Froude number was computed for all gait cycles based on the mean velocity of the horizontal IL marker (v), leg length (l), and the gravitational constant (g) using: $Fr = v^2/(g \cdot l)$. Kinematic parameters were calculated based on the 3D kinematics of the lower legs and trunk. The body was modeled as an interconnected chain of rigid segments: SHO-IL for the trunk, IL-GT for the pelvis, GT-LE for the thigh, LE-LM for the shank, and LM-VM for the foot. The main limb axis was defined as the virtual line connecting GT and VM. Joint and elevation angles were generated accordingly. A total of 101 parameters were estimated for each gait cycle using a custom-written algorithm (Bach et al., 2021a; Dominici et al., 2012) to provide a comprehensive quantification of locomotor patterns. They can be functionally split into themes such as temporal features, limb endpoint trajectory, stability, joint and segment angles, joint and segment angular velocities, intra- and interlimb coordination, intersegmental coordination, and pendulum mechanism. Parameters that were directly influenced by body size were normalized to leg length. For a detailed list we refer to *Supplementary Material* 4.1. All parameters were visually inspected for outliers due to experimental errors (e.g., partially missing markers) and, if the errors were present, the stride was removed from further analysis (~4 and ~8% of total recorded strides for P1 and P2, respectively).

Electromyography and muscle synergies

Of the recorded muscles, the following 11 (bilateral for the children, unilateral for the adults) muscles TA, MG, LG, SOL, RF, VMO, VLO, BF, TFL, GLM, and ES were retained for further analysis. EMG data were visually inspected, and artifacts were removed using a custom-written burst-detection algorithm (Bach et al., 2021b; Zandvoort et al., 2022). After high-pass (2nd-order bidirectional Butterworth filter at 20 Hz; Bach et al., 2021b; De Luca et al., 2010; Willigenburg et al., 2012) and notch filtering (2^{nd}-order bi-directional Butterworth around k·50 Hz, k = 1,…,10, with half-bandwidth of 0.5 Hz), the EMG data were rectified using the modulus of the analytic signal and finally low-pass filtered (bi-directional 2^{nd}-order Butterworth filter at 10 Hz) to obtain the corresponding EMG envelopes (Bekius et al., 2021; Dominici et al., 2011; Oliveira et al., 2016). These envelopes were time-normalized to 200 samples per gait cycle computed relative to the ipsilateral foot contact.

Before applying the muscle synergy analysis, the amplitude of the EMG activity was normalized to the mean activity for each muscle, interpolated in case of missing values (for a maximum of 50% of the stride) within one stride, and finally concatenated for each session in

a [#strides × #samples] × #muscles matrix ([n × 200] × 11). Post-hoc analysis of the interpolation revealed that the mean interpolation was 4.5% for P1 (range: 0.5%-19.5%) and 4.6% for P2 (range: 0.5%-34%) in approximately 22% and 22.6% of the total number of strides, respectively. The gaps were not necessarily consecutive. No interpolation was done on the adult data. Muscle synergies were calculated using weighted non-negative matrix factorization (WNMF) algorithm (with a maximum of $2{\cdot}10^6$ iterations, and a completion threshold of 10^{-6}) to account for missing strides (Goudriaan et al., 2022; Li & Ngom, 2013). There were missing data in few strides where no EMG was recorded for one or two muscles (Goudriaan et al., 2022; Li & Ngom, 2013; Shuman, Goudriaan, Desloovere, Schwartz, & Steele, 2019). WNMF decomposes the original EMG matrix into a small set of temporal activation patterns (C) and weighting coefficients (W):

$$EMG = \sum_{i=1}^{N} C_i \cdot W_i + \epsilon, \qquad N \leq \#\text{muscles}$$

With ϵ denoting the residual error. To assess the quality of the reconstruction, the reconstruction accuracy (Bach et al., 2021b; Kerkman et al., 2020; Kerkman et al., 2022; Zandvoort et al., 2019) was determined using the Frobenius norm of the residuals

$$RA = 1 - \frac{\|EMG - (W \cdot C)\|_F}{\|EMG\|_F}$$

We determined the number of synergies for further analysis via the “best linear fit” proposed by Cheung et al. (2005). For this, one computes the mean squared error for each linear fit of the reconstruction quality for first 1-10 synergies, then 2-10 until calculated for 9-10 synergies. When the mean squared error drops below 10^{-4} the reconstruction quality is said to plateau defining the number of synergies to retain. To align the number of synergies across sessions, the best linear fit method was applied to each session of the children and the adults, respectively, and the median number of synergies across these 13 sessions that fulfilled this criterion was chosen, thus avoiding a bias towards the mean in the case of outliers.

The output of the WNMF is not ranked and as such post-hoc sorting has to be applied to compare synergies across sessions. To do so, the weighting coefficients were grouped using hierarchical clustering during which we ensured that the maximum number of clusters corresponded to the maximum number of synergies (i.e., a maximum of three clusters were allowed with a three-synergy solution). For the synergy analysis, the grand average of all strides for each synergy was determined per session.

To quantify differences in the duration of the temporal activation patterns of the muscle synergies, we estimated the full width at half-maximum (FWHM) per activation pattern and stride. Here we first subtracted the minima of the activity patterns – in the case of several

peaks, the FWHM was calculated for the main peak, i.e., the peak with the highest amplitude and in case of boundary peaks, an assumption was made that the shape of the peak was symmetric (Cappellini et al., 2006). Timing differences were determined via the center-of-activity (CoA) per activation pattern and stride (Labini, Ivanenko, Cappellini, Gravano, & Lacquaniti, 2011; Sylos-Labini et al., 2014; Yakovenko, Mushahwar, VanderHorst, Holstege, & Prochazka, 2002). The CoA is particularly useful when multiple peaks are present or when low activity does not allow for identifying a single peak. CoA also makes the comparison across sessions feasible. Here, we defined it as

$$CoA = \tan^{-1}\left[\frac{\sum_{t=1}^{200}(\cos\theta_t \cdot EMG_t)}{\sum_{t=1}^{200}(\sin\theta_t \cdot EMG_t)}\right]$$

where, θ denotes an angle that varies between 0-360° corresponding to 0-100% of the gait cycle (t=200 samples). The FWHM and the CoA for the extracted synergies were retained and added to the list of gait parameters for further analysis to have a spatial as well as temporal measure for the activation patterns of the muscle synergies (*Supplementary Material* 4.1).

PCA and clustering

We sought to quantify how running develops over time from the first independent steps. Strides from trials in which the children were instructed to run (that were labelled either fast walking or running) were included. We chose for this 'blind' approach as our previous research revealed that in very young children the presence of a flight phase is not a solid indicator for the presence of running (Bach et al., 2021a). We employed principal component analysis (PCA) in combination with clustering of several parameters extracted from the kinematics and muscle synergies for all strides (Bach et al., 2021a). PCA served to reduce covariation between parameters and clustering to find unbiased classification.

For every participant, parameters were combined in a [(number of sessions × number of strides) × number of parameters] matrix [1730 × 107] and z-scored prior to PCA, see *Supplementary Material* 4.1 for a full overview of the parameters. The z-scoring was applied to ensure that all parameters could potentially contribute to the same degree in the PCA (if the variance differs between parameters it may cause a bias in the PCA-ranking). We selected the three leading principal components (PCs) and included them in the clustering, as this turned out sufficient for our classification purposes (Bach et al., 2021a; Courtine et al., 2009; Dominici et al., 2012; Friedli et al., 2015; Phinyomark, Hettinga, et al., 2015). The degree to which the different parameters influence the first three PCs can be given by their $loadings = \upsilon \cdot \sqrt{\lambda}$, where υ denotes the eigenvector of a PC and λ its eigenvalue. We considered a parameter as a strong contributor if the corresponding loadings exceeded the 95% confidence interval $CI_{95} = 1.96/\sqrt{n}$ where n = 107 parameters.

Finally, we applied hierarchical clustering with correlation distance (Bach et al., 2021a). We first built a dendrogram (Milligan, 1980; Murtagh & Contreras, 2011; Xu & Wunsch, 2005) using average links (unweighted pair group method with arithmetic mean). The cophenetic correlation coefficient was determined (CCC; Sokal & Rohlf, 1962) to establish the degree of fit of the clustering technique. The Calinzki-Harabasz stopping rule (Milligan & Cooper, 1985) and visual inspection were utilized in unison to determine the optimal number of clusters, with the inspection focusing on categorization of first steps walking and running and the classification of mature and immature running. We distinguished mature from immature locomotion by computing the average pairwise correlation distance from every stride belonging to a distinct cluster to the adults running. Put differently, the average pairwise correlation distance served as a measure for gait maturity with the adult gait pattern as reference.

Statistics

Means and standard deviations are provided unless otherwise specified. To investigate whether the dimensionless speed Fr and the FWHM of the muscle activation patterns were different between sessions for each participant and comparable to the adults, we used a non-parametric test, the Kruskal-Wallis test, as the data were not normally distributed, confirmed using a Kolmogorov-Smirnov goodness-of-fit hypothesis test. If a statistically significant effect was found, a Bonferroni correction was applied to account for multiple comparisons. With 7 mixed within-between participants (6 sessions for the toddlers and 1 session for the adults), the used significance threshold was $\alpha = 0.05/7 = 0.007$.

Results

Our child participants were comparable in terms of age as well as time in months since first independent steps. P2 started walking at 10.6 months whereas P1 started walking at 11.9 months. Both children were relatively early walkers. The median age of independent walking lies between 11.4 months (Piper & Darrah, 1994) and 13.0 months (Storvold et al., 2013). The different sessions were comparable and within a few weeks of each other in terms of walking age. All results were ordered based on the walking age to investigate the influence of walking age.

The first sessions, the FS sessions, were recorded within 9 days of when the children performed at least four independent strides, and for these sessions only walking was recorded. In the subsequent sessions, the children were instructed to either walk or run, but only strides from trials when instructed to run (that were labelled as fast walking or running during the experiment, see *2.2 Setup* for further details) were analyzed.

Six out of the seven sessions for each child were retained for further analysis with the first session being the session containing the first independent steps (FS). The +2 months sessions were excluded due to insufficient data quality or an insufficient amount of data recorded. See Figure 4.1 for an overview of all included sessions and respective ages and walking ages for P1 and P2.

The mean number of strides included per session was (mean ± std) 133 ± 73 strides for the toddlers' sessions and a total of 105 strides for the adults (range 14-24 per participant). The FS session for P1 had an exceptionally large number of strides that could be included. To make the number of strides more balanced across sessions, only overground strides with a velocity of more than 0.5 km/h were retained, reducing the total number of strides from 729 to 254 strides for this specific session. Several strides with a Froude number exceeding 1.5 were excluded from the sessions +19 and +32 for both P1 (∼25 strides in total) and P2 (∼60 strides in total) as they were deemed to be sprinting and as such were not comparable to the other data.

The FS sessions had only strides with double support phases whereas the remaining sessions had a mixture of strides with double support and flight phase. The double support and flight phases were expressed as a percentage of the gait cycle. Double support phases were present in all sessions (after the FS sessions) of P1 and P2, with a tendency towards an increased amount of flight phase in the last sessions. The flight phase was shorter than in the adults. The linear regression of the double support phase revealed a significant effect of session, no effect on participant, and only a small interaction effect between session and participant (cf., Figure 4.2 and *Supplementary Material* 4.2). The linear regression of the flight phase revealed a significant effect of both session and participant and an interaction effect as well. The normalized speed (Froude number) of the two FS sessions was significantly different from all other sessions for that participant and to that of the adults ($p < 1 \times 10^{-14}$ for all sessions for both participants). The normalized speeds ranged between 0.34 and 0.69 for the running sessions and three sessions of P1 (+6, +13, and +19, $p < 2 \times 10^{-9}$) and two sessions of P2 (+13 and +19, $p < 2 \times 10^{-7}$) were significantly different from the adults, cf. Figure 4.2.

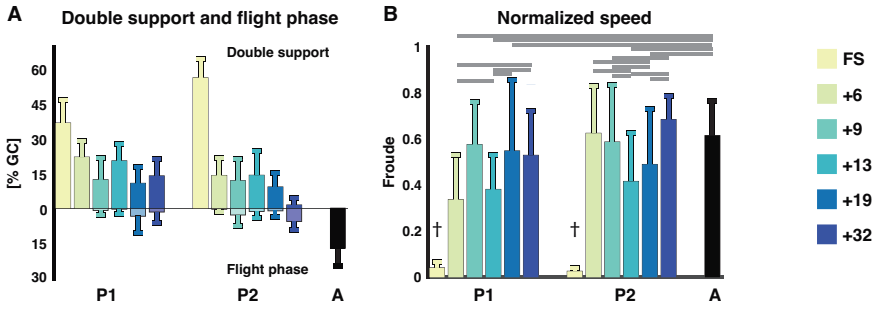

Figure 4.2: Temporal gait parameters. A) Flight phase and double support phase as a percentage of the gait cycle (mean±std). Double support phases are on the top with flight phases being the negative percentages below. B) The normalized speed expressed as the Froude number ($v^2/g \cdot l$) for each session and participant (mean±std). † Denotes a significant difference between current session and all other sessions for that participant as well as adults ($p < 0.007$). Horizontal lines denote significant differences between the Froude numbers for the sessions. FS: First steps, %GC: percentage gait cycle, +6, +9, +13, +19, +32 refers to the number of months since onset of independent walking.

Like the presence of a flight phase, the Froude number might also not be a good indicator of whether a child is running. The Froude number, the normalized speed, is useful to determine the optimal speed at which to transition from walking to running or vice versa, and in adults this transition occurs at a Froude value of 0.5 (Gatesy & Biewener, 2009; Kram, Domingo, & Ferris, 1997) which the adults exceeded in this study. The mean of the Froude numbers of the toddlers also exceeded 0.5 (P1: 0.58±0.18, 0.55±0.31, 0.53±0.19 for sessions +9, +19, +32 and P2: 0.63±0.21, 0.59±0.25, 0.69±0.10 for sessions +6, +9, +32, respectively) except for +6 (0.34±0.20) and +13 (0.38±0.15) for P1 and +13 (0.42±0.21) and +19 (0.49±0.24) for P2. See above and Figure 4.2 for statistics. However, it is possible to walk at a Froude value higher than 0.5, it is just not as energetically efficient.

PCA and Clustering

The first three principal components (PCs) accounted for >45% of the total variance of the data. The scatterplots in Figure 4.3, detail the spread of data in the 3 PC spaces. We observed that PC1 can distinguish between the FS sessions and the remaining sessions, whereas PC2 seemed to distinguish adult running and later sessions from the early sessions. The loadings associated with these three PCs (*Supplementary Material* 4.1 and 4.3) were all within the CI_{95} except for three. The three parameters not contributing were parameters 74, 79, and 88, i.e., the phase relationship between the two limbs (a measure for interlimb coordination), projection of 1st eigenvector on the shank axis (a measure intersegmental coordination; Bekius et al., 2021; Bianchi, Angelini, & Lacquaniti, 1998; Borghese, Bianchi, & Lacquaniti, 1996; Dominici et al., 2010; Ivanenko, Dominici, et al., 2007), and ratio of left to right leg cycle duration (a measure for intersegmental coordination).

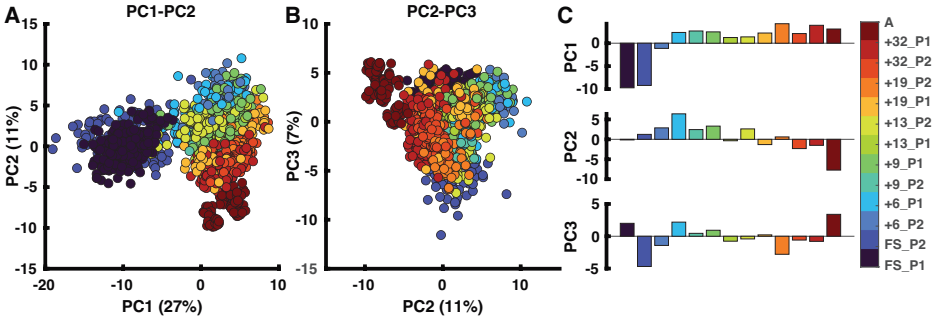

Figure 4.3: Principal component analysis (PCA). In the two left panels, each dot represents one stride. A) PCA results in PC1-PC2 space. B) The outcome of the PCA in PC2-PC3 space. C) The weightings of all sessions ordered based on walking age, so not ordered per participant. PC1 distinguishes the FS sessions from the other sessions with PC2 distinguishing "mature" from "immature" running. PC: Principal component, FS: First steps, +6, +9, +13, +19, +32 refers to the number of months since onset of independent walking.

We found three clusters, see *Supplementary Material* 4.3 for details. The clustering results are depicted in Figure 4.4A. Every node represents strides from a certain session ordered from lowest to highest walking age from left to right. The lines connecting the sessions to the clusters represent the number of strides larger than ten percent that is present in a certain cluster. The cluster nodes are sized based on the number of strides in each cluster. The three-cluster solution resulted in one cluster that included the adults ("A" on the lower far right of the circle) which could be interpreted as the mature running cluster (C1 cluster), one containing the immature running strides (C2 cluster) and one that included the "walking" strides (C3 cluster). The "walking" cluster contained all strides of the two FS sessions as well as a percentage of strides each from the following sessions (session [% strides]): +6 P1 (81%), +6 P2 (99%), +9 P1 (31%), +9 P2 (52%), +13 P2 (51%). The "immature running" cluster contained some strides from all sessions, except the two FS sessions, +6 P2 and the adults running. Finally, the "mature running" cluster contained all strides from the adults, 32% from +32 P1, 40% from +19 P1, and 16% of the strides from +13 P1. At first glance, P1 and P2 had similar developmental trajectories but a closer look revealed clear differences in that, in contrast to P2, P1 did reach mature running while immature running occurred intermintly within sessions from 9/13 months from onset of independent walking onwards (cf., Figure 4.4B).

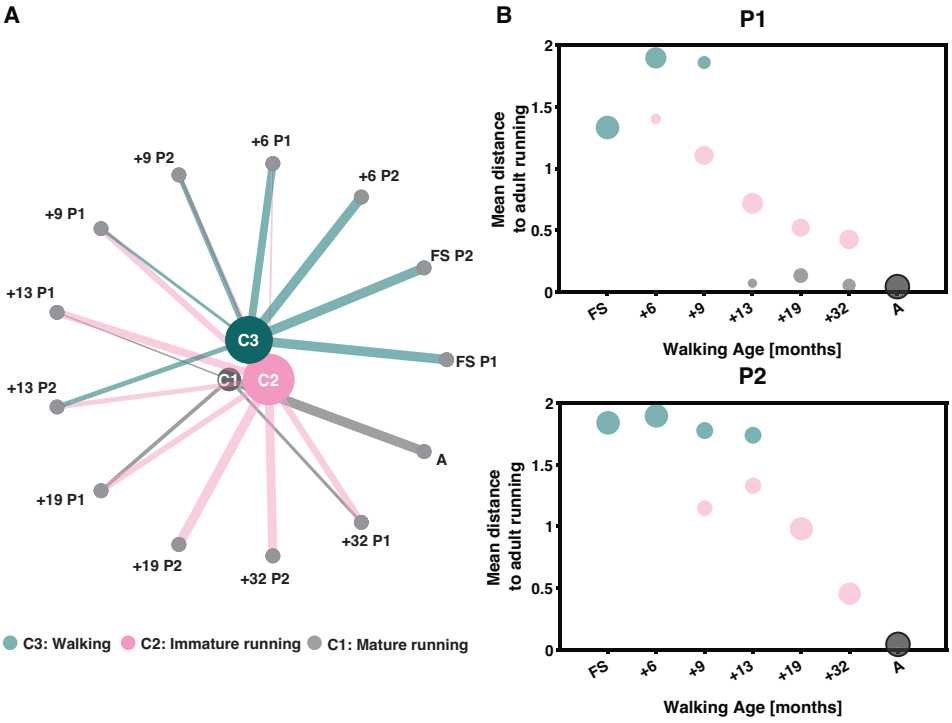

Figure 4.4: Clustering output. A) Output of clustering ordered based on walking age (time since onset of walking in months) with the youngest session on the right and increasing in walking age in anticlockwise direction. The size of the clusters depends on the number of strides they contain (the larger the node the more strides they contain), similarly are the lines from each node to a cluster a representation of the number of strides from that session that belongs to each cluster larger than 10%. B) Average pairwise correlation distance from each session to those of the adults as a function of walking age (months) for P1 and P2, respectively. Sizing of dots follow the sizing of lines in panel A. FS: First steps, +6, +9, +13, +19, +32 refers to the number of months since onset of independent walking.

Muscle synergies

The differences in the developmental trajectories shown in Figure 4.5 (panel B) may appear quantitatively subtle but – in fact – they are of qualitative nature. P2 shows an improvement in the running maturity which evolves gradually but does not reach full maturity over the observation period. On the other hand, P1 did reach a mature running pattern over the last few recording sessions, but apparently the immature pattern coexisted even once mature running could be accomplished. In searching for the causes underlying these difference, we here dwell more on the result of the analysis of the accompanying muscle synergies. Before going into detail, we would like to note that lateral gastrocnemius (LG) was not analyzed for the FS and +6 sessions of P1 and erector spinae (ES) for +6 of P1. This was due to poor data quality.

The reconstruction accuracy (RA) revealed different numbers of muscle synergies between sessions with median of three muscle synergies (IQR: 3:4.5) across all sessions. The RA was 64.2 ± 1.8, 64.1 ± 2.6, and 66.3 for P1, P2, and the adults, respectively, for three synergies. The temporal activation patterns of the first of the three synergies had the most activity at foot contact, the weight acceptance phase, with the knee extender muscles (RF, VM, VL, and RF muscles) being the predominant influencers both for toddlers and adults with some contribution also of the TFL and GLM muscles (cf. Figure 4.5). The second components were related to end of stance, the propulsion phase, with the largest contributions of MG, LG, and SOL. The third synergy was more variable with activity from TA and ES with most activity at swing. Synergies were comparable across sessions for P1 and P2. For P1, the most notable development in the muscle synergies in time after onset of independent walking, was the increase in amplitude, especially in synergy 1. This increase in amplitude across age/time since onset of independent was not clear to the same extent in P2.

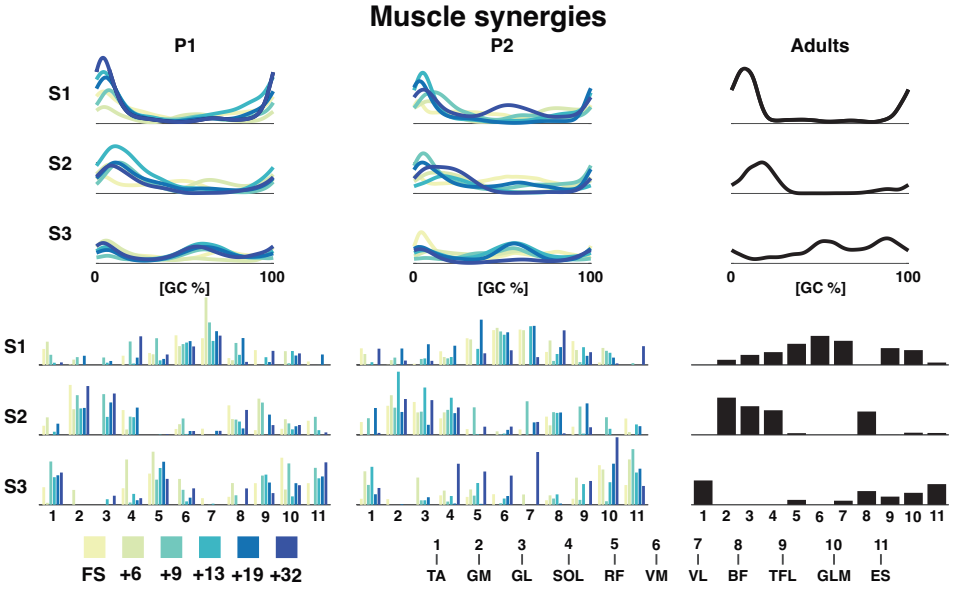

Figure 4.5: Muscle synergies for P1, P2, and adults. The top graphs are the grand average temporal activation patterns for each session as a function of the gait cycle and the three synergies. Amplitude is in arbitrary units. The lower bar graphs are the weighting coefficients for the muscle synergies. The naming of the muscles can be seen below. TA: tibialis anterior, GM: gastrocnemius medialis, GL: gastrocnemius lateralis, SOL: soleus, RF: rectus femoris, VM: vastus medialis, VL: vastus lateralis, BF: biceps femoris, TFL: tensor fascia latae, GLM: gluteus maximus, ES: erector spinae, +6, +9, +13, +19, +32 refers to the number of months since onset of independent walking.

FWHM and CoA mark the ability to quickly contract a muscle and the timing of the muscle contraction, respectively. The FWHM of the temporal patterns of the three synergies was comparable across sessions with a large variance between strides (cf. Figure 4.6). The most

pronounced differences were found between the FWHM of the sessions of P2 and the adults (e.g., FS, +6, +13, +19, and +32 all had a p<0.0001 for synergy 1, +6, +13, +32 were all p<0.001 for synergy 2) with some in-between significant differences between the sessions within P1 and P2. Synergy 3 of P2 had a characteristic pattern of a reduction of the FWHM from the first running session (+6) to the last running session (+32) with significant p-values of p<0.0001 for the +6 session compared to +19, +32, and adults and p=0.0067 for the +6 session compared to the +13 session.

The CoA of the synergies were way more variable in the children than in the adults. In the latter the CoAs were within the same 25% of the gait cycle across strides (between 0-25% of the gait cycle for synergy 1 and 2, and within 63 and 83% of the gait cycle for synergy 3). For the first and third pattern, the range of the CoA for P1 and P2 covered all percentages of the gait cycle for all sessions. Most noteworthy is the mean CoA for the second temporal pattern which occurred later in the FS sessions (31.6% ± 18.5% and 56.3% ± 18.7% of the gait cycle) for P1 and P2, respectively, compared to the mean over the other sessions, which ranged from 13.8% to 16.0% for P1 and 13.6% to 20.2% for P2 ($p < 6 \times 10^{-4}$ and $p < 2 \times 10^{-16}$, respectively). Here, the adult patterns were similar with a mean of 13.3% ± 3.6% of the gait cycle for the second component.

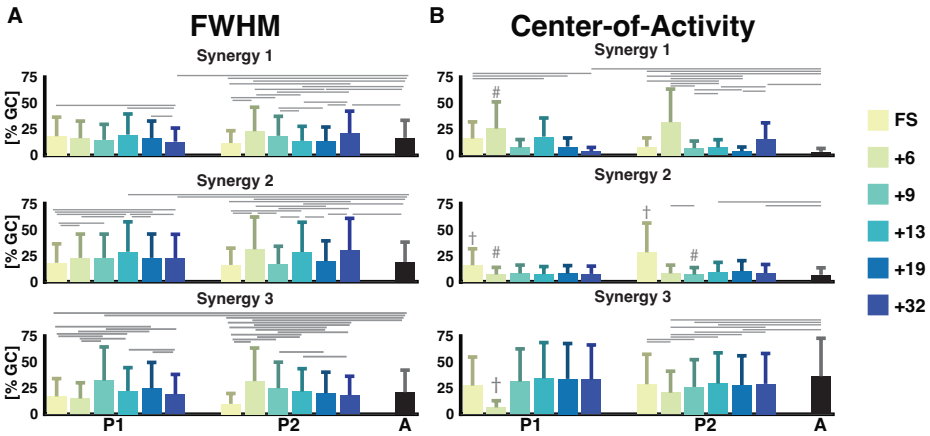

Figure 4.6: Full-width half-maximum and center-of-activity of muscle synergies. Color notation as to the right. (A) The full-width half-maximum (FWHM) was calculated for the main peak of each stride for each muscle synergy. It is represented as a percentage of the gait cycle. (B) The center-of-activity (CoA) was expressed as the percentage of the gait cycle. The horizontal lines represent a significant difference, p < 0.007 within a participant and the adults. The dagger (†) represents a significant difference between session and all other sessions. A hash (#) represents a significant difference between session and all later sessions and adults. GC: gait cycle, FWHM: full-width at half-maximum, A: adults, FS: first steps, +6, +9, +13, +19, +32 refers to the number of months since onset of independent walking.

Discussion

PCA and Clustering – Classifying running maturity

We succeeded to classify the development of running maturity over the span of six recording sessions of almost three years in two toddlers matched on walking age. That is, our shotgun approach combining PCA and hierarchical clustering enabled us to estimate the maturity of very early development of running.[1] After walking the first independent steps, our participants developed the capacity of running, though to different degrees of maturity. It appears that mature running patterns can coexist next to immature ones, which occur earlier in the course of developement.

As said, in particular in P1, several sessions had strides in two different clusters. Since the data were collected not only during overground running but also on the treadmill it might have been that the more mature strides were recorded overground and the more immature ones on the treadmill. A lack of treadmill experience may hence have cause the 'return' to the immature mode of locomotion . However, analysis of the strides falling into the more mature or immature clusters did not reveal such a pattern, see *Supplementary Material* 4.3.

Remarkably, the FS session of P1 was relatively close to mature running in terms of the average pairwise distance to the adults. While this might hint at shortcomings of our clustering approach (see also below), already in PC1-PC2 space the first step session (very dark blue) was indeed close to the adults. In a future study we will compare new walkers to very experienced runners. There we will also include adult walking, i.e., experienced walking, and expect that the FS strides will becloser to this cluster than to adult running.

In the current two children we cannot pinpoint a moment when the running pattern differs from the walking pattern and becomes like the adult running pattern. This is mostly due to a substantial variability between and within sessions in the majority of outcome variables. We would like to stress anyway that we were able to show that the two toddlers seemingly display different paths towards running maturity.

[1] While this – in principle – supports the combination of kinetic, kinematic, and electromyographic data in a single 'shotgun' approach, it leaves the question of which factors or parameters are causing the (differences in) development open. However, the parameters dominating the PCA can be readily determined. We briefly illustrate this by investigating whether a reduced number of parameters may lead to results similar to the ones reported in the body text. For this sake we retained only loadings contributing >0.6 and repeated the cluster analysis. In total 46 parameters were included in the second analysis (see *Supplementary Material* 4.4). These cluster results differed from our main ones in that more sessions/strides were considered "mature" running and more strides/sessions were considered "immature" running instead of walking. Thus, clustering seems less sensitive to individual differences in the strides with a reduced number of parameters. Put differently, parameters not contributing more than 60% to the PCA are still relevant when clustering.

Muscle synergies – What underlies running maturity?

We determined three muscle synergies. This number is smaller than in many other studies on running where the number is usually four or more (Bach et al., 2021b; Cappellini et al., 2006; Cheung et al., 2020; Santuz, Ekizos, Janshen, et al., 2018). We chose to determine the number of muscle synergies based on finding the plateau of the reconstruction accuracy (RA) using the linear-fit method introduced by Cheung et al. (2005). Whether or not this explains this discrepancy with the literature is unclear. A recently method proposed by Ballarini, Ghislieri, Knaflitz, and Agostini (2021) where the consistency and similarity of both activation patterns and weighting coefficients were determined may shed light on this. However, most methods of determining the number of synergies require setting some threshold which leaves this an open issue for future research (Sylos-Labini et al., 2022); see *Supplementary Material* 4.5 for an alternative to the reconstruction accuracy (RA) used here.

Synergy 2 shows a phase shift as evidenced in the CoA from 30-50% of the gait cycle for the FS session to around ~15% of the gait cycle for the later sessions. The phase shift occurs from the +6 session and is stable across the running sessions, which indicates that a contraction of the foot flexors matching the shorter stance phase is important for even early running patterns.

The analysis of FWHM of the temporal activation patterns of the muscle synergies allowed us to quantify the duration of activity of the muscles contributing to this particular synergy. FWHM of motor primitives or muscle synergies has previously been hypothesised to be a measure for robustness of the motor control (Martino et al., 2015; Martino et al., 2014; Mileti et al., 2020; Santuz et al., 2020; Santuz, Ekizos, Eckardt, et al., 2018). For both synergy 1 and 2, we found the most differences from the adult patterns to the patterns of P2 and not P1, which indicates similar widening between P1 and the adult pattern already from an early running pattern. It is likely that this trend was indeed an underlying reason for why the running patterns of this participant has been considered to mature earlier than P2. It is likely that this trend was indeed an underlying reason for why the running patterns of this participant has been considered to mature earlier than P2. We also observed that for both synergy 1 and 2 that there was first an increase followed by a reduction in the FWHM from the +13 session. This is the same timepoint at which the very mature strides appeared. In P2, the +6 and +32 sessions for synergy 1 both differed from most of the other sessions with a decrease in the FWHM from the +6 session to the +19 session with the +6 and +32 sessions being similar. The decrease from 6 months since onset of independent walking until +19 months could be due to an improved ability to narrow the duration of the activation pattern and reduce the overlap of the muscle synergies at the weight acceptance phase, where the increase in the FWHM at 32 months could be explained by a possible altered running pattern that is not yet finetuned.

Methodological choices and Limitations

The EMG was processed by normalizing the amplitude to the mean of the data across strides. According to Besomi et al. (2020), a normalization to the mean can lead to a reduction in the inter-individual variation in amplitude. Obtaining a more optimal normalization via maximal voluntary contraction may, however, not be feasible, especially in young children. Yet, we must admit that normalization to the mean might have resulted in some unwarranted high weighting for some muscles (Besomi et al., 2020).

The main limitation of this study is the lack of power by only having two participants. Without a doubt this limits the ability to generalize our results. Despite the lack of generalizability, we consider it a valuable starting point, first in methods and – more importantly, in clarifying that time since onset of independent walking does not appear to be a solid indicator of the maturity of running patterns in very young children.

The two clusters, C3 “walking” and C2 “immature running” were so close to each other that they are just overlapping in terms of our measure of maturity, the mean pairwise correlation distance to that of the adults. This may suggest that a cluster solution with three clusters may not have been optimal. However, the mean pairwise distance to the adults did not change with an altered number of clusters. We are hence convinced that our measure can be used for determining the “order of maturity”. On the other hand, the FS session of P1 can be considered more mature than +6 and +9, two sessions containing running strides. Apparently, the distance measure and linkage method used to create the dendrogram was less optimal than in our previous study (Bach et al., 2021a). However, a combination of other distance measures and linkage methods did not yield better cophenetic correlation coefficients (CCC). The only a Euclidian distance measure with either average (CCC: 0.83) or centroid algorithms (CCC: 0.84) showed comparable results but cause problems, e.g., dendrogram with non-monotonic links.

Future research should be focused on investigating larger number of children. When doing so, we advocate combining many kinematic and neuromuscular parameters to fully investigate the development of the running patterns in very young children.

Conclusion

Our study is unique in that the development of running was monitored longitudinally over a three-years span with highly frequent assessments of kinetics, kinematics, and electromyography. It provides a first view on the effect of time since onset of independent walking on the development of running. Running development followed different trajectories that we quantified ‘blindly’ via a shotgun approach after combining various biomechanical and neuromuscular parameters. Evidently, the development of running can take different

trajectories including the co-existence of immature and mature running within the same session in a child. Muscle synergy analysis may help explaining why the development can differ between children, though there is a long way to clarifying this with statistical robustness.

Supplementary Material 4.1

List of parameters and their normalizations before being z-scored and included into the PCA.

Table S4.1: Included parameters in the principal component analysis.

PARAM	DETAILED EXPLANATION	UNIT [NORM]
TEMPORAL FEATURES		
1	Stride duration	s
2	Froude velocity	
3	Stance duration	s
4	Percentage swing duration	% GC
5	Percentage stance duration	% GC
6	Percentage double support	% GC
7	Percentage flight phase	% GC
8	Stride length (1D)	[1/l]
9	Stride length (3D)	[1/l]
LIMB ENDPOINT (VM) TRAJECTORY		
10	Step length	[1/l]
11	Step height	[1/l]
12	Maximum backward position	[1/l]
13	Maximum forward position	[1/l]
14	Maximum velocity during swing	m/s
15	Relative timing of max velocity during swing	% GC
16	Acceleration at swing onset	m/s^2
17	Endpoint velocity	m/s
18	Orientation of velocity vector at swing onset	rad
19	Position of ankle with respect to hip at FC	[1/l]
20	Position of ankle with respect to hip at FO	[1/l]
21	Position of ankle with respect to hip at SE	[1/l]
STABILITY		
22	Lateral displacement of foot during swing	[1/l]
23	Step length	[1/l]
24	Step width (ML)	[1/l]
25	Hip midpoint variability (ML)	
26	Hip midpoint variability (vert)	
27	Variability of sagittal trunk oscillations	
28	Variability in vel. of sagittal trunk oscillations	
29	Variability of Medio-lateral hip rotations	
30	Amplitude of trunk Medio-lateral movement	deg
31	Amplitude of trunk Vertical movement	deg
32	Variability of Medio-lateral trunk movement	
33	Variability of Vertical trunk movement	
JOINT AND SEGMENTAL ANGLES		
34	Hip elevation angle (min)	deg
35	Thigh elevation angle (Min)	deg
36	Shank elevation angle (Min)	deg
37	Foot elevation angle (Min)	deg
38	Main-leg elevation angle (Min)	deg
56	Main-leg elevation angle (Amp)	deg
57	Hip joint angle (Amp)	deg
58	Knee joint angle (Amp)	deg
59	Ankle joint angle (Amp)	deg
60	Main-leg medio-lateral angle (Amp)	deg
LEG/JOINT ANGULAR VELOCITY		
61	Main-leg velocity (Min)	deg/s
62	Hip joint velocity (Min)	deg/s
63	Knee joint velocity (Min)	deg/s
64	Ankle joint velocity (Min)	deg/s
65	Main-leg velocity (Max)	deg/s
66	Hip joint velocity (Max)	deg/s
67	Knee joint velocity (Max)	deg/s
68	Ankle joint velocity (Max)	deg/s
69	Main-leg velocity (Amp)	deg/s
70	Hip joint velocity (Amp)	deg/s
71	Knee joint velocity (Amp)	deg/s
72	Ankle joint velocity (Amp)	deg/s
INTRA-LIMB COORDINATION		
73	Correlation between the two limbs AP direction	
74	Phase relationship between the two limbs	
INTERSEGMENTAL COORDINATION		
75	Percentage of variance (1st u)	
76	Percentage variance (2nd u)	
77	Percentage variance (3rd u)	
78	Projection of 1st u on thigh axis	
79	Projection of 1st u on shank axis	
80	Projection of 1st u on foot axis	
81	Projection of 2nd u on thigh axis	
82	Projection of 2nd u on shank axis	
83	Projection of 2nd u on foot axis	
84	Projection of 3rd u on thigh axis	
85	Projection of 3rd u on shank axis	
86	Projection of 3rd u on foot axis	
87	Area of the gait loop	deg^2
88	Ratio of left to right leg cycle duration	
INTERLIMB COORDINATION		
89	Phase difference hip and thigh elev. angles	
90	Phase difference thigh and shank elev. angles	
91	Phase difference shank and foot elev. angles	
92	Max r (hip and thigh elevation angles)	
93	Max r (thigh and shank elevation angles)	

39	Hip elevation angle (Max)	deg	94	Max r (shank and foot elevation angles)	
40	Thigh elevation angle (Max)	deg	95	Max r (hip and knee joint angles)	
41	Shank elevation angle (Max)	deg	96	Max r (knee and ankle joint angles)	
42	Foot elevation angle (Max)	deg	**PENDULUM/SPRING MECHANISM**		
43	Main-leg elevation angle (Max)	deg	97	Amplitude of vertical hip displacement	m
44	Hip joint angle (Min)	deg	98	Amplitude of ML hip displacement	m
45	Knee joint angle (Min)	deg	**TRUNK SEGMENTAL AND JOINT ANGLES**		
46	Ankle joint angle (Min)	deg	99	Trunk elevation angle (Min)	deg
47	Main-leg abduction (Min)	deg	100	Trunk elevation angle (Max)	deg
48	Hip joint angle (Max)	deg	101	Trunk elevation angle (amp)	deg
49	Knee joint angle (Max)	deg	**MUSCLE SYNERGIES**		
50	Ankle joint angle (Max)	deg	102	Full-width half-maximum – Synergy 1	% GC
51	Main-leg abduction (Max)	deg	103	Full-width half-maximum – Synergy 2	% GC
52	Hip elevation angle (Amp)	deg	104	Full-width half-maximum – Synergy 3	% GC
53	Thigh elevation angle (Amp)	deg	105	Center of activity – Synergy 1	% GC
54	Shank elevation angle (Amp)	deg	106	Center of activity – Synergy 2	% GC
55	Foot elevation angle (Amp)	deg	107	Center of activity – Synergy 3	% GC

Param: parameter; Norm: normalization; l, leg-length; FC: foot contact, FO: foot off, SE: swing end; AP: anterior-posterior; ML: medio-lateral, W: body weight; SS: single support; d: stride length; min: minimum; max: maximum; amp: amplitude; u: eigenvector.

Supplementary Material 4.2

To quantify the influence of the session and participants on the ability to run with either a double support (DS) phase or a flight phase (FP), a linear regression model was fitted to all data with either DS or FP as the response variable and the session, participant and the interaction between session and participant as predictors. $p < 0.05$ were considered significant for this purpose. We fitted a least squares exponential function of the dependence of Froude on the ability to run with a flight phase and double support phase, respectively and report the adjusted R^2 values. A two-sample t-test was performed on the Froude values for the treadmill strides and overground strides for each session.

Table S4.2: Statistics on double support phase and flight phase

	Factor	*Estimate*	*SE*	*t*	*p-value*
DS	Intercept	42.62	1.70	25.11	$< 2 \times 10^{-16}$
	Session	-4.84	0.35	-13.98	$< 2 \times 10^{-16}$
	Participant	-1.83	1.09	-1.68	0.09
	Session:Participant	-0.47	0.20	-2.31	0.02
FP	Intercept	3.42	0.65	5.29	$< 2 \times 10^{-7}$
	Session	-1.27	0.13	-9.61	$< 2 \times 10^{-16}$
	Participant	-3.31	0.42	-7.98	$< 2 \times 10^{-16}$
	Session:Participant	1.45	0.08	18.64	$< 2 \times 10^{-16}$

DS: Double support phase, FP: Flight phase, SE: Standard error, t: t-statistics

The Froude value for strides on the treadmill were in all cases significantly lower than the Froude value for strides recorded while locomoting overground as can be seen in Table S4.3. Not all sessions contained strides recorded during both modalities.

Table S4.3: Comparisons of the Froude values for treadmill and overground strides

Participant	*Froude – OVG*	*Froude - TM*	*p-value*
FS P1	0.04		$< 2 \times 10^{-16}$
FS P2	0.02	0.04	9.5×10^{-6}
+6 P1	0.34		
+6 P2	0.63		
+9 P1	0.58		
+9 P2	0.65	0.45	1.7×10^{-5}
+13 P1	0.59	0.32	$< 2 \times 10^{-16}$
+13 P2	0.51	0.25	3.3×10^{-16}
+19 P1	0.86	0.41	1.5×10^{-15}
+19 P2	1.04	0.40	$< 2 \times 10^{-16}$
+32 P1	1.06	0.50	$< 2 \times 10^{-16}$
+32 P2	1.03	0.68	$< 2 \times 10^{-16}$
A		0.62	

Missing values are due to no strides recorded for that modality for that session. A: Adults, OVG: Overground, TM: Treadmill, FS: First steps

There was a strong inverse relationship between the Froude value and the DS phase (R^2 = 0.79) meaning that the lower the Froude value, the more DS was present (cf., Figure S4.1). However, there no significant relationship (R^2 = 0.27) between the Froude value and the amount of FP and there is almost no flight phase present with a Froude value between 0 and 0.4. The strong presence of a relationship between the double support phase and the normalized speed, but the lack of the same relationship between the flight phase and the normalized speed indicates that for running the ability to run with a flight phase is not merely a function of running at a certain speed, but more factors influence this ability.

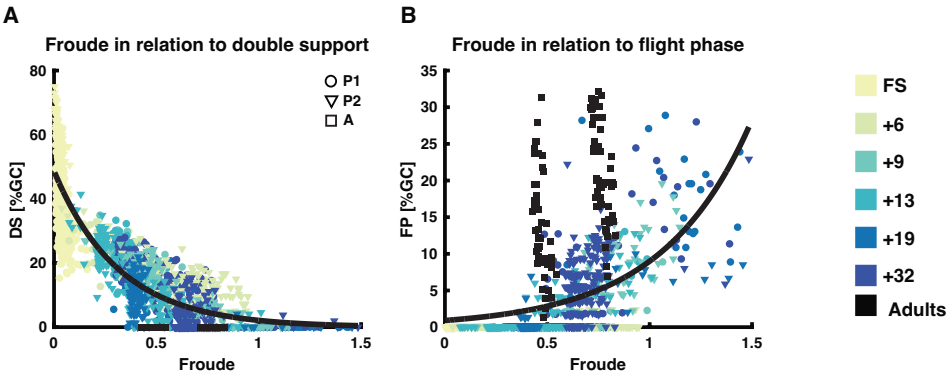

Figure S4.1: Relationship between Froude and DS and FP. A) Relationship between double support expressed as a percentage of the gait cycle as a function of the Froude value. A least-squares exponential function was fitted and resulted in an adjusted R^2 = 0.79 which means a decrease in double support is correlated to an increase in dimensionless speed. B) Relationship between flight phase expressed as a percentage of the gait cycle as a function of the Froude value. A least-squares exponential function was fitted and resulted in an adjusted R^2 = 0.27 which means no relation between the amount of flight phase and dimensionless speed. DS: Double support, FP: Flight phase, %GC: percentage gait cycle, +6, +9, +13, +19, +32 refers to the number of months since first steps, i.e., the walking age.

Supplementary Material 4.3

Loadings explaining the contribution to each PCA. First parameter to the right, parameter 107 on the left. See *Supplementary Material* 4.1 for overview of the different parameters. The darker the color (red or blue) the higher the contribution to the relevant PC.

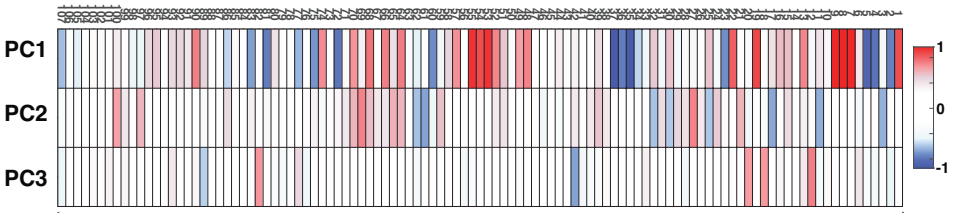

Figure S4.2: Loadings for PC1-PC3. Color coding refers to the contribution of each loading. The darker the color the higher the contribution. See Table S4.1 for overview of all 107 parameters.

We first built a dendrogram using average links (unweighted pair group method with arithmetic mean) of the first three PCs. The cophenetic correlation coefficient (CCC) for the correlation distance measure with average links was 0.84 which was comparable or higher than other combinations of distance measure and linkage methods. Combining a visual inspection of the dendrogram with the Calinzki-Harabasz stopping rule, resulted in three clusters. The Calinzki-Harabasz stopping rule run from 1-10 clusters revealed a cluster solution of two to be the most optimal, however the visual inspection resulted in three clusters to also allow for a possible separation, not only between walking in the FS sessions and the running in the other sessions but also between immature and mature running.

Dendrogram describing the split of clusters. The y-axis is a measure for the distance between clusters as measured by the correlation distance. The taller the links between two lead nodes, the longer the leaf nodes (or clusters) are located from each other in 3D space.

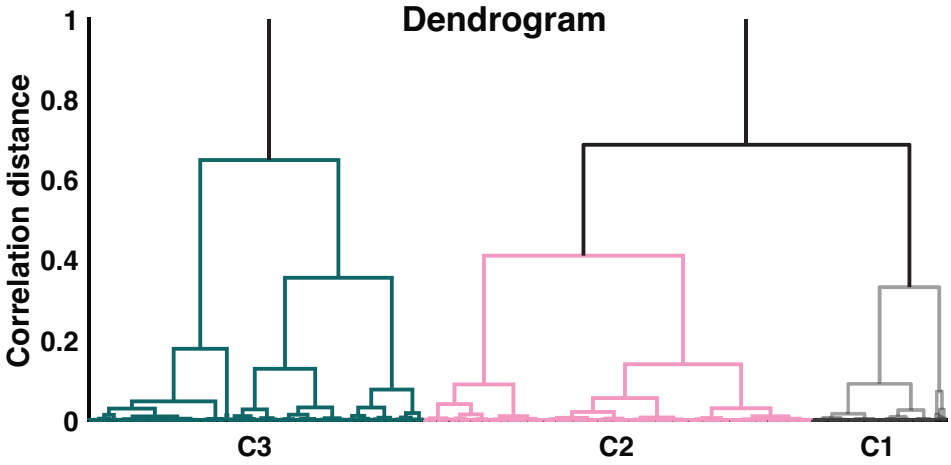

Figure S4.3: Dendrogram for clustering results.

Table S4.4 represents the strides that belong to each cluster for treadmill and overground locomotion, respectively. What is clear in this overview is that the modality (treadmill or overground locomotion) does not account for the maturity of the strides.

Table S4.4: Overview of overground and treadmill strides for each cluster

Participant	*Cluster 1*		*Cluster 2*		*Cluster 3*		*Total strides*
	OVG	TM	OVG	TM	OVG	TM	
FS P1					254		254
FS P2					77	22	99
+6 P1			9		38		47
+6 P2			1		108		109
+9 P1	1		19		9		29
+9 P2	2	5	31	29	64	8	139
+13 P1	1	15	16	63	6	1	102
+13 P2			35	43	68	14	160
+19 P1	13	29	18	45	2		107
+19 P2		2	12	78	1		93
+32 P1	9	69	6	163			247
+32 P2		23	5	209	2		239
A		103		2			105

Missing values are due to no strides recorded for that modality for that session. Red values represent strides that are not included in the cluster results as they account for less than 10% of the total number of strides. A: Adults, OVG: Overground, TM: Treadmill, FS: First steps

Supplementary Material 4.4

To investigate if a smaller number of parameters lead to similar results as the full analysis a second analysis was done with the loadings contributing >0.6 to either of the three PCs. This reduced number of loadings means that 46 parameters were analyzed in total. See Table S4.5 below for parameters.

Table S4.5: List of parameters included into PCA in reduced analysis.

PARAM	DETAILED EXPLANATION	NEW PARAM
TEMPORAL FEATURES		
1	Stride duration	1
2	Froude velocity	2
3	Stance duration	3
4	Percentage swing duration	4
5	Percentage stance duration	5
6	Percentage double support	6
8	Stride length (1D)	7
9	Stride length (3D)	8
LIMB ENDPOINT (VM) TRAJECTORY		
10	Step length	9
12	Maximum backward position	10
13	Maximum forward position	11
14	Maximum velocity during swing	12
18	Orientation of velocity vector at swing onset	13
19	Position of ankle with respect to hip at FC	14
20	Position of ankle with respect to hip at FO	15
21	Position of ankle with respect to hip at SE	16
STABILITY		
23	Step length	17
24	Step width (ML)	18
28	Variability in vel. of sagittal trunk oscillations	19
JOINT AND SEGMENTAL ANGLES		
36	Shank elevation angle (Min)	20
37	Foot elevation angle (Min)	21
38	Main-leg elevation angle (Min)	22
43	Main-leg elevation angle (Max)	23
49	Knee joint angle (Max)	24
50	Ankle joint angle (Max)	25
53	Thigh elevation angle (Amp)	26
54	Shank elevation angle (Amp)	27
55	Foot elevation angle (Amp)	28
56	Main-leg elevation angle (Amp)	29
58	Knee joint angle (Amp)	30
LEG/JOINT ANGULAR VELOCITY		
61	Main-leg velocity (Min)	31
62	Hip joint velocity (Min)	32
65	Main-leg velocity (Max)	33
67	Knee joint velocity (Max)	34
69	Main-leg velocity (Amp)	35
70	Hip joint velocity (Amp)	36
71	Knee joint velocity (Amp)	37
INTRA-LIMB COORDINATION		
73	Correlation limb-arm AP direction	38
INTERSEGMENTAL COORDINATION		
75	Percentage of variance (1st u)	39
76	Percentage variance (2nd u)	40
78	Projection of 1st u on thigh axis	41
82	Projection of 2nd u on shank axis	42
83	Projection of 2nd u on foot axis	43
84	Projection of 3rd u on thigh axis	44
INTERLIMB COORDINATION		
91	Phase difference shank and foot elev. angles	45
TRUNK SEGMENTAL AND JOINT ANGLES		
101	Trunk elevation angle (amp)	46

Param: parameter; Norm: normalization; l, leg-length; FC: foot contact, FO: foot off, SE: swing end; AP: anterior-posterior; ML: medio-lateral, W: body weight; SS: single support; d: stride length; min: minimum; max: maximum; amp: amplitude; u: eigenvector.

The three PCs explained more than 70% of the variance of the original dataset (PC1: 48%, PC2: 14%, and PC3: 10%). All parameters included contributed more than the 95%CI. PC1 distinguished the first sessions from the other sessions with no clear effect of PC2 and PC3.

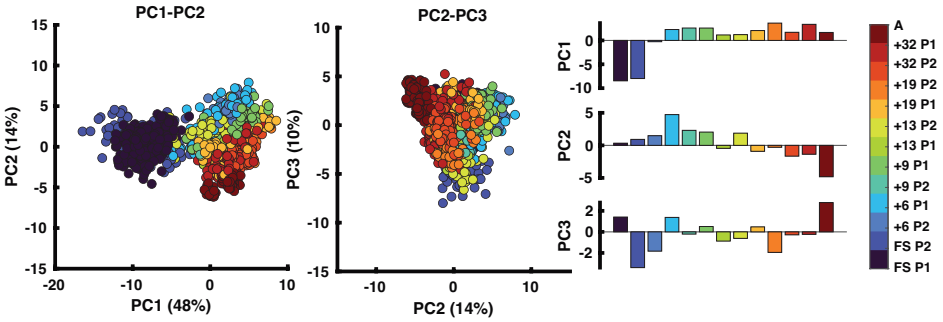

Figure S4.4: Output of Principal Component Analysis (PCA) on 46 parameters. A) PC1-PC2 space. B) PC2-PC3 space. Color coding as to the right. Each dot represents one stride.

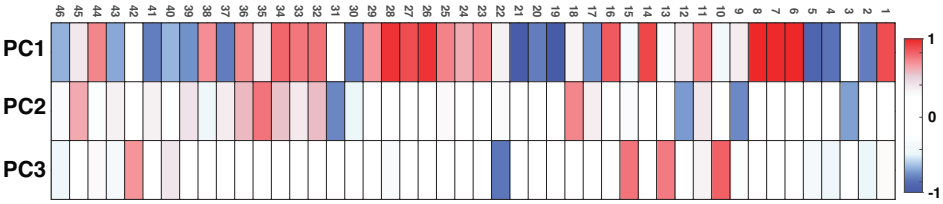

Figure S4.5: Loadings for PC1-PC3. Color coding refers to the level of contribution with the darkest colors providing the highest loadings. For information on which parameters are which, refer to Table S4.5.

The loadings for the three PCs were all high for PC1 and they all contributed more than 0.6 to any of the three PCs.

The clustering was done in similar way as the original analysis with a correlation distance and average linkage. A dendrogram was created and the cophenetic correlation coefficient was 0.80 for this cluster solution, see Figure S4.6.

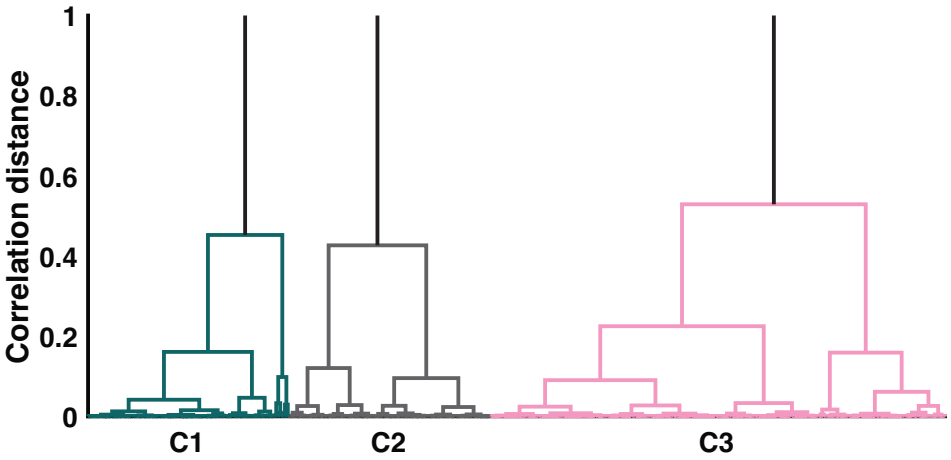

Figure S4.6: Dendrogram for reduced analysis. Colors represent each their cluster. The y-axis of the plot refers to the correlation distance. Cluster 1 (C1) and cluster2 (C2) are closest to each other with C3 being on the far right.

The Calinzki-Harabasz rule resulted in an optimal number of 2 clusters, however, the visual inspection of the dendrogram revealed that three clusters resulted in the least inconsistent links and so the three-cluster solution was used – this also made the supplemental analysis comparable to the main analysis.

The cluster solution with only a subset of the parameters resulted in a slightly different solution of the clusters than the main analysis. More sessions are now clustered in the adult cluster, i.e., the "mature running" cluster (c.f., Figure S4.7A). This applies to +19 of P2 and more strides from +13 of P1 also now fall in the mature cluster. Similarly, are there fewer strides/sessions falling into the "walking" cluster such as the two +6 and +9 sessions. This indicates that a reduced number of parameters means that the clustering is less sensitive to the individual differences in the strides. The trend that P1 has a faster development toward a mature pattern than P2 is still present in this analysis.

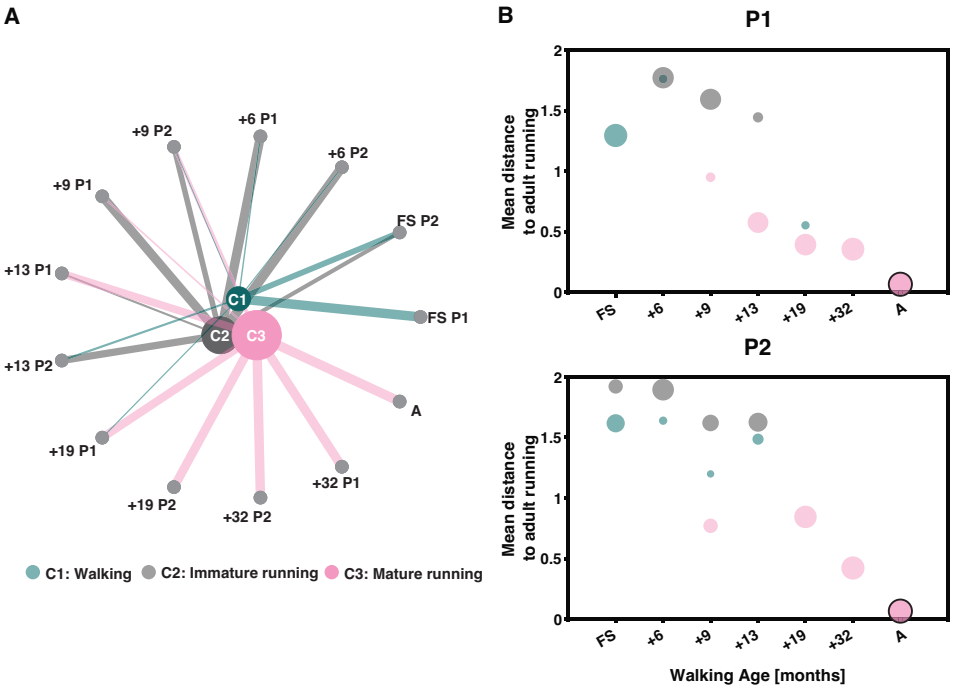

Figure S4.7: Output of clustering. A) Output of clustering ordered based on walking age (months) with the youngest session on the right and increasing in walking age in anticlockwise direction. The size of the clusters depends on the number of strides they each contain (the larger the cluster node the more strides they contain), similarly are the lines from each node to a cluster a representation of the number of strides from that session that belongs to each cluster larger than 10%. B) Calculated average pairwise correlation distance from each session to those of the adults as a function of walking age (months). Sizing of dots follow the sizing of lines in panel A. C) calculated average pairwise correlation distance to the adults as a function of maturity. Note that some sessions contribute to more than one cluster and thus are repeated on the upper x-axis. The color notation is similar as in (A) and (B). D) Output of clustering based on maturity of the gait patterns with the most immature gait pattern on the far right with increasing maturity in anticlockwise direction. FS: First steps

That all parameters contributed more than 0.6 to the PCA indicates that they are all relevant for the analysis and thus are a good starting point if one wants to pinpoint the exact parameters influencing the maturity of gait patterns in very young children.

Supplementary Material 4.5

The reconstruction accuracy (RA) has the advantage of exploiting the Frobenius norm which is the optimization method also used for the (W)NMF. However, the VAF method is more widely used, so we also compared the RA to the VAF for the chosen number of synergies. We determined VAF as the mean-uncentered VAF.

$$VAF = 1 - \frac{\|EMG - W \cdot H\|^2}{\|EMG\|^2}$$

where W and H represent the weighting coefficients and activation patterns of the synergies, respectively. When using VAF, a common method to determine the number of synergies needed is that they should explain a minimum of 80-90% of the data. Three synergies explain a mean of 87.16% ± 1.29%, 87.07% ± 1.89%, and 88.66% for P1, P2, and adults, and the next added synergies only add 3.34% ± 0.40%, 3.79% ± 1.04%, and 3.14%, respectively. Thus, despite the number of synergies being lower than in other studies, the three synergies still explain a large portion of the original data and adding another synergy does not add any substantial variance to the data.

Chapter 5

PREDICTING VERTICAL GROUND REACTION FORCES FROM 3D ACCELEROMETRY USING RESERVOIR COMPUTERS LEADS TO ACCURATE GAIT EVENT DETECTION

Bach, M. M., Dominici, N., & Daffertshofer, A.

Front. Sports Act. Living, 2022, 4:1037

Abstract

Accelerometers are low-cost measurement devices that can readily be used outside the lab. However, determining isolated gait events from accelerometer signals, especially foot-off events during running, is an open problem. We outline a two-step approach where machine learning serves to predict vertical ground reaction forces from accelerometer signals, followed by force-based event detection. We collected shank accelerometer signals and ground reaction forces from 21 adults during comfortable walking and running on an instrumented treadmill. We trained one common reservoir computer using segmented data using both walking and running data. Despite being trained on just a small number of strides, this reservoir computer predicted vertical ground reaction forces in continuous gait with high quality. The subsequent foot contact and foot off event detection proved highly accurate when compared to the gold standard based on co-registered ground reaction forces. Our proof-of-concept illustrates the capacity of combining accelerometry with machine learning for detecting isolated gait events irrespective of mode of locomotion.

Introduction

Estimating the presence of a step using mobile devices can be realized with fair accuracy and relative ease (de Ruiter, van Oeveren, Francke, Zijlstra, & van Dieen, 2016; Moe-Nilssen & Helbostad, 2004; Norris, Kenny, & Anderson, 2016; van Oeveren, 2021; van Oeveren, de Ruiter, Beek, Rispens, & van Dieen, 2018). Yet, many details of the stepping cycle remain opaque such as foot contact and foot off moments, but also more detailed gait characteristics, such as loading responses in (ambulant) clinical contexts. In most of the current literature on wearables, event estimations are rule-based and often require searching for an area of interest (Pérez-Ibarra, Williams, Siqueira, & Krebs, 2018; Prasanth et al., 2021). This is true for data from inertial measurement units but also for data derived from only accelerometers. Algorithms are optimized for either walking (Ben Mansour, Rezzoug, & Gorce, 2015; Greene et al., 2010; Gurchiek, Garabed, & McGinnis, 2020; Mico-Amigo et al., 2016; Pacini Panebianco, Bisi, Stagni, & Fantozzi, 2018; Rueterbories, Spaich, & Andersen, 2014; Selles, Formanoy, Bussmann, Janssens, & Stam, 2005; Trojaniello et al., 2014) or running (Bergamini et al., 2012; Khandelwal & Wickstrom, 2017; Lee, Mellifont, & Burkett, 2010; McGrath, Greene, O'Donovan, & Caulfield, 2012; Mitschke, Heß, & Milani, 2017; Mo & Chow, 2018; Purcell, Channells, James, & Barrett, 2006; Sinclair, Hobbs, Protheroe, Edmundson, & Greenhalgh, 2013) and vary depending on sensor location and type, and on speed. As it stands, they may not generalize to other settings.

Machine learning approaches may provide welcome alternatives. They have been employed to predict stepping moments and gait phases by extracting different features recorded from inertial measurement units (Abaid, Cappa, Palermo, Petrarca, & Porfiri, 2013; Chen, Qi, Guo, & Yu, 2017; Mannini, Genovese, & Maria Sabatini, 2014; Mannini & Sabatini, 2011; Martinez-Hernandez & Dehghani-Sanij, 2018; Meng, Martinez-Hernandez, Childs, Dehghani-Sanij, & Buis, 2019; Prado, Cao, Robert, Gordon, & Agrawal, 2019; Robberechts et al., 2021; Su, Smith, & Gutierrez Farewik, 2020; Taborri, Rossi, Palermo, Patane, & Cappa, 2014; Taborri, Scalona, Palermo, Rossi, & Cappa, 2015; Tan, Aung, Tian, Chua, & Yang, 2019; Vu et al., 2018; Yang et al., 2019), 3D marker data (Aung et al., 2013; Kidzinski, Delp, & Schwartz, 2019; Osis, Hettinga, & Ferber, 2016; Osis, Hettinga, Leitch, & Ferber, 2014), electromyography (Morbidoni et al., 2021), pressure sensors (Crea et al., 2012), and textile sensors (Rezaei, Ejupi, Gholami, Ferrone, & Menon, 2018). Across the board, though, these approaches required a priori feature extractions and are, hence, potentially jeopardized by selection bias.

Stepping instants can readily be identified using (the shape of) ground reaction forces (GRFs), typically obtained from force plate signals (Borghese et al., 1996; Roerdink et al., 2008). With these, one can specify single/double support and flight phases and, correspondingly, the mode of locomotion, i.e., walking or running. As such it seems obvious to first seek to estimate the GRF's shape from wearable sensors and to subsequently use these predicted waveforms

to determine gait events. Also here, machine learning has been successful. GRFs during the stance phase, for instance, has been estimated using only acceleration (Davidson, Virekunnas, Sharma, Piche, & Cronin, 2019; Leporace, Batista, & Nadal, 2018; Lim, Kim, & Park, 2019; Ngoh, Gouwanda, Gopalai, & Chong, 2018), a combination of acceleration and angular velocity (Lee & Park, 2020; Pogson, Verheul, Robinson, Vanrenterghem, & Lisboa, 2020; Sharma, Davidson, Muller, & Piche, 2021; Wouda et al., 2018), or marker-based kinematics (Johnson et al., 2021; Komaris et al., 2019). The GRFs during double stance phase could be estimated via marker-based kinematics (Choi, Lee, & Mun, 2013; Oh, Choi, & Mun, 2013) and the GRFs during the full gait cycle using accelerometers placed on the torso (Guo et al., 2017). Yet, these approaches often appeared tailored to the data under study rendering their generalizability questionable, but more importantly, in almost all cases, they only managed to predict GRFs for the stance phase, whereas the (duration of the) swing phase is of great importance when investigating running.

A recent review revealed that the shape of the GRF can most accurately be estimated from accelerometry (Horsley et al., 2021) and another found neural networks as a promising tool to do so (Ancillao et al., 2018). This triggered the idea of estimating vertical GRF waveforms from acceleration signals of the lower extremities via reservoir computers, more specifically via echo state networks (ESNs) (Goodfellow, Bengio, & Courville, 2016; Jaeger & Haas, 2004; Maass, Natschlager, & Markram, 2002). ESNs are 'minimal' forms of recurrent neural networks. Thanks to the reservoir's 'complex' structure, they may come with great computational capacities (Lukoševičius & Jaeger, 2009; Pathak, Hunt, Girvan, Lu, & Ott, 2018). In the absence of feedback, one can train them with a very simple and robust rule: optimizing output weights by mere linear regression. This is particularly appealing when considering that typical datasets on gait are fairly limited in size and that any implementation of machine learning in wearable devices should come with low computational costs.

In the following, we conceptually prove that a single reservoir computer can accurately predict vertical GRF waveforms from shank accelerometer signals, which allows for detecting gait events during walking and running with particularly high precision.

Methods

Participants

We included data of 21 healthy young adults (13 male / 8 female) in the analysis with a mean $\pm$ standard deviation age, height, and weight of 20.8 $\pm$ 1.0 years, 181.7 $\pm$ 10.3 cm, 71.1 $\pm$ 9.8 kg, respectively. The recorded speeds were 1.24 $\pm$ 0.12 m/s for walking and 2.20 $\pm$ 0.14 m/s for running. The participants provided written informed consent in compliance with the Declaration of Helsinki. The experimental design was approved by The Scientific and Ethical

Review Board of the Faculty of Behavioural & Movement Sciences, Vrije Universiteit Amsterdam, Netherlands (File number: VCWE-2022-008R1).

Experimental protocol

Participants walked and ran at their preferred speeds on an instrumented dual-belt treadmill (Motek Medical BV, Culemborg, Netherlands) in tied-belt mode wearing their own shoes. The preferred walking and running speeds were determined for each participant followed by a familiarization. The preferred speeds were determined by starting at either 2 km/h or 6.5 km/h for walking and running, respectively, and slowly increasing the speed by 0.1 km/h until the participant felt it was comfortable (Jordan, Challis, & Newell, 2007). Subsequently, the same process was repeated at a speed 1.5 km/h above this by now slowly decreasing the speed by 0.1 km/h until a new or the same preferred speed was reached. If the two speeds differed more than 0.4 km/h from each other, a third iteration was done, and irrespective of two or three iterations, the mean of the determined preferred speeds was used. The participants were instructed to step with each foot on a separate belt to be able to record the time series of the ground reaction forces from one leg. For each participant a walking and a running trial were recorded of each five minutes in length. Only consecutive strides absent of artefacts (stepping on the wrong belt) were retained leaving an average of 72 strides per trial for analysis (range: 49-116 strides).

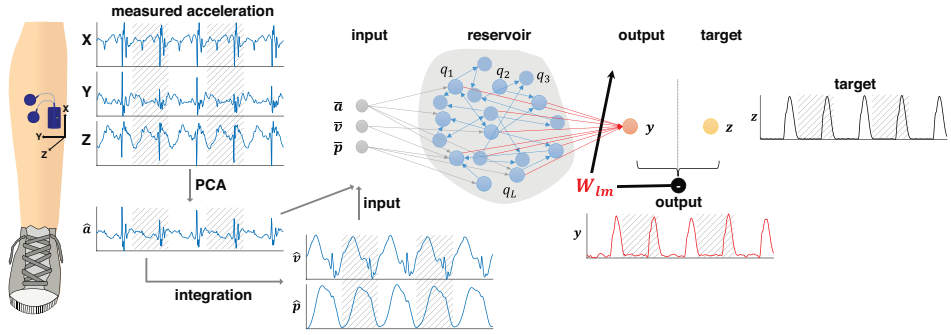

Figure 5.1: A reservoir computer was implemented to predict the vertical ground reaction forces. Tri-axial accelerometer data were recorded from the shank. The accelerometer data were re-oriented using a principal component analysis (PCA). The first prinicipal component ($\hat{a}$) was integrated to obtain the velocity ($\hat{v}$) and position ($\hat{p}$) data. The input $\boldsymbol{x}$ consisting of the normalised accelerometer ($\bar{a}$), velocity ($\bar{v}$), and position ($\bar{p}$) data were subsequently mapped onto the sparsely, randomly connected reservoir $\boldsymbol{q}$. This reservoir generated the output $\boldsymbol{y}$, the predicted normalised vertical ground reaction forces (in red), via output weights $\boldsymbol{W}$. When training, the output was compared to the target $\boldsymbol{z}$, i.e. the measured vertical ground reaction forces (in black). Minimising the difference between generated output and target served to adjust the weights (denoted here as W_{lm}). For training, data were segmented into strides, here represented by hatched and unhatched areas. Testing was conducted on continuous data. Data from walking and running were pooled.

Tri-axial accelerometers, built into the probe of the wireless bipolar surface electromyography system (Mini wave plus, Zerowire; Cometa, Bareggio, Italy), were mounted on the right

and left tibia, respectively (see Figure 5.1). The accelerometers were not placed in the same exact position due to inexperienced researchers. Accelerometer data were sampled at 2,000/14 Hz (=142.86 Hz) which in the following will be referred to as ~143 HZ, with a sensitivity of $\pm$ 16g, which was sufficient to avoid clipping. The vertical GRFs were sampled at 1 kHz and re-sampled to ~143 Hz.

A single reservoir computer was trained to predict ipsilateral continuous vertical ground reaction forces based on the shank accelerometer data recorded during walking and running. Figure 5.1 contains a schematic of the pre-processing steps and the implemented machine learning approach. Further details are presented in the following.

Data processing

Accelerometer signals a were first 'standardized' to their principal axes using principal component analysis (PCA) (Moe-Nilssen, 1998; Rispens et al., 2014):

$$a = \left(a_x, a_y, a_z\right) \xrightarrow{\text{PCA}} \hat{a}$$

with $\hat{a}$ along the direction of maximum variance and being the only principal component that was retained. $\hat{a}$ was integrated twice over time (after a bi-directional high pass Butterworth filter with cut-off at 1 Hz, 2nd order) to generate likewise standardized velocities $\hat{v}$ and positional data $\hat{p}$:

$$\hat{v} = \int_0^t \hat{a} \cdot dt \quad \text{and} \quad \hat{p} = \int_0^t \hat{v} \cdot dt$$

Per subset (trial) these signals were normalized (Halilaj et al., 2018) by means of

$$\hat{a} \to \bar{a} = \frac{\hat{a}}{\text{range}(\hat{a})} \quad \text{and} \quad \hat{v} \to \bar{v} = \frac{\hat{v}}{\text{range}(\hat{v})} \quad \text{and} \quad \hat{p} \to \bar{p} = \frac{\hat{p}}{\text{range}(\hat{p})}$$

before combining them as three-dimensional input data

$$x = (\bar{a}, \bar{v}, \bar{p}) \in \mathbb{R}^{3 \times T}$$

with T indicating the number of samples in time. Vertical ground reaction forces F_z were normalized. With this, the target signal for our machine learner (see below) could be defined as z-score (Halilaj et al., 2018)

$$z = \bar{F}_z = \left(F_z - \mu(F_z)\right) / \sigma(F_z) \in \mathbb{R}^{1 \times T}$$

with μ and σ denoting the mean and standard deviation over time per trial.

Stepping moments (foot contact and foot off events) were identified based on the measured F_z through mere thresholds: First, the F_z was scaled to a range [0 1], then weakly filtered with a polynomial Savitzky-Golay filter (1st order, ± 30 ms = in total 9 samples) (Savitzky & Golay, 2002). The foot contact was defined as the last point below a threshold (12.5% of the maximum of the data) nearest the ascend of the F_z of the stance phase; similarly, the foot off was defined as the first point crossing the same threshold nearest the descending F_z (Borghese et al., 1996; Ghoussayni, Stevens, Durham, & Ewins, 2004).

Data were split according to the defined foot off events for further analysis. We considered 36 samples in time on either side of the foot off as transients when correcting for learning errors in the beginning or end of the data. These transients also served to ensure that data were independent of the true events as 36 samples represent different percentage of the stride for walking and running, respectively.

Reservoir computer

We adopted the leaky ESN implementation by (see also Jaeger, 2001; Jaeger, 2002); Jaeger and Haas (2004). In brief, we built a reservoir of N nodes $q = (q_1, q_2, \dots, q_N) \in \mathbb{R}^{N\times T}$ that received an input $x = (x_1, x_2, \dots, x_K) \in \mathbb{R}^{K\times T}$ and generated output $y = (y_1, y_2, \dots, y_M) \in \mathbb{R}^{M\times T}$. During the supervised training mode output was compared with target $z = (z_1, z_2, \dots, z_M) \in \mathbb{R}^{M\times T}$ by means of the L_2-norm (Lukoševičius, 2012); cf. Figure 5.1.

The reservoir dynamics can be written as

$$dq = \tau^{-1}[-\gamma q + \tanh(Cq + Fx)]dt + d\varepsilon$$

where $C \in \mathbb{R}^{N\times N}$ denotes the connectivity of the reservoir. Here, C was set as a sparse, random matrix specified by a sparseness parameter; its weights were normalised for a given spectral radius (the relative magnitude of the leading eigenvalue of C). $F \in \mathbb{R}^{N\times K}$ was set to be a dense matrix allowing for an optional scaling of the input values when mapping them onto the reservoir. The quantity ε stands for uniformly distributed, uncorrelated noise, i.e., $\varepsilon \in \varepsilon\mathcal{U}(-1,1)$, with ε being reasonably small. The output is given by

$$y = Wq$$

with $W \in \mathbb{R}^{M\times N}$, which is the matrix of the to-be-learned output weights.

Learning was realized by ridge regression, i.e.

$$\|z - q\| = \|z - Wq\|_2 \to \min \Rightarrow W = Q^{-1}z$$

where $Q = [q_1, \dots, q_T]$ and $(\cdot)^{-1}$ denotes the pseudo-inverse. In the case of multiple time series, i.e. S steps (see below), we defined $Q = \left[q_1^{(1)}, \dots, q_{T_1}^{(1)}; q_1^{(2)}, \dots, q_{T_2}^{(2)}; \dots; q_1^{(S)}, \dots, q_{T_S}^{(S)}\right]$ and accordingly we used $z = \left[z^{(1)}; \dots; z^{(S)}\right]$.

The network parameters were set as follows: $N = 1000$, $\text{spectral radius} = 0.5$, $F = [0.1; 0.5]$, $\tau = 1$, $\gamma = 0.5$ and $\varepsilon = 10^{-4}$. The noise was primarily added to minimize the risk of overfitting and we put $\varepsilon = 0$ after learning.

Stepping moments from the predicted vertical ground reaction forces

Stepping moment identification of the predicted vertical ground reaction force waveforms was implemented in the same way as for the measured vertical ground reaction forces (see above).

Estimation of gait events such as foot contact and foot off from vertical GRF waveforms are considered the gold standard in movement analysis. An example of the detection algorithm during walking and running can be found in Figure 5.2. One sample difference between the events based on the measured and predicted vertical GRF waveforms equaled ~7 ms due to the relatively low sampling frequency, common to wearable accelerometers.

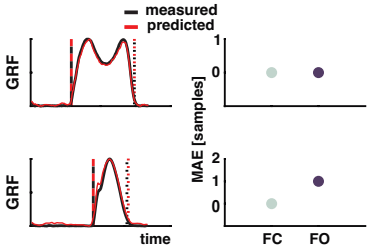

Figure 5.2: Example of the estimation of foot contact and foot off events from measured and predicted ground reaction forces. Top: walking, bottom: running. Left side: Measured vertical GRF waveforms are depicted in black and the predicted ones in red. The vertical dashed lines represent foot contact (black: measured, red: predicted) and the dotted lines represent foot off (black: measured, red: predicted). Right side: Differences in samples between events based measured and predicted vertical GRF. One sample equal ~7 ms. Abbreviations: MAE: mean absolute error, FC: Foot contact, FO: Foot off.

Statistical evaluation

The normalized root mean square error ϵ and the coefficient of determination R^2 served for quality assessment of the predicted vertical ground reaction forces. We defined them as follows:

$$\epsilon = \frac{\langle \|z - y\|_2 \rangle}{\text{range}(z)} \quad \text{and} \quad R^2 = 1 - \frac{\langle \|z - y\|_2^2 \rangle}{\langle \|z - \langle z \rangle\|_2^2 \rangle}$$

Prediction of stepping moments were validated using the mean absolute error defined as

$$\frac{1}{t}\sum_{i=1}^{t}\left|E_{\text{target},i} - E_{\text{prediction},i}\right|$$

where, $E_{\text{target},i}$ and $E_{\text{prediction},i}$ refer to target and prediction events $i = 1, \ldots, t$, respectively.

We evaluated the training via cross-validation with 50% of the data segmented and subsequently used for training, 25% continuous data for validation, and the remaining 25% continuous data for testing. We performed 100 repetitions with a random draw each time. A continuation rule was used, such that if the R^2 of the validation data were all positive, the testing could be employed, and the training was satisfactory. A maximum of 100 repetitions were allocated for validation and in cases where the validation criteria was not satisfied, the training was stopped. In all cases, the number of strides used from each trial during training was reduced to 25 to ensure a balanced design.

Two scenarios served to assess the robustness of the reservoir computer as sketched in Figure 5.3.

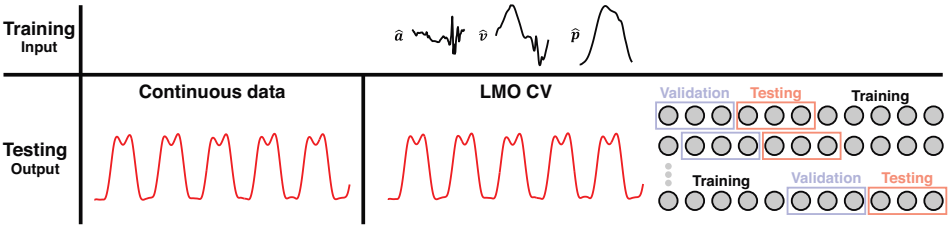

Figure 5.3: Schematic of the different testing scenarios used for validating the robustness of the reservoir computer. A random trace of a walking trial is shown here. The input data ($\hat{a}, \hat{v}, \hat{p}$) were first segmented into strides (we considered 36 samples in time on either side of the foot off as transients when correcting for any learning errors in the beginning or end of the data). The first scenario, the training is performed on segmented data and the testing on continuous data. The continuous data (in red) represents the output of the reservoir, the vertical GRF waveforms. Secondly, the training was performed on segmented data, testing was done on continuous, but a leave-M-out cross-validation (LMO CV) was employed (split: 50/25/25% for training, validation, and testing, respectively). The vertical GRF in red represents the output of the trained reservoir during testing. Abbreviations: LMO CV: Leave-M-out cross-validation.

Training on segmented data – validating and testing on continuous data

The applicability of our machine learning approach on continuous data were verified by training the reservoir computer on single strides and subsequent testing on continuous data from each trial (see Figure 5.3). First, we extracted a random 50% of continuous data from each trial before segmenting the remaining data into strides. The continuous data was split in two so 25% of the data were used for validation and testing, respectively. The segmented data were pooled across trials and conditions before being used for training. Training was validated by verifying the mean R^2 over the validation set to be positive (see above for definition). Whenever validation did not pass with success, training was repeated using the same subset but other randomly chosen initial conditions (here in all cases validation was passed on first

attempt). The entire process was repeated 100 times to allow for statistical evaluation as mentioned earlier.

Additionally, we estimated the minimum amount of data needed to secure a good reconstruction quality ($R^2 > 0.95$), so the training data were reduced. We repeated the training 100 times from 4% of the total dataset to 50% of the total dataset. The validation and test sets remained 25% each for all runs (here the smaller training set sizes required re-learning but eventually validation was passed with success).

Leave-M-out cross-validation

To test the machine learner's ability to work as a classifier across participants, it was first trained and validated on a subgroup of participants and then tested on others that was unknown to the machine learner. The cross-validation split was performed based on trials. M trials were held out and the remaining 42-M trials were split 75/25% of the total dataset for training and validation. A total of 42 repetitions were performed. In the main text we report the result for $M = 1$ while the range $M = 1,2 \dots ,6$ is depicted in *Supplementary Material* 5.2.

Unless specified otherwise, means and standard deviations are provided and were calculated as either the grand averages or the standard deviations across the 100 repetitions.

Results

A total of 3020 strides were included from 42 trials (1249 walking strides [21 trials] and 1771 running strides [21 trials]). Here, we would like to note that we only show results of the right-side analysis, as the left-side results were very similar. Given this similarity one may pool data across sides to increase the sample size but, as will become clear, this was not needed.

The performance of 100 repetitions in predicting GRF waveforms exceeded 95% when combining walking and running data. The coefficients of determination R^2 were 0.96 ± 0.00 and the normalized root-mean squared errors ϵ were $6.8 \pm 0.3\%$ (mean $\pm$ SD); cf. Figure 5.4. On average, the subsequently extracted foot contact and foot off events deviated from those based on the measured vertical GRF waveforms by 3 and 4 samples. This corresponds to mean absolute errors of 21.9 ± 6.5 ms and 29.1 ± 16.0 ms for foot contact and foot off events, respectively. Here we would like to add that the likewise convincing results when training the network on only walking or on only running are provided as Supplementary Material 5.1.

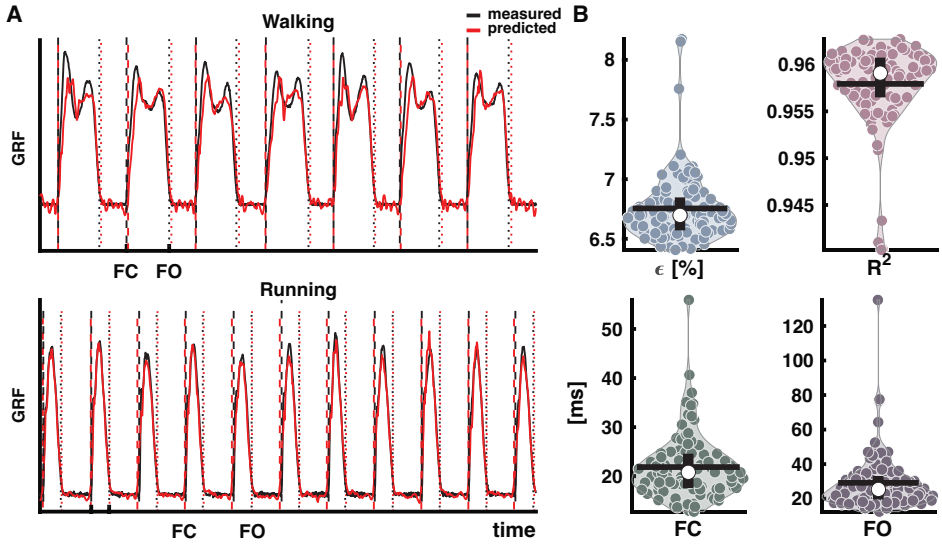

Figure 5.4: Output of reservoir computer trained on segmented data and validated and tested on continuous data pooled over conditions. (A) Vertical ground reaction force (GRF) waveforms of four randomly selected strides from each condition from a random trial and a random selected training run out of the 100, with the measured vertical GRF waveforms in black and predicted in red. The vertical dashed lines represent the foot contact events (black: measured, red: predicted), the vertical dotted lines the foot off events (black: measured, red: predicted). (B) Normalized root-mean squared error (ϵ), coefficient of determination (R^2), mean absolute error of foot contact and foot off. The white dots in the violin-plots illustrate the medians. Black horizontal lines represent the mean and vertical black lines the 1st and 3rd quartiles. Every dot represents one of the 100 training runs, and the width of the violins is determined by the frequency. Abbreviations: GRF: ground reaction forces, FC: foot contact, FO: foot off.

To estimate the smallest number of strides needed for a mean reconstruction accuracy above 95%, we changed the size of the training set from 4 to 50% for the total dataset size (again with maximum 25 strides per trial for the training); cf. Figure 5.5. The size of the validation and test sets were kept fixed at 25% each to guarantee identical accuracy demands. An average of approximately 222 strides, ~17% of the total dataset sufficed to reach R^2 = 0.95 $\pm$ 0.01 with ϵ = 7.2 $\pm$ 0.3% and a mean absolute error of the foot contact (foot off) of 26.4 $\pm$ 9.3 ms (35.8 $\pm$ 15.8 ms).

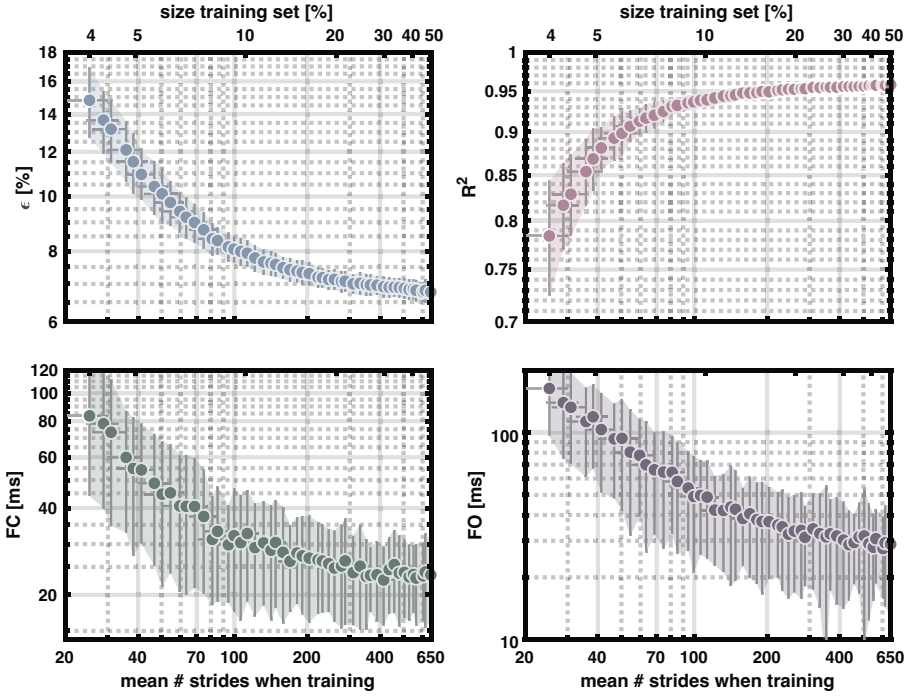

*Figure 5.5: Output of reservoir computer with training data ranging from 4-50% of the total dataset and validating and testing with 25%, respectively. Upper left panel: normalized root-mean squared error (**ϵ**), upper right panel: coefficient of determination (R^2), lower left panel: mean absolute error of foot contact, and lower right panel: mean absolute error of foot off. Upper x-axes show the percentage of the total dataset used for training and the lower x-axes the corresponding mean number of strides. Each dot represents the mean value for 100 repetitions. The vertical error-bars and colored areas represent the standard deviation of the corresponding measure. The horizontal error-bars represent the standard deviation in the number of strides across the 100 repetitions. Abbreviations: FC: foot contact, FO: foot off.*

Finally, to test whether our approach allows for predicting vertical GRFs in trials that in their entirety were not part of the learning set, we performed a leave-M-out cross-validation. Training was realized in the held-in trials using a 75%-25% split of learning and validation (in the training set we used a maximum number of 25 strides per trial). For $M = 1$, the mean R^2 reached 0.91 ± 0.12, with an error ϵ of $9.1 \pm 3.6\%$. One trial was a clear outlier in the leave-one-out analysis, and when re-calculating the means without this trial, the mean R^2 and the error ϵ were 0.93 ± 0.04 and $8.6 \pm 2.3\%$, respectively. The corresponding mean absolute errors for foot contact and foot off were 63.7 ± 167.1 ms and 140.9 ± 224.3 ms for all included trials and 49.0±138.9 ms and 129.8 ± 215.1 ms when not taking the outlier trial into account. For an overview of the results of $M = 1$ to $M = 6$, we refer to *Supplementary Material* 5.2.

Discussion

Reservoir computers are a promising tool to predict vertical GRF waveforms based on accelerometer data measured at the shank during walking and running. Accurately predicted GRF waveforms facilitate the detection of gait phases and events. We showed that this 'simple' machine learning approach has excellent prediction accuracy of continuous vertical GRF waveforms independent of the type of locomotion. Put differently, reservoir computers can be used for predicting vertical GRF waveforms for gait of unknown type with excellent performance. This has great potential for uses outside the lab and for collecting large amounts of data. Without a doubt the growing amount of data available for biomechanical analysis in running will greatly drive the field forwards (Novacheck, 1998). Machine learning combined with wearable sensors may be the solution to increase the amount of data recorded.

Using machine learning for activity recognition and gait phase recognition based on gait features extracted from biomechanical data, which may be measured with wearable sensors (Farrahi, Niemela, Kangas, Korpelainen, & Jamsa, 2019; Figueiredo et al., 2018) has become increasingly popular. The most common techniques to classify gait events or predict GRF waveforms using machine learning are hidden Markov models (Abaid et al., 2013; Chen et al., 2017; Chen, Salim, & Yu, 2015; Crea et al., 2012; Guenterberg et al., 2009; Mannini et al., 2014; Mannini & Sabatini, 2012; Taborri et al., 2014; Taborri et al., 2015; Yuwono, Su, Guo, Moulton, & Nguyen, 2014), neural networks such as deep neural networks (more than 1 hidden layer) (Davidson et al., 2019; Prado et al., 2019; Rezaei et al., 2018; Vu et al., 2018; Wouda et al., 2018; Yang et al., 2019); feed-forward neural networks (Choi, Jung, Lee, Lee, & Mun, 2019; Choi, Jung, & Mun, 2019; Choi et al., 2013; Komaris et al., 2019; Lee & Park, 2020; Lim et al., 2019; Ngoh et al., 2018; Oh et al., 2013); long short-term models (Choi, Jung, Lee, et al., 2019; Choi, Jung, & Mun, 2019; Kidzinski et al., 2019; Robberechts et al., 2021; Sharma et al., 2021; H. X. Tan et al., 2019); convolutional neural networks (Johnson et al., 2021; Su et al., 2020); support vector machines (Morbidoni et al., 2021; Nutakki et al., 2020; Rezaei et al., 2018); (multilayer) perceptron models (Leporace et al., 2018; Mijailovic, Gavrilovic, Rafajlovic, Đuric-Jovicic, & Popovic, 2009; Morbidoni et al., 2021; Pogson et al., 2020; Robberechts et al., 2021), as well as random forest classifiers (Morbidoni et al., 2021; Rezaei et al., 2018; Yang et al., 2019), K-nearest neighbors (Chu, Jiang, & Menon, 2017; Morbidoni et al., 2021; Sharma et al., 2021), and other types of machine learning using, e.g., Bayesian models (Martinez-Hernandez & Dehghani-Sanij, 2018; Meng et al., 2019; Nutakki et al., 2020; Yuwono et al., 2014), Gaussian mixture model (Aung et al., 2013), and principal component analysis (Osis et al., 2016; Osis et al., 2014; Pogson et al., 2020; Yuwono et al., 2014). Reservoir computers have the great advantage of low computational costs while still showing excellent performance. They merely require a handful of time series for training and avoid any a priori feature extraction. Reservoir computers even seem to be promising as a tool to successfully

reproduce locomotor patterns observed during walking and running (de Graaf, Mochizuki, Thies, Wagner, & Le Mouel, 2022).

There have been several studies conducted on predicting GRFs based on wearables, the vast majority for the stance phase only. Utilizing these machine learning techniques properly requires foot contact and foot off to be known. This, however, can only be accomplished by either co-registering footswitches or ground reaction forces, or by implementing a rule-based detection of the gait events. This is exactly what we sought to circumvent. Rule-based detections based on accelerometers during running, searching for a specific peak or valley in some area of interest, are not as precise as an event detection based on vertical ground reaction forces.

We did not restrict the prediction to only the stance phase – we included the entire gait cycle and showed that this worked well on continuous data. We also did not time-normalize the gait cycles and did not impose any other constraints into the timing of the signals. As such, our predictions are robust against variations in speed and stride durations/lengths as well as the type of locomotion. For training the reservoir computer, data were segmented based on the ground truth events, though when these are unknown, the data could be segmented in any way, or they may not be segmented at all; cf. Figure 5.4. We are convinced that our approach is suitable for lab as well as outdoor use. One very recent study (Alcantara, Edwards, Millet, & Grabowski, 2022) predicted continuous vertical GRFs from trunk accelerations using a long short-term model network with good accuracy during sloped running. The pre-processing involved several filtering and feature extraction steps. By contrast, here we succeeded to reduce the number of pre-processing steps and applied only very weak filtering, i.e., the inputs are by and large the time series (derived from) vertical acceleration.

We validated the use of accelerometer data to estimate the vertical GRF waveform. We used accelerometer data collected by a sensor that could, in fact, also be used for electromyography data collection. The sensors were not aligned in the same way for all participants, which Tan, Chiasson, Hu, and Shull (2019) found can negatively affect the precision of the detection of GRFs using machine learning. However, variability in orientation and position is likely to occur if participants mount their own devices or in large-scale studies. By correcting the orientation of the accelerometers using principal component analysis we circumvent these potential problems and underline the robustness of our method and its applicability in many settings.

Even a small number of strides sufficed to achieve a high reconstruction accuracy. While strides from all participants were pooled for this analysis, it is unlikely that the strides randomly drawn into the training sets were representative for all trials/conditions and that this was also the case for the test sets. We evaluate this via leave-M-out cross-validation, as the test-set should be unknown to the machine (Halilaj et al., 2018). Admittedly, the

reconstruction accuracy was not as high, but we consider it still satisfactory. The resulting event detection of the leave-M-out cross-validation, did not perform satisfactorily because of an introduction of jitter into the swing phase of the GRF which led many events to be detected too early or too late. We trust that a revision of the event detection algorithm can result in an improved FS and FO estimation compared to the gold standard.

We would like to note that we did not optimize the machine learner to perform the absolute best it can do. Our primary aim was to show that even in its 'simplest' form, a reservoir computer with ridge-regression-based output weights can perform well. Apparently, this (off-line) approach has its limits as, during learning, one must store all network states which can put pressure on computer memory. The alternative online learning may be realized via recursive least squares regression (Haykin, 2014), that has recently be adopted by Sussillo and Abbott (2009). Along these lines one may add online feedback and change the reservoir's connectivity for the network's dynamics to reach the chaotic regime (currently we used a spectral radius of 0.5 but values larger than 1 may accelerate online learning; Sussillo & Abbott, 2009; Yildiz, Jaeger, & Kiebel, 2012). For our proof-of-concept, however, fine-tuning the reservoir might be considered overfitting, which let us decide not to progress along this direction. The most optimal settings will probably depend on the dataset under study.

Our accelerometers had a relatively low sampling rate (2000/14 Hz ≈ 143 Hz), which prevents better estimation than 7 ms (i.e., one frame equals 7 ms). An accelerometer with higher sampling frequency will arguably lead to higher accuracy of the predicted events compared to the ground truth. A sampling frequency of 60-200 Hz is not uncommon when recording kinematics (Fellin, Rose, Royer, & Davis, 2010; Hreljac & Marshall, 2000; O'Connor, Thorpe, O'Malley, & Vaughan, 2007; Zeni, Richards, & Higginson, 2008) and the accuracy is not worse than the accuracy one could obtain using kinematic data. A frequently employed detection algorithm for kinematic gait event detection is the coordinate-based detection algorithm where the distance between the sacrum and foot is used to predict foot contact and foot off events (Zeni et al., 2008, currently cited >800 times). A review on this and other detection algorithms (Fellin et al., 2010) during running revealed that the coordinate-based detection algorithm has an absolute error of 29 ms for foot contact and 98 ms for foot off (sampling frequency: 200 Hz) whereas the best performing algorithms has an accuracy of 24 ms for foot contact (the foot vertical position (Alton, Baldey, Caplan, & Morrissey, 1998, >600 citations)) and 6 ms for foot off (the peak knee extension algorithm (Dingwell, Cusumano, Cavanagh, & Sternad, 2001, >600 citations)). For comparison, the best estimation possible with a sampling frequency of 200 Hz is 5 ms, i.e., current algorithms have an accuracy between one and ~ 20 samples. Our approach is comparable to or exceeding this accuracy. Being cheap and easy to collect, being usable outside the lab and for long time-periods are, hence, not the only advantages of accelerometers – they also come with formidable accuracy in step detection when properly combined with reservoir computers.

Our machine learning approach performs well for a dataset comprised of both walking and running data despite a relatively small number of participants and a relatively small number of strides. To investigate its ability for each condition separately, we refer to *Supplementary Material* 5.1, where we show that training and testing on only one type of locomotion improves the already excellent reconstruction accuracy. The outputs of the reservoir computer can easily be modified to provide other outputs such as other components of the GRF or the center-of-pressure. By including all three components of the GRF, energetics of the center-of-mass can be estimated during overground/track running which in turn can provide even more information about the locomotion type. Of course, the energetics will be in arbitrary units given our GRF prediction rely on normalize (z-scored) values. To expand the prediction from z-scored GRF to GRF containing information about the body weight of the participant, a more diverse group of participants are needed for training data. However, despite this shortfall, we believe that this is feasible. All data for this study were recorded on the treadmill. The next step will be to apply reservoir-based prediction to accelerometer data (or gyroscope data) obtained at other parts of the body, e.g., hip mounted (e.g., activity trackers), arm mounted (e.g., sport watches, smartphones) or head mounted (e.g., augmented/virtual reality glasses) to broaden applicability in daily living contexts as well as in clinical populations as machine learning algorithms might perform worse on clinical gait (Bastien, Gosseye, & Penta, 2019). This certainly calls for expanding the current dataset with overground/outdoor locomotion. We expect our findings to be transferable to overground settings. A large meta-analysis suggests that neither vertical ground reaction forces, nor peak tibial accelerations are significantly different between treadmill and overground running (Van Hooren et al., 2020). However, this might not be true when accelerations, decelerations, turns, etc. are considered.

As a final note we would like to recall that our reservoir computer did not include a feedback loop. Adding feedback may allow for not only predicting the GRF accompanying tibial accelerations but eventually also the GRF in forthcoming strides. We trust that future studies will pursue this generalization as it is beyond the scope of our proof-of-concept study. Given our prediction results, however, we can stress that all the information needed for predicting (vertical) ground reaction forces seems to be present in the (principal component of) accelerometer signals. The use of the latter, hence, provides more opportunities than commonly thought.

Our data and code are made freely available and are ready to use on other datasets and can be extended for use in experiments and clinic.

Conclusion

Reservoir computers are an excellent candidate to correctly predict vertical ground reaction force waveforms from accelerometer signals for a small number of participants and strides.

The predicted time series can serve to estimate stepping moments with particularly high accuracy. The ease in training procedure, which requires only a (very) limited number of steps and without prior knowledge about the type of locomotion lets us advocate this machine learning approach to be further expanded to be applied on future applications in both research and clinic.

Supplementary Material 5.1

To investigate if training the reservoir computer on each condition separately resulted in even better prediction values, we trained and validated on stride-segmented data and tested its prediction capacity for continuous gait data for each condition separately. For each trial, 25% of the continuous data was selected for testing, another 25% of the continuous data was selected for validation and the remaining 50% was segmented into strides (with a maximum of 25 strides per trial) and subsequently pooled across all trials and used for training totaling a 50/25/25% split for training, validation, and testing respectively. For both walking and running the quality of performance of predicting vertical GRF waveforms exceeded 97%: the coefficients of determination R^2 were 0.97 ± 0.00 and 0.97 ± 0.02, respectively, and the normalized root-mean squared errors ϵ were $5.9 \pm 0.4\%$ and $5.6 \pm 0.3\%$, respectively (mean $\pm$ SD); cf. Figure S5.. On average, the subsequently extracted foot contact (foot off) events deviated from those based on the measured vertical GRF waveforms by 2.4 (2.5) samples for walking and 1.9 (2.3) samples for running. This corresponds to mean absolute errors of 17.3 ± 12.2 ms (17.5 ± 11.3 ms) for walking and 13.5 ± 3.9 ms (16.1 ± 8.5 ms) for running.

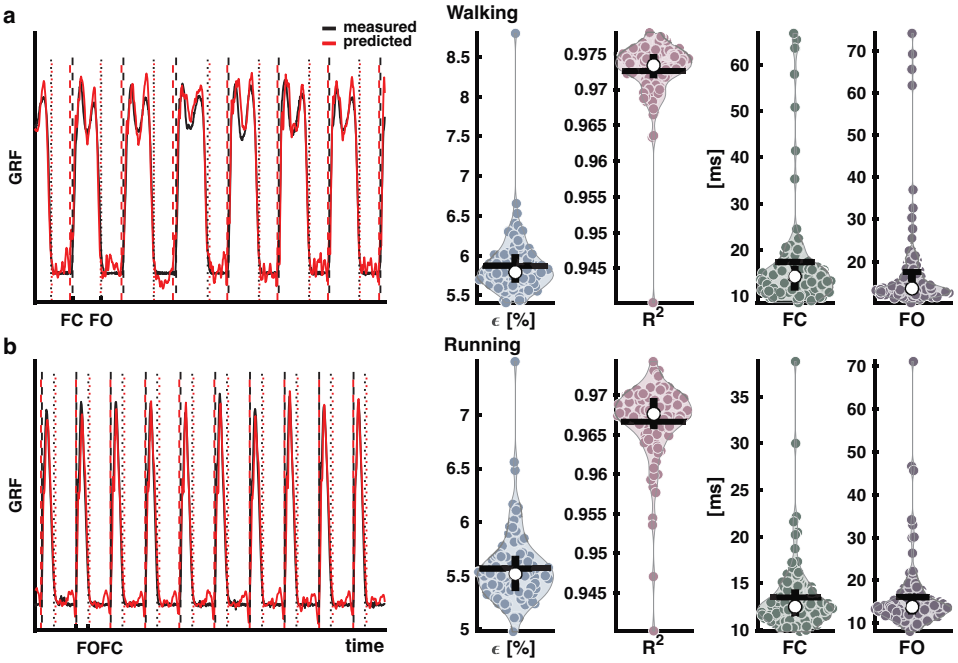

Figure S5.1: Output of the reservoir computer trained on segmented data and validated and tested on continuous data. a: Walking condition, b: Running condition. Left panels: Vertical ground reaction force (GRF) waveforms of four randomly selected strides from a random trial and a random selected iteration out of the 100, with the measured vertical GRF waveforms in black and predicted in red. The vertical dashed lines represent the foot contact events (black: measured, red: predicted), and the vertical

dotted one the foot off events (black: measured, red: predicted). Right side panels: Normalised root-mean squared error (ϵ), coefficient of determination (R^2), mean absolute error of foot contact and foot off. The white dots in the violin-plots illustrate the medians. Black horizontal lines represent the mean and vertical black lines the 1st and 3rd quartiles. Every dot represents one of the 100 iterations. Abbreviations: GRF: ground reaction forces, FC: foot contact, FO: foot off.

As a final test of the validity of the machine learner, we ran the leave-M-out cross-validation for M = [1,2…6]. The leave-M-out iterations were all repeated 42 times to ensure no bias in the random selection of trials. The results can be found in Figure S5.2. The poor results found in the leave-one-out cross-validation stems from one trial with particularly large errors, here indicated as outliers.

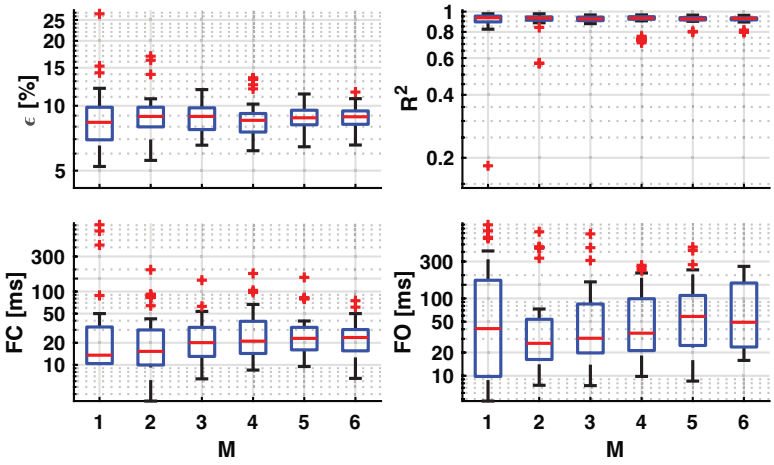

Figure S5.2: Result of the leave-M-out cross validation. A leave-M-out cross-validation with M ranging from 1 to 10 was carried out. Upper left panel: normalised root-mean squared error (ϵ), upper right panel: coefficient of determination (R^2), lower left panel: mean absolute error of foot contact, and lower right panel: mean absolute error of foot off. Red horizontal lines indicate the median, the boxes represent the 25th and 75th percentile. Outliers are indicated with red plus. Note the large outliers in the M=1.

Chapter 6

EPILOGUE

The understanding of the development of running in children is limited, specifically the underlying mechanisms of the motor control. In this thesis I studied the motor control of the development of running in children by combining neuromuscular and biomechanical measures using novel techniques and state of the art statistics. Hereby, I introduced a frame of reference for the factors underlying the development of running in children.

The cross-sectional study in **Chapter 2** was my attempt to understand whether the most common classifiers for running can be used in children. I also sought to unravel how to determine the degree of maturity in children while locomoting on a treadmill. This study was entirely focused on the biomechanical aspects of locomotion. It shows that neither flight phase nor the in-phase oscillations of kinetic and potential energies of the center-of-mass (CoM) are proper indicators of running in children. This implies that these two measures cannot be used in (young) children despite their prevalence in classifying types of locomotion in adults. With the adult walking and running patterns defined as the mature ones, children locomotion can sometimes not be linked to either of them, at least not in a unique fashion. As such they are also not sensitive enough to distinguish between immature and mature locomotory patterns, especially in the children older than 3.5 years. That is, having a flight phase or in-phase oscillations of the kinetic and potential energies are not valid determinants of the degree of maturity in the gait patterns of children.

My next objective was to investigate the development of neuromuscular control of locomotion in children and to correlate this control to the ability to run with a flight phase. In **Chapter 3** I assessed muscle activity and in particular the number and structure of muscle synergies and related them to the ability to run with a flight phase. Despite my expectations we only found a weak correlation between age and the duration of the contraction of the medial gastrocnemius muscle. Significant differences in the phase shift of this muscle across the four groups were absent. There was an increase in the number of muscle synergies related to the ability to run with a flight phase and in this case, the oldest children, while the number of synergies was lowest for the adults. My interpretation is that this increased number of synergies in older children compared to younger children is related to motor learning and exploration.

To further detail the development of locomotion, I investigated the running in a longitudinal design assessing two children from their first independent steps until ~32 months of walking experience. In **chapter 4** I combined both biomechanics and neuromuscular control of locomotion. By using a similar method as in **Chapter 2** and comparing the running development of the two toddlers to a group of adults, I was able to determine that the development of running can take different trajectories including the co-existence of immature and mature running within the same session in a child.

Recording large amounts of data is simple to do on a treadmill and most of the experimental data in this thesis were also recorded on a treadmill. However, a treadmill does not necessarily represent natural locomotion, so in **Chapter 5** I explored avenues to record outside of the lab. We employed recursive neural networks (reservoir computers) to predict vertical ground reaction force data from shank accelerometer data in adults with high accuracy which in turn lead to a high accuracy in the gait event detection. The machine learner was able to handle a combination of running and walking data.

Implications

The purpose of this thesis was to attempt to elucidate the motor control of the development of running in children. To achieve that goal, several research questions were posed that I will answer below.

Q1. *How suitable are the common classifiers in running for children learning to run?*

I found that it cannot be determined whether a (young) child is running based on the presence of a flight phase or the in-phase oscillations of the energetics of the CoM. A new definition should be investigated and agreed upon.

Whitall and Getchell (1995) found the use of a walk-run strategy in all four newly runners they investigated, despite the visual appearance of the children running. The authors speculated that this pattern might have been due to faster development of the ability of generating speed compared to the ability to control the vertical displacement of the center-of-mass. We found the same walk-run strategy in this thesis in a group of children aged 1-9 years old. Children investigated for this thesis either only use a double support phase, a flight phase, or use a combination of a flight phase and a double support phase. This walk-run strategy is statistically different from walking in its amount of double support phase as well as in discernable amplitudes and patterns of muscle activity. The work in this thesis highlights that the presence of a flight phase should not be used to determine whether a gait pattern is walking or running in children.

The relative recovered energy of the CoM and the in-phase oscillations of kinetic and potential energy of the CoM are both considerably larger in children compared to adults and as such, can also not directly be used as a proxy for when a child is running. Some research that includes running in children make it a point to exclude data when children do not show a flight phase (Cheung et al., 2020; Kratschmer, Bohm, & Doderlein, 2019) or when the exchange of energy exceeds a set threshold (Legramandi, Schepens, & Cavagna, 2013; Schepens et al., 1998). Yet, excluding these data points can mean excluding data relevant for the understanding of development and emergence of the mature running pattern.

Since children do not seem to have a flight phase or in-phase oscillations of the kinetic and potential energies while running, they cannot be making full use of the spring-mass model (c.f., **Chapter 1**). This finding corresponds to the hypothesis put forth by Whitall and Getchell (1995) that the vertical displacement of the CoM does not follow that of the adult. Overall, it implies that children make use of either a combination of the inverted pendulum model (i.e., the walking model) and the spring mass model (i.e., the running model) or a modified spring mass model with less compression during the stance phase of the stance leg.

Running using a walk-run strategy during development is useful to explore the degrees of freedom that is available to the child within boundaries that are already well-explored, i.e., having a (shorter than normal) double support phase. As development is not linear, the ability to run with a flight phase is also not static and sometimes the child makes use of the flight phase and other times not. We saw this not only within sessions in **Chapters 2, 3, and 4** but also across sessions in the longitudinal study in **Chapter 4**.

The following two questions are interlinked and are thus answered together.

Q2. *How to determine the degree of maturity in locomotory patterns in children?*

Q3. *What is the longitudinal development of running in very young children?*

To determine the degree of maturity in gait in children, advanced statistical methods should be combined with many parameters to capture the subtle differences across development. These analyses should be performed on a cross-sectional group as well as longitudinally.

The words ‘development’ and ‘maturation’ may be used interchangeably. In this thesis however, I use them in different contexts. Development is continuous whereas maturity implies an end-goal: you reach a stage of maturity. Broadly speaking, the development in the context of the motor control of running in children implies the general development of running. I used maturity as the preferred term when discussing gait patterns because the end-goal is a gait pattern corresponding to that of the healthy young adult. The degree of maturity is therefore indicative for the developmental stage.

Determining the degree of maturity requires understanding the mechanisms behind what constitutes a mature pattern. Several attempts have been made to qualify when a mature gait pattern has been established. Walking is thought to reach maturity between 7 and 12 years of age depending on the gait parameters investigated. Sutherland et al. (1980) argued that a combination of growth and maturation altered the spatiotemporal parameters of the walking pattern until around four years of age, whereas mostly growth accounted for the changes in the following years. The peak positive acceleration of the shank during walking was considered mature around 7 years of age (Tirosh, Orland, Eliakim, Nemet, & Steinberg,

2017), whereas the muscle activity patterns most likely does not mature until the age of 12 years at fast and slow walking (Tirosh et al., 2013). Maturity in running is only reached around 12 years in terms of the peak positive acceleration of the shank (Tirosh et al., 2017). Finding a common denominator that encapsulates all facets of the gait pattern seems to remain a challenge. And, maturity within one gait pattern may not correspond to maturity in another.

While much research has been carried out in adults to establish the differences between walking and running in e.g., knee angles (Nilsson, Thorstensson, & Halbertsma, 1985; Novacheck, 1998; Sasaki & Neptune, 2006) or muscle synergies (Cappellini et al., 2006; Santuz et al., 2020; Yokoyama et al., 2016), this effort does not necessarily cover all facets of the differences between the two patterns. So, when determining the maturity, it was clear that all aspects should be considered.

My hypothesis was that not one parameter was sufficient to determine the degree of maturity and thus, I utilized a shotgun approach where we used unsupervised learning to determine patterns in the data. The results of this work highlight that maturity of the gait pattern is influenced by many parameters and with high probability too subtle to discriminate with the naked eye. Since most strides were recorded on the treadmill, one may argue that treadmill locomotion influenced the results negatively. For instance, impacting the finding that a mature running pattern seems to precede a mature walking pattern in some children aged 40 to 106 months when locomoting on the treadmill as shown in **Chapter 2**. In new runners, i.e., children with between 6 and 32 months of walking experience in **Chapter 4**, there is a tendency to increased maturation with an increased walking age. Yet, when investigating on a stride-to-stride basis, the tendency is less clear arguably due to large variability within each session that is not dependent on whether locomotion is on treadmill or overground.

Treadmill locomotion is indeed a new experience for most children, especially those younger than nine years and of course treadmill locomotion may have an influence on the results. Adult treadmill and overground locomotion differ in some kinematic measures but with such small magnitudes that it cannot be considered relevant (Van Hooren et al., 2020). In a group of 24 children aged 6-18 years, joint kinematics were similar between overground and treadmill running whereas the joint moments were significantly different for knee, hip, and ankle. Some children may naturally alter their gait pattern(s) due to their unfamiliarity with the treadmill.

Regardless of whether treadmill running affected the results or not in **Chapters 2 and 4**, it is important to move away from a paradigm where only a few parameters are considered when wanting to understand healthy development and move towards more comprehensive and advanced statistical methods in very young as well as older children.

Q4. *What is the neuromuscular control of running in children?*

The expectation that children fine-tune their neuromuscular control linearly over time could not be confirmed in **Chapter 3**. In fact, what I observed was an inverted u-shape in terms of the number of synergies they employ. I will interpret this finding in the context of the degrees-of-freedom "problem" first introduced by Bernstein (1967).

It is commonly believed that there is a certain number of degrees-of-freedom available to control movements as the central nervous system cannot control all possible combinations of movements without computational overload. When children learn to run, they not only have to comply with the biomechanical constraints available to them but also the neuromuscular constraints. Thus, it is straightforward to hypothesize that the relatively small number of muscle synergies in the youngest children (2-3.5 years) is due to an attempt to limit the number of degrees of freedom available to them. Perhaps, they are constraining the neuromuscular space to better control and explore the biomechanical space, whereas when children get older, they have finetuned their biomechanical constraints and are now exploring in the neuromuscular space to find the most optimal control strategy. It is not clear in that case how the control strategy is determined. In adulthood, the most optimal control strategies are found, and exploration is no longer needed to keep the system(s) optimized. Thus, an inverted u-shape of the number of synergies could support the hypothesis of a reduction of the degrees-of-freedom with both inexperience and with expertise.

A newer interpretation of the work of Bernstein is that there is not talk of redundant degrees-of-freedom, however it is a matter of a "principle of abundance" meaning that having some flexibility or variability in movement patterns make them more robust to perturbations and secondary tasks (Latash, 2012). Additionally, it has been argued that the elimination of redundant degrees-of-freedom is a primitive and inconvenient method only used at the beginning of mastering a motor skill (Loeb, 2021; Whiting, 1983). When applying this way of thinking about motor control to the findings in **Chapter 3** one could argue that there is indeed some elimination of the redundant degrees of freedom in the beginning of mastering a skill in the young children which can be evidenced in the reduced number of synergies. However, this thinking does not explain why there is an equally low number of synergies in the adults with an increased number of synergies in the older children. The increased number of synergies in the older children could perhaps instead be explained by flexibility to withstand the perturbations of the unfamiliar movements on (or of) the treadmill.

Whether the inverted u-shape of the number of synergies can be explained by exploration, a larger number of muscle synergies was found in novice runners that decreased with increased running experience (Cheung et al., 2020) or in gymnasts walking a narrow beam (Sawers, Allen, & Ting, 2015). However, in rowing and cycling the number of muscle synergies did not

change with skill level (Park & Caldwell, 2022; Turpin, Guevel, Durand, & Hug, 2011; Zych, Rankin, Holland, & Severini, 2019). These differing findings indicate that the number of synergies may not be the sole indicator for learning.

Q5. *How can ground-reaction forces be estimated from shank accelerometer data?*

By combining a recurrent neural network and shank accelerometer data it is possible to accurately predict the shape of vertical ground reaction forces. From these, the gait events can be determined in a data set combining walking and running data.

Almost all running data recorded in children are recorded in a lab and often on a treadmill. Most labs do not stimulate natural movement in children, thus, there is a great need to move research out of the lab into a more naturalistic environment. Machine learning combined with accelerometers seems to be a great first step to achieve that goal. Accelerometers are cheap and easy to mount. This means that investigating running in children could be done, e.g., in a playground or on a football pitch.

Future research

To further elucidate which parameters are responsible for the maturity of the gait pattern in very young children, new methods could be used to extract the exact parameters underlying the clustering. Either by statistical analyses such as bootstrapping or by utilizing new methods where other advanced statistical methods are being used. What the research in this thesis highlights, is that many parameters as well as advanced statistical methods are necessary to further push the field forwards.

To improve our understanding of development of gait in children, the amount of available data should be clearly increased. We cannot rely on only one piece of the puzzle to explain development of motor control in children and thus by combining already collected data and the knowledge developed, our understanding will improve. With new methods being developed to record outside the lab we need to record children in more realistic environments such as playgrounds etc. By capturing natural(istic) movements, the understanding of the development will improve.

There are no good solutions at this stage on how to define running in (very) young children since the presence of a flight phase does not seem ideal. One could use the prescribed type of locomotion to separate walking from running which is not a very reliable measure and is not a generalizable entity. My suggestion would be to use the dimensionless speed instead, i.e., the Walking Froude value to separate walking from running. In adults, the transition from walking to running takes place at around 0.5 Froude on earth (Alexander, 1989; Gatesy & Biewener, 2009; Hreljac, 1995; Kram et al., 1997). In children over 10 years of age, the

transition speed is similar, between 0.43 and 0.47 (Kung, Fink, Legg, Ali, & Shultz, 2019), and does not seem to be dependent on being as energetically efficient as possible (Tseh, Bennett, Caputo, & Morgan, 2002). The transition speed is to my knowledge not investigated in younger children. The underlying mechanisms for the transition from walking to running is minimizing the metabolic cost of locomotion by improving mechanical efficiency and the muscle activity levels (Kung, Fink, Legg, Ali, & Shultz, 2018). An alternative to the Froude value could be the cadence with which the walk-run transition occurs. This cadence might be informative about classification of gait in children and adolescents (Ducharme et al., 2021). Whether the Froude number or the cadence are sensitive enough to be able to discriminate walking from running in very young children warrants further investigations.

The findings in this thesis are a snapshot of typical running development in healthy and typically developing (very) young children. When a good definition for running has been established, the next steps would be to investigate whether running in children with developmental diseases are also affected in their running patterns. Here, I am thinking of children such as children with developmental coordination disorder (DCD), cerebral paresis (CP), and Duchenne muscular dystrophy. In fact, gait asymmetries that are not present during walking may be present during running in children with CP (Bohm & Doderlein, 2012) while for some children with cerebral paresis, some gait parameters improve when running compared to walking (Kratschmer et al., 2019). In children with DCD, running kinematics do not change between overground and treadmill running (Chia, Licari, Guelfi, & Reid, 2014), and their kinematics do not differ significantly from typically developing children (Chia, Licari, Guelfi, & Reid, 2013). However, children with DCD are generally slower and perform worse in timed running tests compared to typically developing children (Smith, Ward, Williams, & Banwell, 2021). This indicates that running could be interesting to further investigate in a group of neurologically deficient children.

Likewise informative could be to investigate children with obesity or overweight. Overweight/obese children have altered running patterns such as increased ground reaction forces combined with unscaled joint moments and they spend longer time in the stance phase (Bowser & Roles, 2021). Children who are obese/overweight are slower than normal weight children and the distance they can cover in nine minutes is even a predictor for overweight (Silva et al., 2020). The slower paces and longer stance phases may indicate a more immature pattern. In that case, finding the causality between the overweight and the delayed maturity of the running patterns might give insights into the risk factors of overweight in children.

Closing remarks

Circling back to the overarching question of this thesis: The work in this thesis supports the notion that development of running in children is not a linear process. Generally, I believe

that children at a very young age constrain the degrees of freedom available to them which results in a reduced space for movement, both in terms of biomechanics and neuromuscular control. The older a child becomes, the more it makes use of exploration. Here, I mean that the child has homed in on the most basic patterns but are now exploring new patterns to find the most optimal locomotory pattern. What this optimization depends on, e.g., whether it is the cost of transport, the computational cost or something else, is not possible to discern from the work in this thesis.

Based on my findings I must conclude that it is not possible to distinguish biomechanical constraints from neuromuscular constraints. They work in interplay and are equally important to elucidate the motor control of running in children. Development of motor control is subtle and – as such – it cannot be determined with just a few parameters.

To get a grip on abnormal development, we must understand normal development. The work in this thesis highlights that normal development is not only highly variable between children but is also not linear within one child when starting to run. Running is a very important daily task for most children and mastering running is important for participation in daily life. Children with disabilities might not be able to participate in these tasks but by understanding what normal development is, we can faster identify the children who do not develop normally and facilitate their next steps.

Traditional measures for defining running do not discriminate running in children.

To conclude on the title of this thesis. There is indeed more to the story than flight phase, which may indeed be the end point, but is not the starting point.

BIBLIOGRAPHY

Abaid, N., Cappa, P., Palermo, E., Petrarca, M., & Porfiri, M. (2013). Gait detection in children with and without hemiplegia using single-axis wearable gyroscopes. *PLoS One, 8*(9), e73152. doi:10.1371/journal.pone.0073152

Alcantara, R. S., Edwards, W. B., Millet, G. Y., & Grabowski, A. M. (2022). Predicting continuous ground reaction forces from accelerometers during uphill and downhill running: a recurrent neural network solution. *PeerJ, 10*, e12752. doi:10.7717/peerj.12752

Alexander, R. (1976). Mechanics of bipedal locomotion. *Perspectives in experimental biology, 1*, 493-504.

Alexander, R. M. (1989). Optimization and gaits in the locomotion of vertebrates. *Physiol Rev, 69*(4), 1199-1227. doi:10.1152/physrev.1989.69.4.1199

Alexander, R. M., & Jayes, A. S. (1983). A Dynamic Similarity Hypothesis for the Gaits of Quadrupedal Mammals. *Journal of Zoology, 201*(Sep), 135-152. Retrieved from <Go to ISI>://WOS:A1983RH79100010

Alton, F., Baldey, L., Caplan, S., & Morrissey, M. C. (1998). A kinematic comparison of overground and treadmill walking. *Clin Biomech (Bristol, Avon), 13*(6), 434-440. doi:10.1016/s0268-0033(98)00012-6

Ancillao, A., Tedesco, S., Barton, J., & O'Flynn, B. (2018). Indirect Measurement of Ground Reaction Forces and Moments by Means of Wearable Inertial Sensors: A Systematic Review. *Sensors (Basel), 18*(8). doi:10.3390/s18082564

Aung, M. S., Thies, S. B., Kenney, L. P., Howard, D., Selles, R. W., Findlow, A. H., & Goulermas, J. Y. (2013). Automated detection of instantaneous gait events using time frequency analysis and manifold embedding. *IEEE Trans Neural Syst Rehabil Eng, 21*(6), 908-916. doi:10.1109/TNSRE.2013.2239313

Bach, M. M., Daffertshofer, A., & Dominici, N. (2021a). The development of mature gait patterns in children during walking and running. *Eur J Appl Physiol, 121*(4), 1073-1085. doi:10.1007/s00421-020-04592-2

Bach, M. M., Daffertshofer, A., & Dominici, N. (2021b). Muscle Synergies in Children Walking and Running on a Treadmill. *Front Hum Neurosci, 15*, 637157. doi:10.3389/fnhum.2021.637157

Baggen, R. J., van Dieën, J. H., Van Roie, E., Verschueren, S. M., Giarmatzis, G., Delecluse, C., & Dominici, N. (2020). Age-Related Differences in Muscle Synergy Organization during Step Ascent at Different Heights and Directions. *Applied Sciences, 10*(6). doi:10.3390/app10061987

Ballarini, R., Ghislieri, M., Knaflitz, M., & Agostini, V. (2021). An Algorithm for Choosing the Optimal Number of Muscle Synergies during Walking. *Sensors (Basel), 21*(10). doi:10.3390/s21103311

Bastien, G. J., Gosseye, T. P., & Penta, M. (2019). A robust machine learning enabled decomposition of shear ground reaction forces during the double contact phase of walking. *Gait Posture, 73*, 221-227. doi:10.1016/j.gaitpost.2019.07.190

Bekius, A., Bach, M. M., van de Pol, L. A., Harlaar, J., Daffertshofer, A., Dominici, N., & Buizer, A. I. (2021). Early Development of Locomotor Patterns and Motor Control in Very Young Children at High Risk of Cerebral Palsy, a Longitudinal Case Series. *Front Hum Neurosci, 15*, 659415. doi:10.3389/fnhum.2021.659415

Ben Mansour, K., Rezzoug, N., & Gorce, P. (2015). Analysis of several methods and inertial sensors locations to assess gait parameters in able-bodied subjects. *Gait Posture, 42*(4), 409-414. doi:10.1016/j.gaitpost.2015.05.020

Bergamini, E., Picerno, P., Pillet, H., Natta, F., Thoreux, P., & Camomilla, V. (2012). Estimation of temporal parameters during sprint running using a trunk-mounted inertial measurement unit. *J Biomech, 45*(6), 1123-1126. doi:10.1016/j.jbiomech.2011.12.020

Bernstein, N. (1967). *The co-ordination and regulation of movements*. Oxford (osv.): Pergamon.

Berry, M. W., Browne, M., Langville, A. N., Pauca, V. P., & Plemmons, R. J. (2007). Algorithms and applications for approximate nonnegative matrix factorization. *Computational Statistics & Data Analysis, 52*(1), 155-173. doi:10.1016/j.csda.2006.11.006

Besomi, M., Hodges, P. W., Clancy, E. A., Van Dieen, J., Hug, F., Lowery, M., Merletti, R., Sogaard, K., Wrigley, T., Besier, T., Carson, R. G., Disselhorst-Klug, C., Enoka, R. M., Falla, D., Farina, D., Gandevia, S., Holobar, A., Kiernan, M. C., McGill, K., Perreault, E., Rothwell, J. C., & Tucker, K. (2020). Consensus for experimental design in electromyography (CEDE) project: Amplitude normalization matrix. *J Electromyogr Kinesiol, 53*, 102438. doi:10.1016/j.jelekin.2020.102438

Bianchi, L., Angelini, D., & Lacquaniti, F. (1998). Individual characteristics of human walking mechanics. *European Journal of Physiology, 436*(3), 343-356. doi:10.1007/s004240050642

Bizzi, E., & Cheung, V. C. (2013). The neural origin of muscle synergies. *Front Comput Neurosci, 7*, 51. doi:10.3389/fncom.2013.00051

Blickhan, R. (1989). The spring-mass model for running and hopping. *J Biomech, 22*(11-12), 1217-1227. doi:10.1016/0021-9290(89)90224-8

Bohm, H., & Doderlein, L. (2012). Gait asymmetries in children with cerebral palsy: do they deteriorate with running? *Gait Posture, 35*(2), 322-327. doi:10.1016/j.gaitpost.2011.10.003

Bonnaerens, S., Fiers, P., Galle, S., Aerts, P., Frederick, E. C., Kaneko, Y., Derave, W., & D, D. E. C. (2019). Grounded Running Reduces Musculoskeletal Loading. *Med Sci Sports Exerc, 51*(4), 708-715. doi:10.1249/MSS.0000000000001846

Bonnaerens, S., Fiers, P., Galle, S., Derie, R., Aerts, P., Frederick, E., Kaneko, Y., Derave, W., De Clercq, D., & Segers, V. (2021). Relationship between duty factor and external forces in slow recreational runners. *BMJ Open Sport Exerc Med, 7*(1), e000996. doi:10.1136/bmjsem-2020-000996

Boonstra, T. W., Danna-Dos-Santos, A., Xie, H. B., Roerdink, M., Stins, J. F., & Breakspear, M. (2015). Muscle networks: Connectivity analysis of EMG activity during postural control. *Sci Rep, 5*, 17830. doi:10.1038/srep17830

Booth, A. T. C., van der Krogt, M. M., Harlaar, J., Dominici, N., & Buizer, A. I. (2019). Muscle Synergies in Response to Biofeedback-Driven Gait Adaptations in Children With Cerebral Palsy. *Front Physiol, 10*, 1208. doi:10.3389/fphys.2019.01208

Borghese, N. A., Bianchi, L., & Lacquaniti, F. (1996). Kinematic determinants of human locomotion. *J Physiol, 494 (Pt 3)*, 863-879. doi:10.1113/jphysiol.1996.sp021539

Bowser, B. J., & Roles, K. (2021). Effects of Overweight and Obesity on Running Mechanics in Children. *Med Sci Sports Exerc, 53*(10), 2101-2110. doi:10.1249/MSS.0000000000002686

Buurke, T. J., Lamoth, C. J., van der Woude, L. H., & den Otter, A. R. (2016). Synergistic Structure in the Speed Dependent Modulation of Muscle Activity in Human Walking. *PLoS One, 11*(4), e0152784. doi:10.1371/journal.pone.0152784

Cappellini, G., Ivanenko, Y. P., Martino, G., MacLellan, M. J., Sacco, A., Morelli, D., & Lacquaniti, F. (2016). Immature Spinal Locomotor Output in Children with Cerebral Palsy. *Front Physiol, 7*, 478. doi:10.3389/fphys.2016.00478

Cappellini, G., Ivanenko, Y. P., Poppele, R. E., & Lacquaniti, F. (2006). Motor patterns in human walking and running. *J Neurophysiol, 95*(6), 3426-3437. doi:10.1152/jn.00081.2006

Cappellini, G., Sylos-Labini, F., MacLellan, M. J., Sacco, A., Morelli, D., Lacquaniti, F., & Ivanenko, Y. (2018). Backward walking highlights gait asymmetries in children with cerebral palsy. *J Neurophysiol, 119*(3), 1153-1165. doi:10.1152/jn.00679.2017

Carriero, A., Zavatsky, A., Stebbins, J., Theologis, T., & Shefelbine, S. J. (2009). Determination of gait patterns in children with spastic diplegic cerebral palsy using principal components. *Gait Posture, 29*(1), 71-75. doi:10.1016/j.gaitpost.2008.06.011

Cavagna, G. A. (1975). Force platforms as ergometers. *J Appl Physiol, 39*(1), 174-179. doi:10.1152/jappl.1975.39.1.174

Cavagna, G. A., Heglund, N. C., & Taylor, C. R. (1977). Mechanical work in terrestrial locomotion: two basic mechanisms for minimizing energy expenditure. *Am J Physiol, 233*(5), R243-261. doi:10.1152/ajpregu.1977.233.5.R243

Cavagna, G. A., Saibene, F. P., & Margaria, R. (1964). Mechanical Work in Running. *J Appl Physiol, 19*(2), 249-256. doi:10.1152/jappl.1964.19.2.249

Cavagna, G. A., Thys, H., & Zamboni, A. (1976). The sources of external work in level walking and running. *J Physiol, 262*(3), 639-657. doi:10.1113/jphysiol.1976.sp011613

Chen, G., Qi, P., Guo, Z., & Yu, H. (2017). Gait-Event-Based Synchronization Method for Gait Rehabilitation Robots via a Bioinspired Adaptive Oscillator. *IEEE Trans Biomed Eng, 64*(6), 1345-1356. doi:10.1109/TBME.2016.2604340

Chen, G., Salim, V., & Yu, H. (2015). *A novel gait phase-based control strategy for a portable knee-ankle-foot robot.* Paper presented at the 2015 IEEE International Conference on Rehabilitation Robotics (ICORR).

Cheron, G., Bengoetxea, A., Bouillot, E., Lacquaniti, F., & Dan, B. (2001). Early emergence of temporal co-ordination of lower limb segments elevation angles in human locomotion. *Neurosci Lett, 308*(2), 123-127. doi:10.1016/s0304-3940(01)01925-5

Cheron, G., Bouillot, E., Dan, B., Bengoetxea, A., Draye, J. P., & Lacquaniti, F. (2001). Development of a kinematic coordination pattern in toddler locomotion: planar covariation. *Exp Brain Res, 137*(3-4), 455-466. doi:10.1007/s002210000663

Cheung, V. C., d'Avella, A., Tresch, M. C., & Bizzi, E. (2005). Central and sensory contributions to the activation and organization of muscle synergies during natural motor behaviors. *J Neurosci, 25*(27), 6419-6434. doi:10.1523/JNEUROSCI.4904-04.2005

Cheung, V. C. K., Cheung, B. M. F., Zhang, J. H., Chan, Z. Y. S., Ha, S. C. W., Chen, C. Y., & Cheung, R. T. H. (2020). Plasticity of muscle synergies through fractionation and merging during development and training of human runners. *Nat Commun, 11*(1), 4356. doi:10.1038/s41467-020-18210-4

Chia Bejarano, N., Pedrocchi, A., Nardone, A., Schieppati, M., Baccinelli, W., Monticone, M., Ferrigno, G., & Ferrante, S. (2017). Tuning of Muscle Synergies During Walking Along Rectilinear and Curvilinear Trajectories in Humans. *Ann Biomed Eng, 45*(5), 1204-1218. doi:10.1007/s10439-017-1802-z

Chia, L. C., Licari, M. K., Guelfi, K. J., & Reid, S. L. (2013). A comparison of running kinematics and kinetics in children with and without developmental coordination disorder. *Gait Posture, 38*(2), 264-269. doi:10.1016/j.gaitpost.2012.11.028

Chia, L. C., Licari, M. K., Guelfi, K. J., & Reid, S. L. (2014). Investigation of treadmill and overground running: implications for the measurement of oxygen cost in children with developmental coordination disorder. *Gait Posture, 40*(3), 464-470. doi:10.1016/j.gaitpost.2014.05.054

Choi, A., Jung, H., Lee, K. Y., Lee, S., & Mun, J. H. (2019). Machine learning approach to predict center of pressure trajectories in a complete gait cycle: a feedforward neural network vs. LSTM network. *Med Biol Eng Comput, 57*(12), 2693-2703. doi:10.1007/s11517-019-02056-0

Choi, A., Jung, H., & Mun, J. H. (2019). Single Inertial Sensor-Based Neural Networks to Estimate COM-COP Inclination Angle During Walking. *Sensors (Basel), 19*(13). doi:10.3390/s19132974

Choi, A., Lee, J.-M., & Mun, J. H. (2013). Ground reaction forces predicted by using artificial neural network during asymmetric movements. *International Journal of Precision Engineering and Manufacturing, 14*(3), 475-483. doi:10.1007/s12541-013-0064-4

Chu, K. H., Jiang, X., & Menon, C. (2017). Wearable step counting using a force myography-based ankle strap. *J Rehabil Assist Technol Eng, 4*, 2055668317746307. doi:10.1177/2055668317746307

Chvatal, S. A., & Ting, L. H. (2012). Voluntary and reactive recruitment of locomotor muscle synergies during perturbed walking. *J Neurosci, 32*(35), 12237-12250. doi:10.1523/JNEUROSCI.6344-11.2012

Clark, D. J., Ting, L. H., Zajac, F. E., Neptune, R. R., & Kautz, S. A. (2010). Merging of healthy motor modules predicts reduced locomotor performance and muscle coordination complexity post-stroke. *J Neurophysiol, 103*(2), 844-857. doi:10.1152/jn.00825.2009

Courtine, G., Gerasimenko, Y., van den Brand, R., Yew, A., Musienko, P., Zhong, H., Song, B., Ao, Y., Ichiyama, R. M., Lavrov, I., Roy, R. R., Sofroniew, M. V., & Edgerton, V. R. (2009). Transformation of nonfunctional spinal circuits into functional states after the loss of brain input. *Nat Neurosci, 12*(10), 1333-1342. doi:10.1038/nn.2401

Crea, S., De Rossi, S. M., Donati, M., Rebersek, P., Novak, D., Vitiello, N., Lenzi, T., Podobnik, J., Munih, M., & Carrozza, M. C. (2012). Development of gait segmentation methods for wearable foot pressure sensors. *Annu Int Conf IEEE Eng Med Biol Soc, 2012*, 5018-5021. doi:10.1109/EMBC.2012.6347120

d'Avella, A., Portone, A., Fernandez, L., & Lacquaniti, F. (2006). Control of fast-reaching movements by muscle synergy combinations. *J Neurosci, 26*(30), 7791-7810. doi:10.1523/JNEUROSCI.0830-06.2006

d'Avella, A., Saltiel, P., & Bizzi, E. (2003). Combinations of muscle synergies in the construction of a natural motor behavior. *Nat Neurosci, 6*(3), 300-308. doi:10.1038/nn1010

Davidson, P., Virekunnas, H., Sharma, D., Piche, R., & Cronin, N. (2019). Continuous Analysis of Running Mechanics by Means of an Integrated INS/GPS Device. *Sensors (Basel), 19*(6). doi:10.3390/s19061480

Dayanidhi, S., Kutch, J. J., & Valero-Cuevas, F. J. (2013). Decrease in muscle contraction time complements neural maturation in the development of dynamic manipulation. *J Neurosci, 33*(38), 15050-15055. doi:10.1523/JNEUROSCI.1968-13.2013

de Graaf, M. L., Mochizuki, L., Thies, F., Wagner, H., & Le Mouel, C. (2022). Motor pattern generation is robust to neural network anatomical imbalance favoring inhibition but not excitation. *BioRxiv*, 2022.2004.2021.489087. doi:10.1101/2022.04.21.489087

De Luca, C. J., Gilmore, L. D., Kuznetsov, M., & Roy, S. H. (2010). Filtering the surface EMG signal: Movement artifact and baseline noise contamination. *J Biomech, 43*(8), 1573-1579. doi:10.1016/j.jbiomech.2010.01.027

de Ruiter, C. J., van Oeveren, B., Francke, A., Zijlstra, P., & van Dieen, J. H. (2016). Running Speed Can Be Predicted from Foot Contact Time during Outdoor over Ground Running. *PLoS One, 11*(9), e0163023. doi:10.1371/journal.pone.0163023

DeCann, B., Ross, A., & Culp, M. (2014). *On Clustering Human Gait Patterns.* Paper presented at the 2014 22nd International Conference on Pattern Recognition.

Delis, I., Panzeri, S., Pozzo, T., & Berret, B. (2014). A unifying model of concurrent spatial and temporal modularity in muscle activity. *J Neurophysiol, 111*(3), 675-693. doi:10.1152/jn.00245.2013

Dewolf, A. H., Mesquita, R. M., & Willems, P. A. (2020). Intra-limb and muscular coordination during walking on slopes. *Eur J Appl Physiol, 120*(8), 1841-1854. doi:10.1007/s00421-020-04415-4

Dewolf, A. H., Sylos-Labini, F., Cappellini, G., Lacquaniti, F., & Ivanenko, Y. (2020). Emergence of Different Gaits in Infancy: Relationship Between Developing Neural Circuitries and Changing Biomechanics. *Front Bioeng Biotechnol, 8*, 473. doi:10.3389/fbioe.2020.00473

Dingwell, J. B., Cusumano, J. P., Cavanagh, P. R., & Sternad, D. (2001). Local dynamic stability versus kinematic variability of continuous overground and treadmill walking. *J Biomech Eng, 123*(1), 27-32. doi:10.1115/1.1336798

Dominici, N., Ivanenko, Y. P., Cappellini, G., d'Avella, A., Mondi, V., Cicchese, M., Fabiano, A., Silei, T., Di Paolo, A., Giannini, C., Poppele, R. E., & Lacquaniti, F. (2011). Locomotor primitives in newborn babies and their development. *Science, 334*(6058), 997-999. doi:10.1126/science.1210617

Dominici, N., Ivanenko, Y. P., Cappellini, G., Zampagni, M. L., & Lacquaniti, F. (2010). Kinematic strategies in newly walking toddlers stepping over different support surfaces. *J Neurophysiol, 103*(3), 1673-1684. doi:10.1152/jn.00945.2009

Dominici, N., Ivanenko, Y. P., & Lacquaniti, F. (2007). Control of foot trajectory in walking toddlers: adaptation to load changes. *J Neurophysiol, 97*(4), 2790-2801. doi:10.1152/jn.00262.2006

Dominici, N., Keller, U., Vallery, H., Friedli, L., van den Brand, R., Starkey, M. L., Musienko, P., Riener, R., & Courtine, G. (2012). Versatile robotic interface to evaluate, enable and train locomotion and balance after neuromotor disorders. *Nat Med, 18*(7), 1142-1147. doi:10.1038/nm.2845

Ducharme, S. W., Turner, D. S., Pleuss, J. D., Moore, C. C., Schuna, J. M., Tudor-Locke, C., & Aguiar, E. J. (2021). Using Cadence to Predict the Walk-to-Run Transition in Children and Adolescents: A Logistic Regression Approach. *J Sports Sci, 39*(9), 1039-1045. doi:10.1080/02640414.2020.1855869

Farley, C. T., & Ferris, D. P. (1998). 10 Biomechanics of Walking and Running: Center of Mass Movements to Muscle Action. *Exercise and sport sciences reviews, 26*(1), 253-286.

Farrahi, V., Niemela, M., Kangas, M., Korpelainen, R., & Jamsa, T. (2019). Calibration and validation of accelerometer-based activity monitors: A systematic review of machine-learning approaches. *Gait Posture, 68*, 285-299. doi:10.1016/j.gaitpost.2018.12.003

Fellin, R. E., Rose, W. C., Royer, T. D., & Davis, I. S. (2010). Comparison of methods for kinematic identification of footstrike and toe-off during overground and treadmill running. *J Sci Med Sport, 13*(6), 646-650. doi:10.1016/j.jsams.2010.03.006

Figueiredo, J., Santos, C. P., & Moreno, J. C. (2018). Automatic recognition of gait patterns in human motor disorders using machine learning: A review. *Med Eng Phys, 53*, 1-12. doi:10.1016/j.medengphy.2017.12.006

Forssberg, H. (1985). Ontogeny of human locomotor control. I. Infant stepping, supported locomotion and transition to independent locomotion. *Exp Brain Res, 57*(3), 480-493. doi:10.1007/BF00237835

Fortney, V. L. (1983). The Kinematics and Kinetics of the Running Pattern of Two-, Four-, and Six-Year-Old Children. *Research Quarterly for Exercise and Sport, 54*(2), 126-135. doi:10.1080/02701367.1983.10605284

Friedli, L., Rosenzweig, E. S., Barraud, Q., Schubert, M., Dominici, N., Awai, L., Nielson, J. L., Musienko, P., Nout-Lomas, Y., Zhong, H., Zdunowski, S., Roy, R. R., Strand, S. C., van den Brand, R., Havton, L. A., Beattie, M. S., Bresnahan, J. C., Bezard, E., Bloch, J., Edgerton, V. R., Ferguson, A. R., Curt, A., Tuszynski, M. H., & Courtine, G. (2015). Pronounced species divergence in corticospinal tract reorganization and functional recovery after lateralized spinal cord injury favors primates. *Sci Transl Med, 7*(302), 302ra134. doi:10.1126/scitranslmed.aac5811

Gatesy, S. M., & Biewener, A. A. (2009). Bipedal locomotion: effects of speed, size and limb posture in birds and humans. *Journal of Zoology, 224*(1), 127-147. doi:10.1111/j.1469-7998.1991.tb04794.x

Ghoussayni, S., Stevens, C., Durham, S., & Ewins, D. (2004). Assessment and validation of a simple automated method for the detection of gait events and intervals. *Gait Posture, 20*(3), 266-272. doi:10.1016/j.gaitpost.2003.10.001

Goodfellow, I., Bengio, Y., & Courville, A. (2016). *Deep learning*: MIT press.

Goudriaan, M., Papageorgiou, E., Shuman, B. R., Steele, K. M., Dominici, N., Van Campenhout, A., Ortibus, E., Molenaers, G., & Desloovere, K. (2022). Muscle synergy structure and gait patterns in children with spastic cerebral palsy. *Dev Med Child Neurol, 64*(4), 462-468. doi:10.1111/dmcn.15068

Goudriaan, M., Shuman, B. R., Steele, K. M., Van den Hauwe, M., Goemans, N., Molenaers, G., & Desloovere, K. (2018). Non-neural Muscle Weakness Has Limited Influence on Complexity of Motor Control during Gait. *Front Hum Neurosci, 12*, 5. doi:10.3389/fnhum.2018.00005

Greene, B. R., McGrath, D., O'Neill, R., O'Donovan, K. J., Burns, A., & Caulfield, B. (2010). An adaptive gyroscope-based algorithm for temporal gait analysis. *Med Biol Eng Comput, 48*(12), 1251-1260. doi:10.1007/s11517-010-0692-0

Guenterberg, E., Yang, A. Y., Ghasemzadeh, H., Jafari, R., Bajcsy, R., & Sastry, S. S. (2009). A method for extracting temporal parameters based on hidden Markov models in body sensor networks with inertial sensors. *IEEE Trans Inf Technol Biomed, 13*(6), 1019-1030. doi:10.1109/TITB.2009.2028421

Guo, Y., Storm, F., Zhao, Y., Billings, S. A., Pavic, A., Mazza, C., & Guo, L. Z. (2017). A New Proxy Measurement Algorithm with Application to the Estimation of Vertical Ground Reaction Forces Using Wearable Sensors. *Sensors (Basel), 17*(10). doi:10.3390/s17102181

Gurchiek, R. D., Garabed, C. P., & McGinnis, R. S. (2020). Gait event detection using a thigh-worn accelerometer. *Gait Posture, 80*, 214-216. doi:10.1016/j.gaitpost.2020.06.004

Hagedoorn, L., Zadravec, M., Olenšek, A., van Asseldonk, E., & Matjačić, Z. (2022). The Existence of Shared Muscle Synergies Underlying Perturbed and Unperturbed Gait Depends on Walking Speed. *Applied Sciences, 12*(4). doi:10.3390/app12042135

Hagio, S., Fukuda, M., & Kouzaki, M. (2015). Identification of muscle synergies associated with gait transition in humans. *Front Hum Neurosci, 9*, 48. doi:10.3389/fnhum.2015.00048

Halaki, M., & Gi, K. (2012). Normalization of EMG Signals: To Normalize or Not to Normalize and What to Normalize to? In G. R. Naik (Ed.), *Computational Intelligence in Electromyography Analysis - A Perspective on Current Applications and Future Challenges* (pp. Ch. 07). Rijeka: InTech.

Halilaj, E., Rajagopal, A., Fiterau, M., Hicks, J. L., Hastie, T. J., & Delp, S. L. (2018). Machine learning in human movement biomechanics: Best practices, common pitfalls, and new opportunities. *J Biomech, 81*, 1-11. doi:10.1016/j.jbiomech.2018.09.009

Hallemans, A., Aerts, P., Otten, B., De Deyn, P. P., & De Clercq, D. (2004). Mechanical energy in toddler gait. A trade-off between economy and stability? *J Exp Biol, 207*(Pt 14), 2417-2431. doi:10.1242/jeb.01040

Hallemans, A., De Clercq, D., & Aerts, P. (2006). Changes in 3D joint dynamics during the first 5 months after the onset of independent walking: a longitudinal follow-up study. *Gait Posture, 24*(3), 270-279. doi:10.1016/j.gaitpost.2005.10.003

Haykin, S. (2014). *Adaptive Filter Theory: International Edition*: Pearson Education.

Hermens, H. J., Freriks, B., Merletti, R., Stegeman, D., Blok, J., Rau, G., Disselhorst-Klug, C., & Hägg, G. (1999). European recommendations for surface electromyography. *Roessingh Research and Development, 8*(2), 13-54.

Hinnekens, E., Berret, B., Do, M. C., & Teulier, C. (2020). Modularity underlying the performance of unusual locomotor tasks inspired by developmental milestones. *J Neurophysiol, 123*(2), 496-510. doi:10.1152/jn.00662.2019

Hof, A. L. (1996). Scaling gait data to body size. *Gait & Posture, 4*(3), 222-223. doi:10.1016/0966-6362(95)01057-2

Horsley, B. J., Tofari, P. J., Halson, S. L., Kemp, J. G., Dickson, J., Maniar, N., & Cormack, S. J. (2021). Does Site Matter? Impact of Inertial Measurement Unit Placement on the Validity and Reliability of Stride Variables During Running: A Systematic Review and Meta-analysis. *Sports Med, 51*(7), 1449-1489. doi:10.1007/s40279-021-01443-8

Hreljac, A. (1995). Effects of physical characteristics on the gait transition speed during human locomotion. *Human Movement Science, 14*(2), 205-216. doi:10.1016/0167-9457(95)00017-m

Hreljac, A., & Marshall, R. N. (2000). Algorithms to determine event timing during normal walking using kinematic data. *J Biomech, 33*(6), 783-786. doi:10.1016/s0021-9290(00)00014-2

Ivanenko, Y. P., Cappellini, G., Dominici, N., Poppele, R. E., & Lacquaniti, F. (2007). Modular control of limb movements during human locomotion. *J Neurosci, 27*(41), 11149-11161. doi:10.1523/JNEUROSCI.2644-07.2007

Ivanenko, Y. P., Cappellini, G., Poppele, R. E., & Lacquaniti, F. (2008). Spatiotemporal organization of alpha-motoneuron activity in the human spinal cord during different gaits and gait transitions. *Eur J Neurosci, 27*(12), 3351-3368. doi:10.1111/j.1460-9568.2008.06289.x

Ivanenko, Y. P., Dominici, N., Cappellini, G., Dan, B., Cheron, G., & Lacquaniti, F. (2004). Development of pendulum mechanism and kinematic coordination from the first unsupported steps in toddlers. *J Exp Biol, 207*(Pt 21), 3797-3810. doi:10.1242/jeb.01214

Ivanenko, Y. P., Dominici, N., Cappellini, G., & Lacquaniti, F. (2005). Kinematics in newly walking toddlers does not depend upon postural stability. *Journal of Neurophysiology, 94*(1), 754-763.

Ivanenko, Y. P., Dominici, N., & Lacquaniti, F. (2007). Development of independent walking in toddlers. *Exerc Sport Sci Rev, 35*(2), 67-73. doi:10.1249/JES.0b013e31803eafa8

Ivanenko, Y. P., Poppele, R. E., & Lacquaniti, F. (2004). Five basic muscle activation patterns account for muscle activity during human locomotion. *J Physiol, 556*(Pt 1), 267-282. doi:10.1113/jphysiol.2003.057174

Ivanenko, Y. P., Poppele, R. E., & Lacquaniti, F. (2006). Motor control programs and walking. *Neuroscientist, 12*(4), 339-348. doi:10.1177/1073858406287987

Jaeger, H. (2001). The “echo state” approach to analysing and training recurrent neural networks-with an erratum note. *Bonn, Germany: German National Research Center for Information Technology GMD Technical Report, 148*(34), 13.

Jaeger, H. (2002). *Tutorial on training recurrent neural networks, covering BPPT, RTRL, EKF and the" echo state network" approach* (Vol. 5): GMD-Forschungszentrum Informationstechnik Bonn.

Jaeger, H., & Haas, H. (2004). Harnessing nonlinearity: predicting chaotic systems and saving energy in wireless communication. *Science, 304*(5667), 78-80. doi:10.1126/science.1091277

Johnson, W. R., Mian, A., Robinson, M. A., Verheul, J., Lloyd, D. G., & Alderson, J. A. (2021). Multidimensional Ground Reaction Forces and Moments From Wearable Sensor Accelerations via Deep Learning. *IEEE Trans Biomed Eng, 68*(1), 289-297. doi:10.1109/TBME.2020.3006158

Jordan, K., Challis, J. H., & Newell, K. M. (2007). Walking speed influences on gait cycle variability. *Gait Posture, 26*(1), 128-134. doi:10.1016/j.gaitpost.2006.08.010

Kaptein, R. G., Wezenberg, D., T, I. J., Houdijk, H., Beek, P. J., Lamoth, C. J., & Daffertshofer, A. (2014). Shotgun approaches to gait analysis: insights & limitations. *J Neuroeng Rehabil, 11*, 120. doi:10.1186/1743-0003-11-120

Kerkman, J. N., Bekius, A., Boonstra, T. W., Daffertshofer, A., & Dominici, N. (2020). Muscle Synergies and Coherence Networks Reflect Different Modes of Coordination During Walking. *Front Physiol, 11*, 751. doi:10.3389/fphys.2020.00751

Kerkman, J. N., Zandvoort, C. S., Daffertshofer, A., & Dominici, N. (2022). Body Weight Control Is a Key Element of Motor Control for Toddlers’ Walking. *Frontiers in Network Physiology, 2*. doi:10.3389/fnetp.2022.844607

Khandelwal, S., & Wickstrom, N. (2017). Evaluation of the performance of accelerometer-based gait event detection algorithms in different real-world scenarios using the MAREA gait database. *Gait Posture, 51*, 84-90. doi:10.1016/j.gaitpost.2016.09.023

Kibushi, B., Hagio, S., Moritani, T., & Kouzaki, M. (2018). Speed-Dependent Modulation of Muscle Activity Based on Muscle Synergies during Treadmill Walking. *Front Hum Neurosci, 12*, 4. doi:10.3389/fnhum.2018.00004

Kibushi, B., Moritani, T., & Kouzaki, M. (2022). Modular control of muscle coordination patterns during various stride time and stride length combinations. *Gait Posture, 94*, 230-235. doi:10.1016/j.gaitpost.2021.04.006

Kidzinski, L., Delp, S., & Schwartz, M. (2019). Automatic real-time gait event detection in children using deep neural networks. *PLoS One, 14*(1), e0211466. doi:10.1371/journal.pone.0211466

Kim, Y., Bulea, T. C., & Damiano, D. L. (2018). Children With Cerebral Palsy Have Greater Stride-to-Stride Variability of Muscle Synergies During Gait Than Typically Developing Children: Implications for Motor Control Complexity. *Neurorehabil Neural Repair, 32*(9), 834-844. doi:10.1177/1545968318796333

Komaris, D.-S., Perez-Valero, E., Jordan, L., Barton, J., Hennessy, L., O'Flynn, B., & Tedesco, S. (2019). Predicting Three-Dimensional Ground Reaction Forces in Running by Using Artificial Neural Networks and Lower Body Kinematics. *IEEE Access, 7*, 156779-156786. doi:10.1109/access.2019.2949699

Kram, R., Domingo, A., & Ferris, D. P. (1997). Effect of reduced gravity on the preferred walk-run transition speed. *J Exp Biol, 200*(Pt 4), 821-826. doi:10.1242/jeb.200.4.821

Kratschmer, R., Bohm, H., & Doderlein, L. (2019). Kinematic adaptation and changes in gait classification in running compared to walking in children with unilateral spastic cerebral palsy. *Gait Posture, 67*, 104-111. doi:10.1016/j.gaitpost.2018.09.031

Kung, S. M., Fink, P. W., Legg, S. J., Ali, A., & Shultz, S. P. (2018). What factors determine the preferred gait transition speed in humans? A review of the triggering mechanisms. *Hum Mov Sci, 57*, 1-12. doi:10.1016/j.humov.2017.10.023

Kung, S. M., Fink, P. W., Legg, S. J., Ali, A., & Shultz, S. P. (2019). Age-dependent variability in spatiotemporal gait parameters and the walk-to-run transition. *Hum Mov Sci, 66*, 600-606. doi:10.1016/j.humov.2019.06.012

Labarrière, F., Thomas, E., Calistri, L., Optasanu, V., Gueugnon, M., Ornetti, P., & Laroche, D. (2020). Machine learning approaches for activity recognition and/or activity prediction in locomotion assistive devices—A systematic review. *Sensors, 20*(21), 6345.

Labini, F. S., Ivanenko, Y. P., Cappellini, G., Gravano, S., & Lacquaniti, F. (2011). Smooth changes in the EMG patterns during gait transitions under body weight unloading. *J Neurophysiol, 106*(3), 1525-1536. doi:10.1152/jn.00160.2011

Latash, M. L. (2012). The bliss (not the problem) of motor abundance (not redundancy). *Exp Brain Res, 217*(1), 1-5. doi:10.1007/s00221-012-3000-4

Lee, D. D., & Seung, H. S. (1999). Learning the parts of objects by non-negative matrix factorization. *Nature, 401*(6755), 788-791. doi:10.1038/44565

Lee, D. D., & Seung, H. S. (2001). *Algorithms for non-negative matrix factorization.* Paper presented at the Advances in neural information processing systems.

Lee, J. B., Mellifont, R. B., & Burkett, B. J. (2010). The use of a single inertial sensor to identify stride, step, and stance durations of running gait. *J Sci Med Sport, 13*(2), 270-273. doi:10.1016/j.jsams.2009.01.005

Lee, M., & Park, S. (2020). Estimation of Three-Dimensional Lower Limb Kinetics Data during Walking Using Machine Learning from a Single IMU Attached to the Sacrum. *Sensors (Basel), 20*(21). doi:10.3390/s20216277

Legramandi, M. A., Schepens, B., & Cavagna, G. A. (2013). Running humans attain optimal elastic bounce in their teens. *Sci Rep, 3*, 1310. doi:10.1038/srep01310

Leporace, G., Batista, L. A., & Nadal, J. (2018). Prediction of 3D ground reaction forces during gait based on accelerometer data. *Research on Biomedical Engineering, 34*(3), 211-216. doi:10.1590/2446-4740.06817

Li, Y., & Ngom, A. (2013). The non-negative matrix factorization toolbox for biological data mining. *Source Code Biol Med, 8*(1), 10. doi:10.1186/1751-0473-8-10

Lim, H., Kim, B., & Park, S. (2019). Prediction of Lower Limb Kinetics and Kinematics during Walking by a Single IMU on the Lower Back Using Machine Learning. *Sensors (Basel), 20*(1). doi:10.3390/s20010130

Liu, W., Mei, Q., Yu, P., Gao, Z., Hu, Q., Fekete, G., Istvan, B., & Gu, Y. (2022). Biomechanical Characteristics of the Typically Developing Toddler Gait: A Narrative Review. *Children (Basel), 9*(3). doi:10.3390/children9030406

Loeb, G. E. (2021). Learning to use Muscles. *J Hum Kinet, 76*, 9-33. doi:10.2478/hukin-2020-0084

Lukoševičius, M. (2012). A Practical Guide to Applying Echo State Networks. In G. Montavon, G. B. Orr, & K.-R. Müller (Eds.), *Neural networks: Tricks of the trade* (pp. 659-686). Berlin, Heidelberg: Springer Berlin Heidelberg.

Lukoševičius, M., & Jaeger, H. (2009). Reservoir computing approaches to recurrent neural network training. *Computer Science Review, 3*(3), 127-149. doi:10.1016/j.cosrev.2009.03.005

Maass, W., Natschlager, T., & Markram, H. (2002). Real-time computing without stable states: a new framework for neural computation based on perturbations. *Neural Comput, 14*(11), 2531-2560. doi:10.1162/089976602760407955

Maclellan, M. J., Ivanenko, Y. P., Massaad, F., Bruijn, S. M., Duysens, J., & Lacquaniti, F. (2014). Muscle activation patterns are bilaterally linked during split-belt treadmill walking in humans. *J Neurophysiol, 111*(8), 1541-1552. doi:10.1152/jn.00437.2013

Mannini, A., Genovese, V., & Maria Sabatini, A. (2014). Online decoding of hidden Markov models for gait event detection using foot-mounted gyroscopes. *IEEE J Biomed Health Inform, 18*(4), 1122-1130. doi:10.1109/JBHI.2013.2293887

Mannini, A., & Sabatini, A. M. (2011). *A hidden Markov model-based technique for gait segmentation using a foot-mounted gyroscope.* Paper presented at the 2011 Annual International Conference of the IEEE Engineering in Medicine and Biology Society.

Mannini, A., & Sabatini, A. M. (2012). Gait phase detection and discrimination between walking-jogging activities using hidden Markov models applied to foot motion data from a gyroscope. *Gait Posture, 36*(4), 657-661. doi:10.1016/j.gaitpost.2012.06.017

Martinez-Hernandez, U., & Dehghani-Sanij, A. A. (2018). Adaptive Bayesian inference system for recognition of walking activities and prediction of gait events using wearable sensors. *Neural Netw, 102*, 107-119. doi:10.1016/j.neunet.2018.02.017

Martino, G., Ivanenko, Y. P., d'Avella, A., Serrao, M., Ranavolo, A., Draicchio, F., Cappellini, G., Casali, C., & Lacquaniti, F. (2015). Neuromuscular adjustments of gait associated with unstable conditions. *J Neurophysiol, 114*(5), 2867-2882. doi:10.1152/jn.00029.2015

Martino, G., Ivanenko, Y. P., Serrao, M., Ranavolo, A., d'Avella, A., Draicchio, F., Conte, C., Casali, C., & Lacquaniti, F. (2014). Locomotor patterns in cerebellar ataxia. *Journal of Neurophysiology, 112*(11), 2810-2821.

McGrath, D., Greene, B. R., O'Donovan, K. J., & Caulfield, B. (2012). Gyroscope-based assessment of temporal gait parameters during treadmill walking and running. *Sports Engineering, 15*(4), 207-213. doi:10.1007/s12283-012-0093-8

McMahon, T. A., & Cheng, G. C. (1990). The mechanics of running: how does stiffness couple with speed? *Journal of Biomechanics, 23*, 65-78.

Meng, L., Martinez-Hernandez, U., Childs, C., Dehghani-Sanij, A. A., & Buis, A. (2019). A Practical Gait Feedback Method Based on Wearable Inertial Sensors for a Drop Foot Assistance Device. *IEEE Sensors Journal, 19*(24), 12235-12243. doi:10.1109/jsen.2019.2938764

Mico-Amigo, M. E., Kingma, I., Ainsworth, E., Walgaard, S., Niessen, M., van Lummel, R. C., & van Dieen, J. H. (2016). A novel accelerometry-based algorithm for the detection of step durations over short episodes of gait in healthy elderly. *J Neuroeng Rehabil, 13*, 38. doi:10.1186/s12984-016-0145-6

Mijailovic, N., Gavrilovic, M., Rafajlovic, S., Đuric-Jovicic, M., & Popovic, D. (2009). Gait phases recognition from accelerations and ground reaction forces: Application of neural networks. *Telfor Journal, 1*(1), 34-36.

Mileti, I., Serra, A., Wolf, N., Munoz-Martel, V., Ekizos, A., Palermo, E., Arampatzis, A., & Santuz, A. (2020). Muscle Activation Patterns Are More Constrained and Regular in Treadmill Than in Overground Human Locomotion. *Front Bioeng Biotechnol, 8*, 581619. doi:10.3389/fbioe.2020.581619

Milligan, G. W. (1980). An examination of the effect of six types of error perturbation on fifteen clustering algorithms. *psychometrika, 45*(3), 325-342.

Milligan, G. W., & Cooper, M. C. (1985). An examination of procedures for determining the number of clusters in a data set. *psychometrika, 50*(2), 159-179. doi:10.1007/bf02294245

Mitschke, C., Heß, T., & Milani, T. (2017). Which method detects foot strike in rearfoot and forefoot runners accurately when using an inertial measurement unit? *Applied Sciences, 7*(9), 959.

Mo, S., & Chow, D. H. K. (2018). Accuracy of three methods in gait event detection during overground running. *Gait Posture, 59*, 93-98. doi:10.1016/j.gaitpost.2017.10.009

Moe-Nilssen, R. (1998). A new method for evaluating motor control in gait under real-life environmental conditions. Part 1: The instrument. *Clin Biomech (Bristol, Avon), 13*(4-5), 320-327. doi:10.1016/s0268-0033(98)00089-8

Moe-Nilssen, R., & Helbostad, J. L. (2004). Estimation of gait cycle characteristics by trunk accelerometry. *J Biomech, 37*(1), 121-126. doi:10.1016/s0021-9290(03)00233-1

Monaco, V., Ghionzoli, A., & Micera, S. (2010). Age-related modifications of muscle synergies and spinal cord activity during locomotion. *J Neurophysiol, 104*(4), 2092-2102. doi:10.1152/jn.00525.2009

Morbidoni, C., Cucchiarelli, A., Agostini, V., Knaflitz, M., Fioretti, S., & Di Nardo, F. (2021). Machine-Learning-Based Prediction of Gait Events From EMG in Cerebral Palsy Children. *IEEE Trans Neural Syst Rehabil Eng, 29*, 819-830. doi:10.1109/TNSRE.2021.3076366

Murtagh, F., & Contreras, P. (2011). Algorithms for hierarchical clustering: an overview. *WIREs Data Mining and Knowledge Discovery, 2*(1), 86-97. doi:10.1002/widm.53

Narayanan, A., Desai, F., Stewart, T., Duncan, S., & Mackay, L. (2020). Application of raw accelerometer data and machine-learning techniques to characterize human movement behavior: a systematic scoping review. *Journal of Physical Activity and Health, 17*(3), 360-383.

Nelson-Wong, E., Howarth, S., Winter, D. A., & Callaghan, J. P. (2009). Application of autocorrelation and cross-correlation analyses in human movement and rehabilitation research. *J Orthop Sports Phys Ther, 39*(4), 287-295. doi:10.2519/jospt.2009.2969

Ngoh, K. J., Gouwanda, D., Gopalai, A. A., & Chong, Y. Z. (2018). Estimation of vertical ground reaction force during running using neural network model and uniaxial accelerometer. *J Biomech, 76*, 269-273. doi:10.1016/j.jbiomech.2018.06.006

Nilsson, J., Thorstensson, A., & Halbertsma, J. (1985). Changes in leg movements and muscle activity with speed of locomotion and mode of progression in humans. *Acta Physiol Scand, 123*(4), 457-475. doi:10.1111/j.1748-1716.1985.tb07612.x

Norris, M., Kenny, I. C., & Anderson, R. (2016). Comparison of accelerometry stride time calculation methods. *J Biomech, 49*(13), 3031-3034. doi:10.1016/j.jbiomech.2016.05.029

Novacheck, T. F. (1998). The biomechanics of running. *Gait Posture, 7*(1), 77-95. doi:10.1016/s0966-6362(97)00038-6

Nutakki, C., Mathew, R. J., Suresh, A., Vijay, A. R., Krishna, S., Babu, A. S., & Diwakar, S. (2020). Classification and kinetic analysis of healthy gait using multiple accelerometer sensors. *Procedia Computer Science, 171*, 395-402.

O'Connor, C. M., Thorpe, S. K., O'Malley, M. J., & Vaughan, C. L. (2007). Automatic detection of gait events using kinematic data. *Gait Posture, 25*(3), 469-474. doi:10.1016/j.gaitpost.2006.05.016

Oh, S. E., Choi, A., & Mun, J. H. (2013). Prediction of ground reaction forces during gait based on kinematics and a neural network model. *J Biomech, 46*(14), 2372-2380. doi:10.1016/j.jbiomech.2013.07.036

Oliveira, A. S., Gizzi, L., Farina, D., & Kersting, U. G. (2014). Motor modules of human locomotion: influence of EMG averaging, concatenation, and number of step cycles. *Front Hum Neurosci, 8*, 335. doi:10.3389/fnhum.2014.00335

Oliveira, A. S., Gizzi, L., Ketabi, S., Farina, D., & Kersting, U. G. (2016). Modular Control of Treadmill vs Overground Running. *PLoS One, 11*(4), e0153307. doi:10.1371/journal.pone.0153307

Oliveira, A. S., Silva, P. B., Lund, M. E., Gizzi, L., Farina, D., & Kersting, U. G. (2013). Effects of perturbations to balance on neuromechanics of fast changes in direction during locomotion. *PLoS One, 8*(3), e59029. doi:10.1371/journal.pone.0059029

Olree, K. S., & Vaughan, C. L. (1995). Fundamental patterns of bilateral muscle activity in human locomotion. *Biol Cybern, 73*(5), 409-414. doi:10.1007/BF00201475

Osis, S. T., Hettinga, B. A., & Ferber, R. (2016). Predicting ground contact events for a continuum of gait types: An application of targeted machine learning using principal component analysis. *Gait Posture, 46*, 86-90. doi:10.1016/j.gaitpost.2016.02.021

Osis, S. T., Hettinga, B. A., Leitch, J., & Ferber, R. (2014). Predicting timing of foot strike during running, independent of striking technique, using principal component analysis of joint angles. *J Biomech, 47*(11), 2786-2789. doi:10.1016/j.jbiomech.2014.06.009

Pacini Panebianco, G., Bisi, M. C., Stagni, R., & Fantozzi, S. (2018). Analysis of the performance of 17 algorithms from a systematic review: Influence of sensor position, analysed variable and computational approach in gait timing estimation from IMU measurements. *Gait Posture, 66*, 76-82. doi:10.1016/j.gaitpost.2018.08.025

Park, S., & Caldwell, G. E. (2022). Muscle synergies are modified with improved task performance in skill learning. *Hum Mov Sci, 83*, 102946. doi:10.1016/j.humov.2022.102946

Pathak, J., Hunt, B., Girvan, M., Lu, Z., & Ott, E. (2018). Model-Free Prediction of Large Spatiotemporally Chaotic Systems from Data: A Reservoir Computing Approach. *Phys Rev Lett, 120*(2), 024102. doi:10.1103/PhysRevLett.120.024102

Pérez-Ibarra, J. C., Williams, H., Siqueira, A. A., & Krebs, H. I. (2018). *Real-time identification of impaired gait phases using a single foot-mounted inertial sensor: Review and feasibility study.* Paper presented at the 2018 7th IEEE International Conference on Biomedical Robotics and Biomechatronics (Biorob).

Phinyomark, A., Hettinga, B. A., Osis, S., & Ferber, R. (2015). Do intermediate- and higher-order principal components contain useful information to detect subtle changes in lower extremity biomechanics during running? *Hum Mov Sci, 44*, 91-101. doi:10.1016/j.humov.2015.08.018

Phinyomark, A., Osis, S., Hettinga, B. A., & Ferber, R. (2015). Kinematic gait patterns in healthy runners: A hierarchical cluster analysis. *J Biomech, 48*(14), 3897-3904. doi:10.1016/j.jbiomech.2015.09.025

Phinyomark, A., Petri, G., Ibanez-Marcelo, E., Osis, S. T., & Ferber, R. (2018). Analysis of Big Data in Gait Biomechanics: Current Trends and Future Directions. *J Med Biol Eng, 38*(2), 244-260. doi:10.1007/s40846-017-0297-2

Piper, M. C., & Darrah, J. (1994). *Motor assessment of the developing infant*: WB Saunders Company.

Pogson, M., Verheul, J., Robinson, M. A., Vanrenterghem, J., & Lisboa, P. (2020). A neural network method to predict task- and step-specific ground reaction force magnitudes from trunk accelerations during running activities. *Med Eng Phys, 78*, 82-89. doi:10.1016/j.medengphy.2020.02.002

Prado, A., Cao, X., Robert, M. T., Gordon, A. M., & Agrawal, S. K. (2019). Gait Segmentation of Data Collected by Instrumented Shoes Using a Recurrent Neural Network Classifier. *Phys Med Rehabil Clin N Am, 30*(2), 355-366. doi:10.1016/j.pmr.2018.12.007

Prasanth, H., Caban, M., Keller, U., Courtine, G., Ijspeert, A., Vallery, H., & von Zitzewitz, J. (2021). Wearable Sensor-Based Real-Time Gait Detection: A Systematic Review. *Sensors (Basel), 21*(8). doi:10.3390/s21082727

Purcell, B., Channells, J., James, D., & Barrett, R. (2006). *Use of accelerometers for detecting foot-ground contact time during running.* Paper presented at the BioMEMS and Nanotechnology II.

Rabbi, M. F., Pizzolato, C., Lloyd, D. G., Carty, C. P., Devaprakash, D., & Diamond, L. E. (2020). Non-negative matrix factorisation is the most appropriate method for extraction of muscle synergies in walking and running. *Sci Rep, 10*(1), 8266. doi:10.1038/s41598-020-65257-w

Rezaei, A., Ejupi, A., Gholami, M., Ferrone, A., & Menon, C. (2018). *Preliminary investigation of textile-based strain sensors for the detection of human gait phases using machine learning.* Paper presented at the 2018 7th IEEE International Conference on Biomedical Robotics and Biomechatronics (Biorob).

Rispens, S. M., Pijnappels, M., van Schooten, K. S., Beek, P. J., Daffertshofer, A., & van Dieen, J. H. (2014). Consistency of gait characteristics as determined from acceleration data collected at different trunk locations. *Gait Posture, 40*(1), 187-192. doi:10.1016/j.gaitpost.2014.03.182

Robberechts, P., Derie, R., Van den Berghe, P., Gerlo, J., De Clercq, D., Segers, V., & Davis, J. (2021). Predicting gait events from tibial acceleration in rearfoot running: A structured machine learning approach. *Gait Posture, 84*, 87-92. doi:10.1016/j.gaitpost.2020.10.035

Roberts, M., Mongeon, D., & Prince, F. (2017). Biomechanical parameters for gait analysis: a systematic review of healthy human gait. *Physical Therapy and Rehabilitation, 4*(1). doi:10.7243/2055-2386-4-6

Roerdink, M., Coolen, B. H., Clairbois, B. H., Lamoth, C. J., & Beek, P. J. (2008). Online gait event detection using a large force platform embedded in a treadmill. *J Biomech, 41*(12), 2628-2632. doi:10.1016/j.jbiomech.2008.06.023

Rose, V. L., & Arellano, C. J. (2021). Simple models highlight differences in the walking biomechanics of young children and adults. *J Exp Biol, 224*(22). doi:10.1242/jeb.243040

Rozumalski, A., Novacheck, T. F., Griffith, C. J., Walt, K., & Schwartz, M. H. (2015). Treadmill vs. overground running gait during childhood: a qualitative and quantitative analysis. *Gait Posture, 41*(2), 613-618. doi:10.1016/j.gaitpost.2015.01.006

Rozumalski, A., Steele, K. M., & Schwartz, M. H. (2017). Muscle synergies are similar when typically developing children walk on a treadmill at different speeds and slopes. *J Biomech, 64*, 112-119. doi:10.1016/j.jbiomech.2017.09.002

Rueterbories, J., Spaich, E. G., & Andersen, O. K. (2014). Gait event detection for use in FES rehabilitation by radial and tangential foot accelerations. *Med Eng Phys, 36*(4), 502-508. doi:10.1016/j.medengphy.2013.10.004

Saibene, F., & Minetti, A. E. (2003). Biomechanical and physiological aspects of legged locomotion in humans. *Eur J Appl Physiol, 88*(4-5), 297-316. doi:10.1007/s00421-002-0654-9

Santuz, A., Brull, L., Ekizos, A., Schroll, A., Eckardt, N., Kibele, A., Schwenk, M., & Arampatzis, A. (2020). Neuromotor Dynamics of Human Locomotion in Challenging Settings. *iScience, 23*(1), 100796. doi:10.1016/j.isci.2019.100796

Santuz, A., Ekizos, A., Eckardt, N., Kibele, A., & Arampatzis, A. (2018). Challenging human locomotion: stability and modular organisation in unsteady conditions. *Sci Rep, 8*(1), 2740. doi:10.1038/s41598-018-21018-4

Santuz, A., Ekizos, A., Janshen, L., Mersmann, F., Bohm, S., Baltzopoulos, V., & Arampatzis, A. (2018). Modular Control of Human Movement During Running: An Open Access Data Set. *Front Physiol, 9*, 1509. doi:10.3389/fphys.2018.01509

Sasaki, K., & Neptune, R. R. (2006). Differences in muscle function during walking and running at the same speed. *J Biomech, 39*(11), 2005-2013. doi:10.1016/j.jbiomech.2005.06.019

Savitzky, A., & Golay, M. J. E. (2002). Smoothing and Differentiation of Data by Simplified Least Squares Procedures. *Analytical Chemistry, 36*(8), 1627-1639. doi:10.1021/ac60214a047

Sawers, A., Allen, J. L., & Ting, L. H. (2015). Long-term training modifies the modular structure and organization of walking balance control. *J Neurophysiol, 114*(6), 3359-3373. doi:10.1152/jn.00758.2015

Schepens, B., Bastien, G. J., Heglund, N. C., & Willems, P. A. (2004). Mechanical work and muscular efficiency in walking children. *J Exp Biol, 207*(Pt 4), 587-596. doi:10.1242/jeb.00793

Schepens, B., & Detrembleur, C. (2009). Calculation of the external work done during walking in very young children. *Eur J Appl Physiol, 107*(3), 367-373. doi:10.1007/s00421-009-1132-4

Schepens, B., Willems, P. A., & Cavagna, G. A. (1998). The mechanics of running in children. *J Physiol, 509 (Pt 3)*, 927-940. doi:10.1111/j.1469-7793.1998.927bm.x

Schepens, B., Willems, P. A., Cavagna, G. A., & Heglund, N. C. (2001). Mechanical power and efficiency in running children. *Pflugers Arch, 442*(1), 107-116. doi:10.1007/s004240000511

Schneider, K., & Zernicke, R. F. (1992). Mass, center of mass, and moment of inertia estimates for infant limb segments. *J Biomech, 25*(2), 145-148. doi:10.1016/0021-9290(92)90271-2

Selles, R. W., Formanoy, M. A., Bussmann, J. B., Janssens, P. J., & Stam, H. J. (2005). Automated estimation of initial and terminal contact timing using accelerometers; development and validation in transtibial amputees and controls. *IEEE Trans Neural Syst Rehabil Eng, 13*(1), 81-88. doi:10.1109/TNSRE.2004.843176

Sharma, D., Davidson, P., Muller, P., & Piche, R. (2021). Indirect Estimation of Vertical Ground Reaction Force from a Body-Mounted INS/GPS Using Machine Learning. *Sensors (Basel), 21*(4). doi:10.3390/s21041553

Sherrill, D. M., Moy, M. L., Reilly, J. J., & Bonato, P. (2005). Using hierarchical clustering methods to classify motor activities of COPD patients from wearable sensor data. *J Neuroeng Rehabil, 2*, 16. doi:10.1186/1743-0003-2-16

Short, M. R., Damiano, D. L., Kim, Y., & Bulea, T. C. (2020). Children With Unilateral Cerebral Palsy Utilize More Cortical Resources for Similar Motor Output During Treadmill Gait. *Front Hum Neurosci, 14*, 36. doi:10.3389/fnhum.2020.00036

Shorten, M., & Pisciotta, E. (2017). Running biomechanics: what did we miss? *ISBS Proceedings Archive, 35*(1), 293.

Shuman, B. R., Goudriaan, M., Desloovere, K., Schwartz, M. H., & Steele, K. M. (2019). Muscle synergies demonstrate only minimal changes after treatment in cerebral palsy. *J Neuroeng Rehabil, 16*(1), 46. doi:10.1186/s12984-019-0502-3

Silva, D. A. S., Lang, J. J., Petroski, E. L., Mello, J. B., Gaya, A. C. A., & Tremblay, M. S. (2020). Association between 9-minute walk/run test and obesity among children and adolescents: evidence for criterion-referenced cut-points. *PeerJ, 8*, e8651. doi:10.7717/peerj.8651

Sinclair, J., Hobbs, S. J., Protheroe, L., Edmundson, C. J., & Greenhalgh, A. (2013). Determination of gait events using an externally mounted shank accelerometer. *J Appl Biomech, 29*(1), 118-122. doi:10.1123/jab.29.1.118

Singh, R. E., Iqbal, K., White, G., & Hutchinson, T. E. (2018). A Systematic Review on Muscle Synergies: From Building Blocks of Motor Behavior to a Neurorehabilitation Tool. *Appl Bionics Biomech, 2018*, 3615368. doi:10.1155/2018/3615368

Smith, M., Ward, E., Williams, C. M., & Banwell, H. A. (2021). Differences in walking and running gait in children with and without developmental coordination disorder: A systematic review and meta-analysis. *Gait Posture, 83*, 177-184. doi:10.1016/j.gaitpost.2020.10.013

Sokal, R. R., & Rohlf, F. J. (1962). The comparison of dendrograms by objective methods. *Taxon, 11*(2), 33-40.

Steele, K. M., Munger, M. E., Peters, K. M., Shuman, B. R., & Schwartz, M. H. (2019). Repeatability of electromyography recordings and muscle synergies during gait among children with cerebral palsy. *Gait Posture, 67*, 290-295. doi:10.1016/j.gaitpost.2018.10.009

Steele, K. M., Rozumalski, A., & Schwartz, M. H. (2015). Muscle synergies and complexity of neuromuscular control during gait in cerebral palsy. *Dev Med Child Neurol, 57*(12), 1176-1182. doi:10.1111/dmcn.12826

Steele, K. M., Tresch, M. C., & Perreault, E. J. (2015). Consequences of biomechanically constrained tasks in the design and interpretation of synergy analyses. *J Neurophysiol, 113*(7), 2102-2113. doi:10.1152/jn.00769.2013

Storvold, G. V., Aarethun, K., & Bratberg, G. H. (2013). Age for onset of walking and prewalking strategies. *Early Hum Dev, 89*(9), 655-659. doi:10.1016/j.earlhumdev.2013.04.010

Su, B., Smith, C., & Gutierrez Farewik, E. (2020). Gait Phase Recognition Using Deep Convolutional Neural Network with Inertial Measurement Units. *Biosensors (Basel), 10*(9). doi:10.3390/bios10090109

Sussillo, D., & Abbott, L. F. (2009). Generating coherent patterns of activity from chaotic neural networks. *Neuron, 63*(4), 544-557. doi:10.1016/j.neuron.2009.07.018

Sutherland, D. H., Olshen, R., Cooper, L., & Woo, S. L. (1980). The development of mature gait. *J Bone Joint Surg Am, 62*(3), 336-353. Retrieved from https://www.ncbi.nlm.nih.gov/pubmed/7364807

Sylos-Labini, F., La Scaleia, V., Cappellini, G., Dewolf, A., Fabiano, A., Solopova, I. A., Mondì, V., Ivanenko, Y., & Lacquaniti, F. (2022). Complexity of modular neuromuscular control increases and variability decreases during human locomotor development. *Communications Biology, 5*(1), 1256. doi:10.1038/s42003-022-04225-8

Sylos-Labini, F., La Scaleia, V., Cappellini, G., Fabiano, A., Picone, S., Keshishian, E. S., Zhvansky, D. S., Paolillo, P., Solopova, I. A., d'Avella, A., Ivanenko, Y., & Lacquaniti, F. (2020). Distinct locomotor precursors in newborn babies. *Proc Natl Acad Sci U S A, 117*(17), 9604-9612. doi:10.1073/pnas.1920984117

Sylos-Labini, F., La Scaleia, V., d'Avella, A., Pisotta, I., Tamburella, F., Scivoletto, G., Molinari, M., Wang, S., Wang, L., van Asseldonk, E., van der Kooij, H., Hoellinger, T., Cheron, G., Thorsteinsson, F., Ilzkovitz, M., Gancet, J., Hauffe, R., Zanov, F., Lacquaniti, F., & Ivanenko, Y. P. (2014). EMG patterns during assisted walking in the exoskeleton. *Front Hum Neurosci, 8*, 423. doi:10.3389/fnhum.2014.00423

Taboga, P., Lazzer, S., Fessehatsion, R., Agosti, F., Sartorio, A., & di Prampero, P. E. (2012). Energetics and mechanics of running men: the influence of body mass. *Eur J Appl Physiol, 112*(12), 4027-4033. doi:10.1007/s00421-012-2389-6

Taborri, J., Rossi, S., Palermo, E., Patane, F., & Cappa, P. (2014). A novel HMM distributed classifier for the detection of gait phases by means of a wearable inertial sensor network. *Sensors (Basel), 14*(9), 16212-16234. doi:10.3390/s140916212

Taborri, J., Scalona, E., Palermo, E., Rossi, S., & Cappa, P. (2015). Validation of Inter-Subject Training for Hidden Markov Models Applied to Gait Phase Detection in Children with Cerebral Palsy. *Sensors (Basel), 15*(9), 24514-24529. doi:10.3390/s150924514

Tan, H. X., Aung, N. N., Tian, J., Chua, M. C. H., & Yang, Y. O. (2019). Time series classification using a modified LSTM approach from accelerometer-based data: A comparative study for gait cycle detection. *Gait Posture, 74*, 128-134. doi:10.1016/j.gaitpost.2019.09.007

Tan, T., Chiasson, D. P., Hu, H., & Shull, P. B. (2019). Influence of IMU position and orientation placement errors on ground reaction force estimation. *J Biomech, 97*, 109416. doi:10.1016/j.jbiomech.2019.109416

Tesio, L., Lanzi, D., & Detrembleur, C. (1998). The 3-D motion of the centre of gravity of the human body during level walking. II. Lower limb amputees. *Clin Biomech (Bristol, Avon), 13*(2), 83-90. doi:10.1016/s0268-0033(97)00081-8

Tesio, L., & Rota, V. (2019). The Motion of Body Center of Mass During Walking: A Review Oriented to Clinical Applications. *Front Neurol, 10*, 999. doi:10.3389/fneur.2019.00999

Ting, L. H., & Macpherson, J. M. (2005). A limited set of muscle synergies for force control during a postural task. *J Neurophysiol, 93*(1), 609-613. doi:10.1152/jn.00681.2004

Tirosh, O., Orland, G., Eliakim, A., Nemet, D., & Steinberg, N. (2017). Tibial impact accelerations in gait of primary school children: The effect of age and speed. *Gait Posture, 57*, 265-269. doi:10.1016/j.gaitpost.2017.06.270

Tirosh, O., Sangeux, M., Wong, M., Thomason, P., & Graham, H. K. (2013). Walking speed effects on the lower limb electromyographic variability of healthy children aged 7-16 years. *J Electromyogr Kinesiol, 23*(6), 1451-1459. doi:10.1016/j.jelekin.2013.06.002

Torres-Oviedo, G., Macpherson, J. M., & Ting, L. H. (2006). Muscle synergy organization is robust across a variety of postural perturbations. *J Neurophysiol, 96*(3), 1530-1546. doi:10.1152/jn.00810.2005

Torricelli, D., Pajaro, M., Lerma, S., Marquez, E., Martinez, I., Barroso, F., & Pons, J. L. (2014). Modular Control of Crouch Gait in Spastic Cerebral Palsy. In *XIII Mediterranean Conference on Medical and Biological Engineering and Computing 2013* (pp. 1718-1721).

Tresch, M. C., Cheung, V. C., & d'Avella, A. (2006). Matrix factorization algorithms for the identification of muscle synergies: evaluation on simulated and experimental data sets. *J Neurophysiol, 95*(4), 2199-2212. doi:10.1152/jn.00222.2005

Trojaniello, D., Cereatti, A., Pelosin, E., Avanzino, L., Mirelman, A., Hausdorff, J. M., & Della Croce, U. (2014). Estimation of step-by-step spatio-temporal parameters of normal and impaired gait using shank-mounted magneto-inertial sensors: application to elderly, hemiparetic, parkinsonian and choreic gait. *J Neuroeng Rehabil, 11*, 152. doi:10.1186/1743-0003-11-152

Tseh, W., Bennett, J., Caputo, J. L., & Morgan, D. W. (2002). Comparison between preferred and energetically optimal transition speeds in adolescents. *Eur J Appl Physiol, 88*(1-2), 117-121. doi:10.1007/s00421-002-0698-x

Turpin, N. A., Guevel, A., Durand, S., & Hug, F. (2011). No evidence of expertise-related changes in muscle synergies during rowing. *J Electromyogr Kinesiol, 21*(6), 1030-1040. doi:10.1016/j.jelekin.2011.07.013

Van de Walle, P., Desloovere, K., Truijen, S., Gosselink, R., Aerts, P., & Hallemans, A. (2010). Age-related changes in mechanical and metabolic energy during typical gait. *Gait Posture, 31*(4), 495-501. doi:10.1016/j.gaitpost.2010.02.008

Van Hooren, B., Fuller, J. T., Buckley, J. D., Miller, J. R., Sewell, K., Rao, G., Barton, C., Bishop, C., & Willy, R. W. (2020). Is Motorized Treadmill Running Biomechanically Comparable to Overground Running? A Systematic Review and Meta-Analysis of Cross-Over Studies. *Sports Med, 50*(4), 785-813. doi:10.1007/s40279-019-01237-z

van Ingen Schenau, G. (1980). Some fundamental aspects of the biomechanics of overground versus treadmill locomotion. *Medicine and Science in Sports and Exercise, 12*(4), 257-261.

van Oeveren, B. (2021). *Running Deciphered: The interpretation of running technique from wearable data.* (PhD). Vrije Universiteit Amsterdam, Amsterdam.

van Oeveren, B. T., de Ruiter, C. J., Beek, P. J., Rispens, S. M., & van Dieen, J. H. (2018). An adaptive, real-time cadence algorithm for unconstrained sensor placement. *Med Eng Phys, 52*, 49-58. doi:10.1016/j.medengphy.2017.12.007

Vasudevan, E. V., Patrick, S. K., & Yang, J. F. (2016). Gait Transitions in Human Infants: Coping with Extremes of Treadmill Speed. *PLoS One, 11*(2), e0148124. doi:10.1371/journal.pone.0148124

Vu, H. T. T., Gomez, F., Cherelle, P., Lefeber, D., Nowe, A., & Vanderborght, B. (2018). ED-FNN: A New Deep Learning Algorithm to Detect Percentage of the Gait Cycle for Powered Prostheses. *Sensors (Basel), 18*(7). doi:10.3390/s18072389

Wenger, N., Moraud, E. M., Gandar, J., Musienko, P., Capogrosso, M., Baud, L., Le Goff, C. G., Barraud, Q., Pavlova, N., Dominici, N., Minev, I. R., Asboth, L., Hirsch, A., Duis, S., Kreider, J., Mortera, A., Haverbeck, O., Kraus, S., Schmitz, F., DiGiovanna, J., van den Brand, R., Bloch, J., Detemple, P., Lacour, S. P., Bezard, E., Micera, S., & Courtine, G. (2016). Spatiotemporal neuromodulation therapies engaging muscle synergies improve motor control after spinal cord injury. *Nat Med, 22*(2), 138-145. doi:10.1038/nm.4025

Whitall, J., & Getchell, N. (1995). From walking to running: applying a dynamical systems approach to the development of locomotor skills. *Child Dev, 66*(5), 1541-1553. doi:10.1111/j.1467-8624.1995.tb00951.x

Whiting, H. T. A. (1983). *Human motor actions: Bernstein reassessed*: Elsevier.

Willigenburg, N. W., Daffertshofer, A., Kingma, I., & van Dieen, J. H. (2012). Removing ECG contamination from EMG recordings: a comparison of ICA-based and other filtering procedures. *J Electromyogr Kinesiol, 22*(3), 485-493. doi:10.1016/j.jelekin.2012.01.001

Wouda, F. J., Giuberti, M., Bellusci, G., Maartens, E., Reenalda, J., van Beijnum, B. F., & Veltink, P. H. (2018). Estimation of Vertical Ground Reaction Forces and Sagittal Knee Kinematics During Running Using Three Inertial Sensors. *Front Physiol, 9*, 218. doi:10.3389/fphys.2018.00218

Xu, R., & Wunsch, D., 2nd. (2005). Survey of clustering algorithms. *IEEE Trans Neural Netw, 16*(3), 645-678. doi:10.1109/TNN.2005.845141

Yakovenko, S., Mushahwar, V., VanderHorst, V., Holstege, G., & Prochazka, A. (2002). Spatiotemporal activation of lumbosacral motoneurons in the locomotor step cycle. *J Neurophysiol, 87*(3), 1542-1553. doi:10.1152/jn.00479.2001

Yang, J., Huang, T.-H., Yu, S., Yang, X., Su, H., Spungen, A. M., & Tsai, C.-Y. (2019). *Machine learning based adaptive gait phase estimation using inertial measurement sensors.* Paper presented at the Frontiers in Biomedical Devices.

Yildiz, I. B., Jaeger, H., & Kiebel, S. J. (2012). Re-visiting the echo state property. *Neural Netw, 35*, 1-9. doi:10.1016/j.neunet.2012.07.005

Yokoyama, H., Ogawa, T., Kawashima, N., Shinya, M., & Nakazawa, K. (2016). Distinct sets of locomotor modules control the speed and modes of human locomotion. *Sci Rep, 6*, 36275. doi:10.1038/srep36275

Yuwono, M., Su, S. W., Guo, Y., Moulton, B. D., & Nguyen, H. T. (2014). Unsupervised nonparametric method for gait analysis using a waist-worn inertial sensor. *Applied Soft Computing, 14*, 72-80. doi:10.1016/j.asoc.2013.07.027

Zandvoort, C. S., Daffertshofer, A., & Dominici, N. (2022). Cortical contributions to locomotor primitives in toddlers and adults. *iScience, 25*(10), 105229. doi:10.1016/j.isci.2022.105229

Zandvoort, C. S., van Dieen, J. H., Dominici, N., & Daffertshofer, A. (2019). The human sensorimotor cortex fosters muscle synergies through cortico-synergy coherence. *Neuroimage, 199*, 30-37. doi:10.1016/j.neuroimage.2019.05.041

Zeni, J. A., Jr., Richards, J. G., & Higginson, J. S. (2008). Two simple methods for determining gait events during treadmill and overground walking using kinematic data. *Gait Posture, 27*(4), 710-714. doi:10.1016/j.gaitpost.2007.07.007

Zych, M., Rankin, I., Holland, D., & Severini, G. (2019). Temporal and spatial asymmetries during stationary cycling cause different feedforward and feedback modifications in the muscular control of the lower limbs. *J Neurophysiol, 121*(1), 163-176. doi:10.1152/jn.00482.2018

SUMMARY

The current understanding of the development of running in children is limited, specifically the underlying mechanisms of the motor control. In this thesis I study the development of running in young children by combining neuromuscular and biomechanical measures using novel techniques and state of the art statistics. Hereby, I introduce a frame of reference for the factors underlying the development of running in children which the other chapters of this thesis are built upon. **Chapter 1** introduces muscle synergies and clustering techniques which are integral to the results in this thesis.

The study in **Chapter 2** focuses on the biomechanics of walking and running on a treadmill of children aged 2-9 years old in a cross-sectional design. Clustering of kinetic and kinematic parameters across strides revealed that there was no direct agreement between chronological age and maturity in young children walking and running when comparing their gait patterns to those of adults. When learning to run, young children made use of a “walk-run-strategy”. This strategy is characterized by the ability to run with a combination of strides with double support and flight phase causing in-phase oscillations of potential and kinetic energies of the center-of-mass.

The study in **Chapter 3** focuses on the neuromuscular control of locomotion in children aged 2-9 years old again on a treadmill and in a cross-sectional design. To that end, I assessed the muscle activity and in particular the number and structure of muscle synergies. Children in this study also used a walk-run strategy when learning to run on a treadmill. Older children incorporated exploratory muscle synergies when “optimizing” their walking and running pattern on the treadmill whereas the youngest children below 3.5 years of age made use of a “simpler” motor control pattern trending toward larger bursts of activation. I believe that the increase in the number of muscle synergies for individual participants was related to motor learning and exploration.

To further detail the development of locomotion, I investigated the running in a longitudinal design assessing two children from their first independent steps until about 32 months after onset of independent walking. In **Chapter 4** I combined both biomechanics and neuromuscular control of locomotion. Using a method like the one used in **Chapter 2** and comparing the running development of the two toddlers to a group of adults, I was able to determine that the development of running can proceed along different trajectories including the co-existence of immature and mature running within the same session in a child.

Collecting large amounts of data is easy to achieve on a treadmill and most of the experimental data presented in this thesis were therefore collected on a treadmill. However, a treadmill does not necessarily represent natural locomotion. So, in **Chapter 5** I explored avenues to record outside of the lab. I employed recursive neural networks (reservoir computers)

to predict vertical ground reaction force data from shank accelerometer data in adults with high accuracy which in turn lead to a high accuracy in the gait event detection.

In **Chapter 6** I reflected on the findings of this thesis and put these into a broader context of what is known about running in children. I showed that neither flight phase nor the in-phase oscillations of kinetic and potential energies of the center-of-mass were proper indicators of running in children from onset of independent walking to 9 years of age. I proposed some aspects of future research such as not focusing on the presence of a flight phase to determine running in children and to apply methods requiring advanced statistics to get proper insights into running in children.

The work in this thesis supports the notion that development of running in children is not a linear process. Generally, I have come to understand that children limit the degrees of freedom available to them resulting in a reduced range of movement, both in terms of biomechanics and neuromuscular control. Based on my findings, I conclude that it is not possible to distinguish biomechanical constraints from neuromuscular constraints. They interact and are equally important in understanding the motor control of running in children. The development of motor control is a subtle process and as such it cannot be characterized with just a few parameters.

SAMENVATTING

Het huidige inzicht in de ontwikkeling van hardlopen bij kinderen is beperkt, vooral wat betreft de onderliggende mechanismen van de motorische sturing. In dit proefschrift onderzoek ik de ontwikkeling van hardlopen bij jonge kinderen door neuromusculaire en biomechanische metingen te analyseren met nieuwe technieken en geavanceerde statistiek. Hiertoe presenteer ik een theoretische kader voor de factoren die ten grondslag liggen aan de ontwikkeling van hardlopen bij kinderen. De overige hoofdstukken in het proefschrift zijn hierop gebaseerd. In **Hoofdstuk 1** beschrijf ik in het bijzonder de spiersynergieën en clusteringstechnieken, die integraal deel uitmaken van de in dit proefschrift gepresenteerde resultaten.

De studie in **Hoofdstuk 2** richt zich op de biomechanica van wandelen en hardlopen op een loopband bij kinderen van 2 tot 9 jaar in een cross-sectioneel design. Clustering van kinetische en kinematische parameters over meerdere stappen bracht geen directe overeenkomst aan het licht tussen chronologische leeftijd en rijpheid bij jonge kinderen, wanneer hun looppatronen worden vergeleken met die van volwassenen. Bij het leren hardlopen maken jonge kinderen gebruik van een "loop-ren-strategie". Deze strategie kenmerkt zich door een combinatie van passen met dubbele steun- en vluchtfase, waardoor in-fase-oscillaties optreden van potentiële en kinetische energieën van het zwaartepunt.

De studie in **Hoofdstuk 3** betreft de neuromusculaire sturing van de voortbeweging bij kinderen van 2 tot 9 jaar, andermaal op de loopband en in een cross-sectioneel design. Daartoe analyseerde ik de spieractiviteit en met name het aantal en de structuur van de aanwezige spiersynergieën. Kinderen bleken ook in deze studie een loop-ren strategie te hanteren bij het leren hardlopen op een loopband. Oudere kinderen maakten gebruik van verkennende spiersynergieën bij het "optimaliseren" van hun wandel- en hardlooppatroon op de loopband, terwijl de jongste kinderen onder de 3,5 jaar gebruik maakten van een "eenvoudiger" motorisch sturingspatroon dat neigde naar grotere uitbarstingen van activering. Ik veronderstel dat de toename van het aantal spiersynergieën voor individuele deelnemers verband houdt met motorisch leren en exploratie.

Om de ontwikkeling van de motoriek verder te detailleren, onderzocht ik het hardlopen in een longitudinale studie waarin twee kinderen vanaf hun eerste zelfstandige stapjes tot ongeveer 32 maanden na het begin van het zelfstandig kunnen lopen werden gevolgd. In **Hoofdstuk 4** richtte ik mij op zowel de biomechanica als de neuromusculaire sturing van de motoriek. Door een soortgelijke methode te gebruiken als in **Hoofdstuk 2** en de hardloopontwikkeling van twee peuters te vergelijken met een groep volwassenen, kon ik vaststellen dat de ontwikkeling van het hardlopen langs verschillende trajecten kan verlopen, waaronder het naast elkaar bestaan van onrijp en rijp lopen binnen dezelfde sessie bij hetzelfde kind.

Het verzamelen van grote hoeveelheden meetgegevens is eenvoudig te realiseren op een loopband en de meeste experimentele in dit proefschrift gepresenteerde meetgegevens zijn

dan ook verzameld op een loopband. Hardlopen op een loopband kan echter afwijken van de natuurlijke hardloopbeweging. In **Hoofdstuk 5** heb ik daarom wegen verkend om het hardlopen buiten het lab te bestuderen. Ik gebruikte daartoe recursieve neurale netwerken (reservoircomputers) om de verticale grondreactiekracht uit versnellingsmeterdata van de schacht bij volwassenen met een hoge nauwkeurigheid te voorspellen, wat op zijn beurt leidde tot een hoge nauwkeurigheid in de detectie van ganggebeurtenissen.

In **Hoofdstuk 6** reflecteer ik op de bevindingen van dit proefschrift en plaats deze in een bredere context van wat er momenteel bekend is over hardlopen bij kinderen. Ik toon aan dat noch de vluchtfase, noch de in-fase-oscillaties van kinetische en potentiële energieën van het zwaartepunt goede indicatoren zijn voor het lopen bij kinderen vanaf het begin van het zelfstandig lopen tot de leeftijd van 9 jaar. Ik stel enkele aspecten van toekomstig onderzoek voor, zoals het niet focussen op de aanwezigheid van een vluchtfase om het hardlopen bij kinderen te bepalen en het toepassen van geavanceerde statistische methoden die geavanceerde statistiek vereisen om goede inzichten te krijgen in het hardlopen bij kinderen.

Het onderzoek in deze dissertatie ondersteunt het inzicht dat de ontwikkeling van hardlopen bij kinderen geen lineair proces is. In het algemeen ben ik tot het inzicht gekomen dat kinderen op zeer jonge leeftijd de voor hen beschikbare vrijheidsgraden beperken, wat resulteert in een verminderde bewegingsruimte, zowel in termen van biomechanica als neuromusculaire sturing. Op basis van mijn bevindingen concludeer ik dat het niet goed mogelijk is biomechanische beperkingen te onderscheiden van neuromusculaire beperkingen. Ze werken in wisselwerking en zijn even belangrijk om de motorische sturing van hardlopen bij kinderen te doorgronden. De ontwikkeling van motorische sturing is een subtiel proces en kan als zodanig niet worden gekarakteriseerd aan de hand van slechts enkele parameters.

ACKNOWLEDGEMENTS

It may be that sometimes the fastest way to get somewhere is to go slow, but that does not mean that it was a boring or an uneventful journey. I have a lot of people I would like to thank for supporting me either directly or indirectly in this journey.

First, I would like to thank my two supervisors **Nadia** and **Andreas**.

Nadia, when I first started my Research Master project with you, you were ready to go on maternity leave with Luna so in the beginning I did not see you a lot, but we still managed to come up with a great project that you believed in so much that you funded a PhD for me from your own personal funding. I am forever grateful for that. We have had many lively discussions during my PhD and have learned a lot along the way.

Andreas. Thank you for helping me come a long way from the RM student who was struggling with programming and time series analysis to the scientist I am today. Your guidance played a large role in my progress. I have enjoyed our discussions. I have learnt a lot from you both. Thank you for your confidence in me.

Thank you to the reading committee, **Heiko Wagner**, **Veerle Seegers**, **Claudine Lamoth**, **Marjolein van der Krogt**, and **Jaap van Dieën** for taking your time to read and evaluate my thesis and coming to Amsterdam. I appreciate your comments and feedback which served to improve the thesis.

Coen and **Saba**, thank you for being my paranymphs. **Coen,** there was never a doubt in my mind that you would be one of the people on stage with me. You and I have shared so many ups and downs, coffees, conference trips, and beers. And now we also succeeded in co-authoring a paper together. I am so happy that we keep the tradition of drinking a coffee together, albeit virtually, it really makes the process and the day so much more gezellig. Thank you for being a good friend.

Saba, we have only known each other for a few years but thank you for all the great times we have had on the playground, in each other's houses, and visiting cafes. Thank you for being a voice of reason and a listening ear, for helping with groceries, and offering to feed my family when I am not home. Your friendship and that of our children will be a lasting one, I'm sure.

To the rest of the BabyGaitLab, past and present members: Thank you for great collaboration and fun times in the lab. **Marije**, you have been a support in many aspects and even if it never resulted in any joint papers, I learnt a lot from you as a person as well as a scientist. I wish you all the best in your new endeavors outside academia, you will be missed. Thank you, **Annike**, for taking me by the hand in Berlin at the autumn school, for fun and challenging discussions, and some great collaboration on our joint papers. I have not worked with someone who is as organized as you. **Ruud** and **Marzieh**, I am looking forward to the big parties we

will have when you finish your theses: I will be your biggest cheerleader. Marzieh, you gave the best virtual presentation in Montreal – that's a real skill I wish I had. Ruud, football is not your only strength – playing and entertaining children must be a hidden (to most) skill of yours! Thank you, **Jennifer**, for the attention and supervision in the beginning of my RM project. I learnt a lot from you about doing experiments in children.

Doing a PhD would not have been the same if I had done it somewhere else. Thank you to all my VU PhD and postdoc colleagues past and present for making it a fun experience. For drinking coffee, eating cake, drinking beer, dancing to the BW band, great laughs, PhD weekends, and outings. **Ali**, **Andrea**, **Anna**, **Anne**, **Anouk**, **Axel**, **Bart**, **Bart**, **Bastian**, **Ben**, **Dan**, **Daniel**, **Daniëlle**, **Edwin**, **Encarna**, **Emily**, **Fang**, **Guido**, **Guido**, **Ilse**, **Ingrid**, **Jakob**, **Jeanine**, **Jens**, **Jian**, **Koen**, **Laure**, **Lisa**, **Leila**, **Lotte**, **Lotte**, **Luke**, **Maaike**, **Mireille**, **Mohammad**, **Moira**, **Nick**, **Niels**, **Nicola**, **Nicolas**, **Nina**, **Pieter**, **Roel**, **Stephan**, **Stephanie**, **Sauvik**, **Tammie**, **Tom**, **Ton**, and **Twan**. **Dirk**, **Puck**, and **Sabrina** you guys hold a special place in my heart for always ensuring a great atmosphere in the office, great laughs, and being a shoulder to cry on.

Daphne, thank you for always being great company in Edinburgh, Montreal, but also in Amsterdam. You have shown me time and time again what being a nice person can lead to and I will always look up to you.

None of this thesis would have been possible without our great technical support, I owe you guys a lot. You were always there to answer stupid questions and you trusted me and Coen with a key to the video room back when doing our research master projects which I am sure contributed to our great successes. Thank you, **Bert**, **Frans-Jozef**, **Lennaert, Leon**, and **Vincent**.

Thank you to the former section of Coordination Dynamics. **Bernadette**, **Lieke**, **Melvyn**, **Sjoerd**, and **John** thank you for always great discussions during our lunch meetings, fun section-outings, and for providing excellent feedback and support during presentations. Thank you also to all other staff members, **Brenda**, **David**, **Eli**, **Jaap**, **Jeroen**, **Maarten**, and **Mirjam**, for chats at the coffee machine and for creating a great scientific environment at the VU.

Thank you to all my friends in the Netherlands, **Alex**, **Alison**, **Iulian**, **Joachim**, **Merian**, **Nicoleta**, **Pia**, **Robert-Jan**, **Thilo**, and all your lovely children, for helping us settle, coffee dates, play dates, trips to the market, birthday celebrations, travels, board game evenings, beers, and all the great things we have done together – they have been a great distraction from a busy work life.

Emma, **Phil** – we may not have seen a lot to each other these last three years due to Corona and Brexit, but just know that you guys are very special to me. I look so much forward to being

able to give you guys a big hug again! Maybe we will have a hike next time where we can be joined by **Fred**, **Leanne**, **Liam, Marta**, **Rob**, and **Steve**.

Now, you must use some translate-tool if you want to be able to read the rest as I will continue in Danish here-on out.

Man kan ikke skrive takke-ord uden at takke alletiders kollegie og påhæng, 37-1., **Adam**, **Caroline**, **David**, **Hans**, **Jesper**, **Juan**, **Kathrine**, **Maggie**, **Maria**, **Mathilde**, **Phil**, **Sisse**, **Thomas**, **Tinna** og alle jeres skønne børn. Tak for alle de gode sommerhusture, skønne nytårsaftener, skønne snakke og besøg igennem årene og bare alletiders selskab. I er simpelthen de bedste!

Tak for dig, **Anne**. Du er min bedste veninde og det har været en ære at kende dig i mere end 15 år. Du har stået ved mig i tykt og tyndt og selvom vi ikke snakker hver uge, så ved vi begge to at vi er lige ved siden af hinanden. Det er så ærgerligt at du ikke kan være der og fejre dagen med mig, men jeg ved at du sidder derhjemme og lytter med og hepper på mig som du jo altid har gjort!

Tak til hele **familien Bach** og **familien Poulsen** – I sørger altid for gode stunder når vi er på besøg i Danmark.

En tak også til min søster og hendes mand, **Astrid** og **Asbjørn** og jeres børn – tak for gode inputs. Tak for alle legene og tak for adspredelserne når vi er hjemme på ferie.

Nu kommer den sværeste sektion at skrive i hele denne afhandling med min fars alt for pludselige død. **Mor** og **far**: tak for al den støtte I har givet gennem årene. Støtte i form af børnepasning, et øre der lytter, skønne ferier, godt selskab, penge her og der, og et varmt hjem der altid var åbent blandt mange ting der slet ikke kan beskrives på så kort en plads. Hvor er det uretfærdigt at far ikke længere er her og ikke kan være med til at fejre den store dag. Hans pludselige død har efterladt et stort hul i alles liv og jeg ved hvor stolt af mig han var og hvor stolt af mig I begge er. Tak er et sølle ord. Jeg elsker jer.

Casper, du er min bedste ven og jeg havde aldrig nået hertil uden dig. Du er min sten. Du er mit lyspunkt og uden din feedback, dine stille skub, og dit gode positive sind var jeg nok aldrig påbegyndt sådan en udfordring. Du har vist mig vejen og jeg vil elsker dig og vil altid elske dig meget højt. Du og **Oliver** og **Ellinor** er dagens lyspunkter. Kære børn. Når I engang er store nok til at læse det her (hvis I nogensinde gider), så føles den her kæmpemæssige kamp nok som et lille blip i tiden der er gået. I gør mig stolte hver dag og jeg elsker jer højere end jeg troede noget muligt.

LIST OF PUBLICATIONS

Bekius, A., **Bach, M.M.**, Van der Krogt, M.M., De Vries, R., Buizer, A.I., & Dominici, N. (2020). Muscle synergies during walking in children with cerebral palsy: a systematic review. *Frontiers in physiology*, 632.

Bach, M.M., Daffertshofer, A., & Dominici, N. (2021). The development of mature gait patterns in children during walking and running. *European journal of applied physiology*, *121*(4), 1073-1085.

Bach, M.M., Daffertshofer, A., & Dominici, N. (2021). Muscle synergies in children walking and running on a treadmill. *Frontiers in human neuroscience*, *15*, 637157.

Bekius, A., **Bach, M.M.**, Van de Pol, L.A., Harlaar, J., Daffertshofer, A., Dominici, N., & Buizer, A.I. (2021). Early development of locomotor patterns and motor control in very young children at high risk of cerebral palsy, a longitudinal case series. *Frontiers in human neuroscience*, *15*, 232.

Bach, M.M., Dominici, N., & Daffertshofer, A. (2022). Predicting vertical ground reaction forces from 3D accelerometry using reservoir computers leads to accurate gait event detection. *Frontiers in Sports and Active Living*, 4. doi:10.3389/fspor.2022.1037438

Bach, M.M., Zandvoort, C.S., Cappellini, G., Ivanenko, Y., Lacquaniti, F., Daffertshofer, A., & Dominici, N. (2023). Development of running is not related to time since onset of independent walking, a longitudinal case study. *Frontiers in Human Neuroscience*.

Amsterdam Movement Sciences

VU VRIJE UNIVERSITEIT AMSTERDAM

Amsterdam UMC University Medical Centers

Amsterdam Movement Sciences conducts scientific research to optimize physical performance in health and disease based on a fundamental understanding of human movement in order to contribute to the fulfillment of a meaningful life.